Raum-Zeit Kodierung mit Niedriger Komplexität für Mehrantennensysteme und Relay-Funknetzwerke

Vom Fachbereich Elektrotechnik und Informationstechnik
der Technischen Universität Darmstadt
zur Erlangung der Würde
eines Doktor-Ingenieurs (Dr.-Ing.)
genehmigte Dissertation

von

Javier Mauricio Paredes Riaño, M.Sc.

geboren in Bucaramanga, Kolumbien

Referent:	Prof. Dr. Alex B. Gershman
Korreferent:	Prof. Dr. Gregori Vázquez
Tag der Einreichung:	01.04.2009
Tag der mündlichen Prüfung :	02.07.2009

D 17
Darmstadt
2009

Gedruckt mit Unterstützung des Deutschen Akademischen Austauschdienstes

Low-Complexity Space-Time Coding for Multi-Antenna Systems and Wireless Relay Networks

Submitted to the
Department of Electrical Engineering and Information Technology
Darmstadt University of Technology, Germany
in partial fulfillment of the requirements
for the degree of
Doctor of Engineering

by

Javier Mauricio Paredes Riaño, M.Sc.

from Bucaramanga, Colombia

D 17
Darmstadt
2009

To my wife Jimena Andrea

Acknowledgments

I am grateful to my advisor Prof. Alex B. Gershman for his permanent advice and support during the realization of my Ph.D. study. The completion of this work would not have been possible without his invaluable suggestions and discussions.

Special thanks to the German Academic Exchange Service (DAAD) for the generous scholarship that I received during my studies.

I would like to express my gratitute to Prof. Anja Klein for the help in writing the Ph.D. proposal for the scholarship that I received from the DAAD and for having introduced me to Prof. Gershman. I thank Prof. Babak H. Khalaj for the fruitful discussions and cooperation, Dr. Mohammend Gharavi-Alkhansari for his cooperation during the first part of my work, and all the past and actual members of the Communication Systems Group who contributed in one way or another in the successful completion of this work.

I want to thank my parents for their overall support and encouragment. Finally, and above all, I am grateful to my wife Jimena Andrea, for her unconditional support, patience, advice, and specially, love.

Javier M. Paredes R.

Zusammenfassung

Der steigende Bedarf an Übertragunsgeschwindigkeit, Verlässlichkeit und Verfügbarkeit von drahtlosen Kommunikationssystemen hat eine intensive Forschung in diesem Bereich während der letzten Jahre ausgelöst.

Mehrantennensysteme ermöglichen bedeutende Performancegewinne, da sich das Signal auf unterschiedlichen unabhängigen Wegen zwischen Sender und Empfänger ausbreitet. Raum-Zeit-Codes wurden entwickelt, um die Vorteile von Mehrantennenkanälen zu nutzen. Bei dem Design von Raum-Zeit-Codes müssen unterschiedliche Tradeoffs abgewogen werden. Gute Raum-Zeit-Codes erzielen einen hohen Diversitätsgewinn und den höchst möglichen Multiplexgewinn. Gleichzeitig sollte die Komplexität für die Codierung und die Decodierung so gering wie möglich sein, um eine schnelle Signalverarbeitung zu erlauben. Im ersten Teil der Dissertation werden neuartige Raum-Zeit-Block-Codes präsentiert, die eine Maximum-Likelihood Decodierung mit niedriger Komplexität ermöglichen. Insbesondere wird ein 2×2 Raum-Zeit-Code mit maximaler Rate, niedriger Decodierungskomplexität und der Eigenschaft der nicht-verschwindenden Determinante vorgestellt. Somit erzielt dieser Raum-Zeit-Code optimale Eigenschaften für den Tradeoff zwischen Diversität und räumlichem Multiplex. Darüber hinaus wird unser Verfahren für Raum-Zeit-Codes mit 3 und 4 Sendeantennen erweitert.

Aufgrund der Anforderungen an die Größe und die Kosten können Mehrantennensysteme in einigen Mobilfunkgeräten nicht angewendet werden. Um trotzdem eine Mehrwegeausbreitung zu realisieren, wurden halbduplexe Relay-Funknetzwerke vorgeschlagen, in denen mehrere Nutzer mit jeweils einer Antenne kooperieren. Die Anforderungen an diese Geräte erfordern verteilte Raum-Zeit-Codes mit niedriger Komplexität. Im zweiten Teil dieser Doktorarbeit wird eine neue Technik für die niederratige rückkopplungsbasierte kooperative Übertragung in Relay-Netzwerken

entwickelt, die maximale Diversität, einfache lineare Maximum-Likelihood Decodierung und kurze Decodierungsverzögerung für eine beliebige Anzahl an Nutzern ermöglicht. Um die Performance dieser Technik in praktischen Szenarien mit Kanälen unterschiedlicher Qualität zu verbessern, werden auf der Grundlage der Kanalstatistiken zweiter Ordnung "Lang-Zeit" Leistung-Gewichte berechnet. Außerdem werden durch differentielle Übertragung die vorgeschlagenen verteilten Raum-Zeit-Codes für Empfänger ohne Kanalinformation verallgemeinert.

Abstract

A rapidly growing demand on transmission rates, coverage and reliability for wireless communication systems has triggered an intensive research in the field of multi-antenna communications. The use of multi-antenna systems provides significant gains by making use of independent propagation paths between the transmitter and the receiver. Space-time coding has been recently proposed to exploit the benefits of the multi-antenna channels. In space-time code design, different tradeoffs have to be taken into account. Good codes should provide a high diversity gain and achieve the highest possible multiplexing gain. At the same time, the encoding/decoding complexity should remain as low as possible to enable computationally efficient signal processing. In this thesis, we propose high-rate high-performance space-time block coding schemes that achieve a significantly reduced maximum likelihood decoding complexity in comparison to other state-of-the-art space-time codes. In particular, we propose a 2×2 full-rate space-time code with non-vanishing determinants that achieves the optimal diversity-multiplexing gain tradeoff while using a fast maximum likelihood decoder. Furthermore, by extending the proposed strategy, we develop space-time codes for 3 and 4 transmit antennas.

In certain cases, the use of multi-antenna systems can become impractical due to restrictions in hardware size and cost. As an alternative to create multi-path propagation environments, half-duplex wireless relay networks have emerged. In such networks, single antenna users cooperate to provide gains similar to that of the multi-antenna channel. Considering the initial restrictions, low-complexity distributed space-time coding schemes are required for relay systems. In the second part of the thesis, we develop a novel low-rate feedback-based distributed approach for cooperative transmission in relay networks that achieves the maximum diversity offered by the relay network, enjoys low-complexity maximum likelihood decoding,

avoids long decoding delays and is applicable to any number of relays. The use of second-order channel statistics to design "long-term" power control weights is considered to further improve the performance of our approach in practical scenarios with channel links of different quality. Moreover, the proposed distributed space-time coding schemes are generalized to the non-coherent receiver case using differential transmission.

Contents

List of Tables

List of Figures

List of Abbreviations

AMPS	Advanced Mobile Phone Service
AF	Amplify-and-Forward
BER	Bit error rate
BLER	Block error rate
bpcu	bits per channel use
bps	bits per second
CDMA	Code Division Multiple Access
CIOD	Coordinate Interleaved Orthogonal Design
CSI	Channel State Information
D-AMPS	Digital AMPS
DAST	Diagonal Algebraic Space-Time
DF	Decode-and-Forward
DMG	Diversity-Multiplexing Gain
DOF	Degrees Of Freedom
DSTC	Distributed Space-Time Coding/Code
EDGE	Enhanced Data Rates for GSM Evolution
FIR	Finite Impulse Response
GPRS	General Packet Radio Service
GSM	Global System for Mobile Communications
HSPA	High Speed Packet Access
IEEE	Institute of Electrical and Electronics Engineers
i.i.d.	Independent and Identically Distributed
LCP	Linear Constellation Precoding
LOS	Line Of Sight
LTE	Long Term Evolution

MIMO	Multiple-Input Multiple-Output
MISO	Multiple-Input Single-Output
ML	Maximum Likelihood
MMI	Maximum Mutual Information
NLOS	Non-Line Of Sight
NMT	Nordic Mobile Telephone
NVD	Non-Vanishing Determinant
OSB-STBC	Orthogonal Structure Based STBC
OSTBC	Orthogonal Space-Time Block Code
PAM	Pulse Amplitude Modulation
PDC	Personal Digital Cellular
pdf	Probability Density Function
QAM	Quadrature Amplitude Modulation
QOSTBC	Quasi Orthogonal Space-Time Block Code
QPSK	Quadrature Phase Shift Keying
SD	Sphere Decoder/Decoding
SER	Symbol Error Rate
SISO	Single-Input Single-Output
SNR	Signal-to-Noise Ratio
STBC	Space-Time Block Code/Coding
STC	Space-Time Coding
TACS	Total Access Communication System
UMTS	Universal Mobile Telecommunications System
WCDMA	Wideband CDMA
WiMAX	Worldwide Interoperability for Microwave Access

List of Notations

$\mathcal{CN}(\mu, \sigma^2)$	Complex Gaussian pdf with mean μ and variance σ^2
j	$\sqrt{-1}$
$\mathrm{Re}\{\cdot\}$	Real part operator
$\mathrm{Im}\{\cdot\}$	Imaginary part operator
$(\cdot)^*$	Complex conjugate
$\lvert\cdot\rvert$	Absolute value
$I_0(\cdot)$	Modified zero-order Bessel function of the first kind
log	Natural logarithm
$\log_2$	Base-2 logarithm
$\lVert\cdot\rVert$	Euclidean norm
$\lVert\cdot\rVert_F$	Frobenius norm of a matrix
$(\cdot)^H$	Hermitian transpose
$[\cdot]_{m,n}$	Entry in the mth row and the nth
$\det(\cdot)$	Determinant operator
$\mathrm{tr}(\cdot)$	Trace of a matrix
$\mathbf{A} \succeq 0$	$\mathbf{A}$ is positive semi-definite
$\mathrm{rank}\{\mathbf{A}\}$	Rank of matrix $\mathbf{A}$
$\mathrm{diag}(\cdot)$	A diagonal matrix of its argument
$\mathbf{I}_n$	$n \times n$ identity matrix
$(\cdot)^T$	Transpose of a matrix
$\mathbb{Z}$, $\mathbb{R}$, $\mathbb{C}$	Set of integer, real and complex numbers, respectively
$\underline{\mathbf{Z}}$	Underlined version of matrix $\mathbf{Z}$, see (3.10).
$\mathrm{mat}_{I,J}(\cdot)$	Inverse of the underline operator: $\mathrm{mat}_{I,J}(\underline{\mathbf{Z}}) = \mathbf{Z}$

$\otimes$	Kronecker product
$\mathrm{E}\{\cdot\}$	Statistical expectation operator
$\mathrm{E}_x\{\cdot\}$	Statistical expectation operator with respect to x
$P(\mathbf{X}, \mathbf{X}')$	Pairwise error probability
$\gcd(a, b, \ldots)$	Greatest common divisor of a, b, ...
$a \bmod b$	The remainder of a divided by b
$\odot$	Schur-Hadamard (element-wise) matrix product
sign	Sign function
$\min\{a, b\}$	Minimum number between a and b
$\mathrm{vec}(\cdot)$	Vectorization of a matrix into a column vector

List of Symbols

N_t	Number of transmit antennas
N_r	Number of receive antennas
T	Block length
j	$\sqrt{-1}$
$h_{m,n}$	Complex baseband channel gain between the n transmit and mth receive antenna
$\mathbf{H}$	$N_r \times N_t$ complex baseband channel matrix
$y_m(t)$	Receive signal at the mth antenna and t time-slot
$\mathbf{Y}$	$N_r \times T$ complex matrix of receive signals
$v_m(t)$	Noise at the mth antenna and t time-slot
$\mathbf{V}$	$N_r \times N_t$ complex white Gaussian noise matrix
σ_v^2	Noise variance
$x_n(t)$	Transmit signal at the nth antenna and t time-slot
$\mathbf{X}$	$N_t \times T$ matrix of transmit signals
$\mathbf{C}_k$	Linear dispersion matrix
$\mathcal{X}, \mathcal{Y}$	Codebook of matrices $\mathbf{X}$, $\mathbf{Y}$, respectively
$\underline{\mathcal{X}}, \underline{\mathcal{Y}}$	Codebook of the underline version of the matrices $\mathbf{X}$, $\mathbf{Y}$, respectively
$\mathbb{H}$	Equivalent channel matrix for the real-valued model
$\mathbb{G}$	Space-time code generator matrix
$\mathbb{G}_{OSTBC}$	Generator matrix of an OSTBC
s_k	Information symbol
K	Total number of information symbols encoded per block
K_o	Total number of information symbols encoded in the OSTBC matrix
$\mathbf{s}, \underline{\mathbf{s}}$	Vector of information symbols and its underline version
ζ	Diversity product

P_i	Average transmit power at the ith node
f_i	Channel between the source and the ith relay
g_i	Channel between the ith relay and the destination
$\mu_{f_i}, \sigma^2_{f_i}$	Mean and variance of channel f_i, respectively
$\mu_{g_i}, \sigma^2_{g_i}$	Mean and variance of channel g_i, respectively
m_{f_i}, m_{g_i}	Second-order moment of f_i and g_i, respectively
$\mathbf{r}_i$	Receive signal at the ith relay
$\mathbf{v}_i$	Noise at the ith relay
$\mathbf{d}_i$	Transmitted signal from the ith relay
$\mathbf{n}$	Noise at the destination node
$\mathbf{A}_i, \mathbf{B}_i$	Distributed linear dispersion matrices
$\mathbf{S}$	Equivalent distributed space-time code
$\mathbf{w}$	Total noise at destination
$\mathbf{h}$	Equivalent channel vector between source and destination
$\mathbf{p}$	Equivalent power vector
P_w	Noise power at destination
P_s	Signal power at destination
R	Number of relays
$\mathbf{b}$	Vector of the binary coefficients b_i
$\boldsymbol{\theta}$	Vector with the real-valued power control coefficients θ_i
$\mathbf{b}_a$	Vector of the binary coefficients b_i with the extended Alamouti code
$\boldsymbol{\theta}_a$	Vector with the real-valued power control coefficients θ_i with the extended Alamouti code
$\mathbf{B}, \boldsymbol{\Theta}$	$\mathbf{b}\mathbf{b}^T$, $\boldsymbol{\theta}\boldsymbol{\theta}^T$, respectively
$\mathbf{B}_a, \boldsymbol{\Theta}_a$	$\mathbf{b}_a\mathbf{b}_a^T$, $\boldsymbol{\theta}_a\boldsymbol{\theta}_a^T$, respectively
u_l	Differential transmitted symbol at time l
$\mathbf{u}_l$	Differential transmitted vector at block l
ϕ_{f_i}, ϕ_{g_i}	$\lvert\mu_{f_i}\rvert^2/\sigma^2_{f_i}$ and $\lvert\mu_{g_i}\rvert^2/\sigma^2_{g_i}$, respectively

Chapter 1

Introduction

Multi-antenna communication systems and wireless relay networks have been an intensive topic of recent research. The aim of this thesis is to develop techniques for exploiting their available gains at a reduced complexity. In this introductory chapter, we present an overview of the context of and motivation for this work, and outline the contributions proposed in this thesis.

1.1 Multi-antenna and Cooperative Communications

Since the invention of wireless telegraphy more than one century ago, wireless communication systems have experienced a tremendous growth and are becoming, nowadays, part of our daily life. The new wireless services increase the demand for higher data transmission rates, reliability, coverage and for a more efficient use of the limited electromagnetic spectrum. For wireless providers, the use of this spectrum have required a multi-billion dollar investment. Two important applications, that have been driving the development recently, are cellular and wireless local area networks. In Table 1.1, the data rates for different generations of wireless systems are shown [76]. It can be clearly observed that there has been a tremendous increase in the data rates, that has strongly motivated rapid advancements of wireless communication systems.

Transmissions over wireless channels experience random time-varying attenuation effects, as they are based on the propagation of electromagnetic waves over the

System Generation	Standard Examples	Data rates
1G	TACS, AMPS, C-NETZ	-
2G	GSM, D-AMPS, PDC	13 Kbps
2.5G	GPRS, EDGE	up to 171 Kbps
3G	UMTS, CDMA2000	384Kbps-2Mbps
Beyond 3G	HSPA, LTE, WiMAX	3.6-150Mbps

Table 1.1: Data rates for different generations of wireless systems

air. Due to the limitations in the transmitted power and the expensive electromagnetic spectrum, different communication paradigms have been explored to improve the transmission quality and increase the transmission rate. *Multiple-input-multiple-output* (MIMO) antenna communications have emerged as one of the most significant developments in this field.

The key feature behind MIMO communication systems is their ability to turn the multipath propagation, provided by the multiple antennas, into a benefit for the user and, therefore, to offer improvements of many orders of magnitude in the system performance, at no extra cost for the spectrum or transmitted power [27]. A fundamental approach to obtain these improvements is space-time signal processing in which the time is complemented with the spatial dimension inherent in the use of multiple spatially distributed antennas.

In order to establish fundamental limits on information transmission for MIMO systems, information theory tools can be used. Since the introduction of the concept of capacity by Shannon in 1948 [80], the information theory has further advanced to establish theoretical limits on multi-antenna information transmission. In [23, 90], the capacity of multi-antenna fading channels was first computed. The results of these studies have shown significant gains in the information rate using multi-antenna transceivers, where the *multiplexing gain*[1] increases linearly with the minimum number of transmit and receive antennas. Aside from the channel capacity, a more practical performance criterion is the error probability. Considering the error probability at high signal-to-noise ratios (SNRs), the performance gain is dictated by the SNR exponent which is called the *diversity gain*. For multi-antenna

[1]The number of independent data streams that can be transmitted simultaneously [93].

channels, it has been shown that the diversity gain available is equal to the product of the number of receive and transmit antennas [88].

Space-Time Coding (STC) for MIMO systems has been proposed as an attractive technique which improves the downlink performance without any need for multiple antennas at the receiver and does not require any channel state information (CSI) at the transmitter. It can be combined with channel coding to provide additional gains. Furthermore, it has been shown to be advantageous for carrier synchronization [94] and robust against non-ideal operating conditions, such as antenna correlation and channel estimation errors at the receiver [87]. In a *space-time code*, the transmission of multiple independent copies of the data signal through different antennas is performed, so that the receiver can have higher probability of decoding the signal correctly. By characterizing the error probability, useful design criteria for space-time codes have been formulated in [88]. The use of STC has progressed in a short period of time from its invention to adoption in the major wireless standards, such as WCDMA, where the transmit diversity provided by space-time coding is used to increase the data rate from 100 Kbps to 384 Kbps [18].

MIMO systems can provide two main types of gains: the diversity and spatial multiplexing gains. Most of the recent research has been focussed on maximazing one of those gains. However, maximizing one type of gain may not necessarily lead to maximizing the other [103]. In [103], a simple characterization is obtained in which both gains can be simultaneously achieved with a *fundamental tradeoff*. This tradeoff can also be viewed as that between the transmission rate and the error probability. The work in [103] has motivated the quest for new space-time coding schemes that enjoy the maximum achievable gains within the *diversity-multiplexing tradeoff*. Besides the optimal diversity-multiplexing gain (DMG) tradeoff benefit, space-time codes are desired to have low complexity to enable fast signal processing in small or cost-limited devices. Recently, space-time codes achieving the optimal DMG have been proposed. However, their decoding complexity is rather high.

Although MIMO systems can provide significant gains in fading channels, the use of multi-antenna transceivers may not be practical in certain scenarios where severe restrictions in size and hardware cost can make the implementation difficult. Fortunately, in wireless networks with multiple single-antenna users, a virtual MIMO channel can be created by sharing the resources of different users to convey the infor-

mation over the network. Each cooperating user, that works as a *relay*, provides an independent path for the transmitted signal. This results in the so-called *cooperative diversity* that can be a good alternative to using multiple antennas at the transmitter and/or receiver. The use of cooperative communications offers interesting tradeoffs in code rates and transmit powers with respect to the single-user non-cooperative transmission. Several studies have demonstrated that user cooperation results in a substantial benefit for the transmission [60]. The performance advantages achieved by the cooperative approach make it very attractive for adoption in future standards. For example, the IEEE 802.16's Relay Task Group is currently working on the extension of mobile WiMAX standard using multihop relay transmission [38].

The basic ideas of cooperative communications were presented in [9] where the capacity of the three-node network, in which one node works as relay in between the transmitter and receiver nodes, was analyzed. Later papers studied the capacity of wireless relay networks and established some basic results in this field, see [25, 48] and references therein. Several cooperative strategies have been developed to exploit the potential gains available in relay networks. Two important examples of these signaling methods are *decode-and-forward* (DF) [77, 78] and *amplify-and-forward* (AF) [49] strategies. In the first method, the signal received at the relays is decoded to recover the information signal and then processed and retransmitted to the receiver. In the second method, the noisy signal received by the relays is amplified and retransmitted to the destination, as the name implies. Both methods use the *half-duplex* mode under which the relays cannot transmit and receive at the same time.

As a counterpart of the standard (centralized) STC in the MIMO system case, the use of *distributed space-time coding* (DSTC) has been proposed for wireless relay networks [50] without any CSI available at either the source or the relays. It has been shown that DSTC can achieve the full diversity gain available in the network (which is equivalent to the number of cooperating nodes). For the AF relay network, DSTC schemes can be derived from the standard MIMO space-time codes [40]. However, certain additional constraints need to be satisfied in the distributed setup. Furthermore, cooperative transmission techniques can modify the structure of the code at the receiver, resulting in a higher decoding complexity. For example, the simple maximum likelihood (ML) decoding complexity of orthogonal space-time

block codes (OSTBCs) is no longer possible when more than two relays are used [41]. As in the case of STC, the decoding complexity becomes prohibitively high for large number of relays. Therefore, an important issue for future cooperative relay networks is to develop distributed coding schemes with a moderate complexity, especially in scenarios where the size and cost restrictions prevent us from using multi-antenna transceivers.

Since the cooperative nodes are generally geographically distributed in a certain wide area, the source-to-relay and relay-to-destination channels can have significant differences in statistics and statistical quality. However, current DSTC approaches do not consider these differences that can be used to improve the performance.

1.2 Thesis Overview and Contributions

In this thesis, new low-complexity STC techniques for wireless communication systems are proposed. In Chapter 3, we develop new space-time codes that achieve a substantially improved performance-to-complexity tradeoff as compared to the current state-of-the-art space-time block codes (STBCs). Chapter 4 proposes a novel low-rate feedback based DSTC approach for cooperative transmission in relay networks that enjoys a low-complexity linear ML decoder and avoids long decoding delays while achieving the maximum diversity.

The outline for the remainder of the thesis is as follows:

Chapter 2: Theoretical Background.
In this chapter, the basics of wireless channels, multi-antenna systems and wireless relay networks are presented.

Chapter 3: STBCs with Fast ML Decoding.
OSTBCs represent an attractive choice of STCs because of their simple ML decoding and full diversity property. However, the code orthogonality property limits their achievable transmission rate. New full-diversity linear dispersion STBCs are designed by augmenting the generator of the lattice of the OSTBCs and optimizing it according to the criterion of the maximal worst codeword difference determinant. Because of the internal OSTBC structure of the proposed designs, the ML decoder can be implemented in a fast way. The full-rate 2×2 proposed STBC is proved to satisfy the non-vanishing determinant property and, therefore, to achieve the

optimal DMG tradeoff. The performances of our new STBCs are shown to be comparable to that of the best STBCs known so far. At the same time, the proposed STBCs offer a substantially reduced computational complexity of ML decoding.

Chapter 3 is based on one journal publication:

- J. Paredes, A. B. Gershman, and M. Gharavi-Alkhansari, "A new full-rate full-diversity space-time block code with non-vanishing determinants and simplified maximum likelihood decoding," *IEEE Trans. Signal Processing*, vol. 56, pp. 2461–2469, June 2008.

and two conference publications:

- J. Paredes, A. B. Gershman, and M. Gharavi-Alkhansari, "A 2x2 space-time code with non-vanashing determinants and fast maximum likelihood decoding," in *Proc. IEEE Int. Conference on Acoustics, Speech and Signal Processing (ICASSP)*, Honolulu, Hawaii, USA, April 2007, pp. 877–880.

- J. Paredes and A. B. Gershman, "High-rate space-time block codes with fast maximum-likelihood decoding," in *Proc. IEEE Int. Conference on Acoustics, Speech and Signal Processing (ICASSP)*, Las Vegas, Nevada, USA, April 2008, pp. 2385–2388.

Chapter 4: Distributed space-time coding with low-rate feedback in relay networks.

In this chapter, we propose a simple low-rate feedback based approach to achieve maximum diversity with a low decoding and implementation complexity in space-time coded wireless relay networks. To further improve the performance of the proposed scheme, the knowledge of the second-order channel statistics is exploited to design long-term power control coefficients through maximizing the receiver SNR with appropriate constraints. The maximization problem can be approximated by a convex feasibility problem whose solution is shown to be close to the optimal one in terms of the error probability. Subsequently, to provide robustness against feedback errors and further decrease the feedback rate, the use of an extended version of the distributed Alamouti code is proposed. It is also shown that using differential transmission, our scheme can be generalized to wireless relay networks without CSI

at the receiver. The improvements in system performance for different scenarios are demonstrated through computer simulations.

Chapter 4 is based on one journal submission:

- J. M. Paredes, B. H. Khalaj, and A. B. Gershman, "Cooperative transmission for wireless relay networks using low-rate feedback," *IEEE Trans. Signal Processing*, Feb. 2009, submitted.

and two conference publications:

- J. M. Paredes, B. H. Khalaj, and A. B. Gershman, "Using orthogonal designs with feedback in wireless relay networks," in *Proc. 9th IEEE Workshop on Signal Processing Advances in Wireless Communications (SPAWC)*, Recife, Brazil, July 2008, pp. 61–65.

- J. M. Paredes, B. H. Khalaj, and A. B. Gershman, "A differential cooperative transmission scheme with low rate feedback," in *Proc. IEEE Int. Conference on Acoustics, Speech and Signal Processing (ICASSP)*, Taipei, Taiwan, April 2009.

Chapter 5: concluding remarks are summarized in this chapter.

Chapter 2

Theoretical Background

2.1 Wireless Channel

In a typical wireless communication system, the transmission of a banwidth-limited signal occurs around a center frequency. Before up-converting the signal to the carrier frequency at the transmitter, the processing is performed in the baseband. At the receiver, down-conversion of the signal is done before further processing is conducted. Therefore, the baseband equivalent model can be used to replace the bandpass signal representation [31], resulting in a much simpler analysis that retains the essence of the process. In what follows, complex-valued baseband signal models are used. As we assume that the signals are band-limited, the discrete-time baseband model can be used to represent the continuous signal by taking the traditional approach based on the sampling theorem [31].

Signal variations in a wireless channel can be mainly classified into two categories: *large-scale fading* and *small-scale fading*. The former refers to variations in the channel produced by the signal path loss which depends on the distance from the transmitter to the receiver and shadowing by large obstacles between them. The small-scale fading takes into account the interference of the multiple signal paths between both terminals [93].

The effect of fading can be modeled as a linear time-varying system with the following discrete-time baseband input/output relation [93]:

$$y(t) = \sum_{l=1}^{L} h_l(t)x(t-l) + v(t) \tag{2.1}$$

where $y(t)$ is the received signal, $h_l(t)$ is the lth complex channel tap impulse response coefficient, L is the total number of channel taps, $x(t)$ is the transmitted signal, $v(t)$ is the additive noise and t is the discrete time. A very common assumption for most communication systems is to consider $v(t)$ as a circular symmetric complex white Gaussian noise with the probability density function (pdf) $\mathcal{CN}(0, \sigma_v^2)$, where $\mathcal{CN}(\cdot, \cdot)$ stands for the complex Gaussian pdf and σ_v^2 is the noise variance. The latter assumption means essentially that the primary source of noise is at the receiver.

In (2.1), two important effects of fading can be observed:

- **Frequency selectivity:** this effect is characterized by the *delay spread* which is defined as the difference between the longest and shortest path where only paths with a significant energy are taking into account. Equivalently, it can be characterized by the *coherence bandwith* which is the inverse of the delay spread. A fading channel is said to be *frequency selective* if the coherence bandwith is comparable or less than the signal bandwidth, or, equivalently, when the delay spread is comparable or larger than the symbol duration. The channel acts in this case as a finite impulse response (FIR) filter. Otherwise the fading channel is said to be *frequency flat*.

- **Time selectivity:** this effect is characterized by the *coherence time* which is defined as the interval of time over which $h_l(t)$ changes significantly as a function of t. Equivalently, it can be characterized by the *Doppler spread* which is the inverse of the coherence time.

In this work, we assumed that the symbol duration is much larger than the channel delay spread and therefore, the channel is frequency flat. From (2.1), we obtain in this case that

$$y(t) = h(t)x(t) + v(t) \tag{2.2}$$

where the index l was dropped.

It is further assumed that the coherence time is large enough to consider the channel as constant during an interval of T symbols ($h_i = h(iT + 1) = \cdots = h(iT + T)$). Then, we have from (2.2) that

$$y(t) = h_i x(t) + v(t) \tag{2.3}$$

for $t = iT + 1, \ldots, (i+1)T$ and $i \geq 0$. Without any loss of generality, we will consider only one interval of T symbols and drop the index i from now on.

To characterize h statistically, we are based on the following assumptions [93]:

A1) There is a large number of statistically independent reflected and scattered paths with random amplitudes.

A2) The carrier wavelength is much less than the distance travelled by the paths, so that the phases of different paths are independent and uniformly distributed.

Using the previous assumptions, the channel can be modeled in either of two ways:

- **Rayleigh fading:** the channel is zero-mean circular symmetric complex Gaussian with the pdf $\mathcal{CN}(0, \sigma_h^2)$, where σ_h^2 is the variance. Note that each channel coefficient is the sum of many paths and therefore, the Central Limit Theorem can be applied. The magnitude $|h|$ is a *Rayleigh* random variable with the pdf

$$p_{|h|}(z) = \frac{z}{\sigma_h^2} e^{-\frac{z^2}{2\sigma_h^2}}, \quad z \geq 0 \tag{2.4}$$

  where $|\cdot|$ stands for the absolute value.

- **Rician fading:** if the line-of-sight (LOS) path is significant, then the channel coefficient has the pdf $\mathcal{CN}(\mu_h, \sigma_h^2)$, where μ_h is the channel mean. The magnitude $|h|$ is a *Rician* random variable with the pdf

$$p_{|h|}(z) = \frac{z}{\sigma_h^2} e^{-\frac{|h|^2+|\mu_h|^2}{2\sigma_h^2}} I_0\left(\frac{|h\,\mu_h|}{\sigma_h^2}\right), \quad z \geq 0 \tag{2.5}$$

  where $I_0(\cdot)$ denotes the modified zero-order Bessel function of the first kind.

The use of diversity techniques is one way to exploit the effects of random channel variations to improve the communication performance. This technique consists of transmitting different replicas of the same information over different random channels which fade independently. Three important diversity techniques are:

- **Time diversity**: the same information is transmitted at different time instants (in different coherence periods).

- **Frequency diversity**: the same information is transmitted in different frequency bands.

- **Space diversity**: the same information is transmitted/received using multiple antennas as it is explained in the next section.

The maximum information rate that can be reliably transmitted (with an arbitrary low error probability) over a communication channel is called the *channel capacity*. The capacity of a complex-valued channel, normalized by the bandwidth, is given by [93]

$$C = \log(1 + \mathrm{SNR}) \tag{2.6}$$

in nats per channel use where log is the natural logarithm. The capacity is given in bits per channel use (bpcu) if the binary logarithm ($\log_2$) is used in (2.6).

2.2 MIMO Systems

Let us consider a system with multiple antennas at the receiver and the transmitter. Fig. 2.1 shows a MIMO channel with N_t transmit and N_r receive antennas where we have focused only on one symbol interval and dropped the time index. Prior to the transmitter block in Fig. 2.1, a stream of binary data is mapped onto complex symbols and K symbols s_k are fed into the transmitter. The transmitter encodes these K symbols into the transmitted signals $\{x_1(t), \ldots, x_{N_t}(t)\}$ that are mapped onto multiple antennas. After the frequency conversion, filtering and amplification are performed, the signals are transmitted through the channel.

At the receiver, the signals are captured by the N_r antennas and the frequency down-conversion, filtering and sampling is performed to obtain $\{y_1(t), \ldots, y_{N_r}(t)\}$. After decoding the received signals, the estimated symbols $\{\hat{s}_1, \ldots, \hat{s}_K\}$ are demodulated and demapped to recover the data.

In Fig. 2.1, we denote the complex baseband channel gains between the nth transmit antenna and the mth receive antenna as $h_{m,n}$, $m = 1, \ldots, N_r$; $n = 1, \ldots, N_t$. The received signal at the mth antenna can be expressed as

$$y_m(t) = \sum_{n=1}^{N_t} h_{m,n} x_n(t) + v_m(t), \quad m = 1, \ldots, N_r \tag{2.7}$$

where $v_m(t)$ is the noise. The channels $h_{m,n}$ are modelled to be statistically independent, as typically a rich local scattering at the receiver and the transmitter is

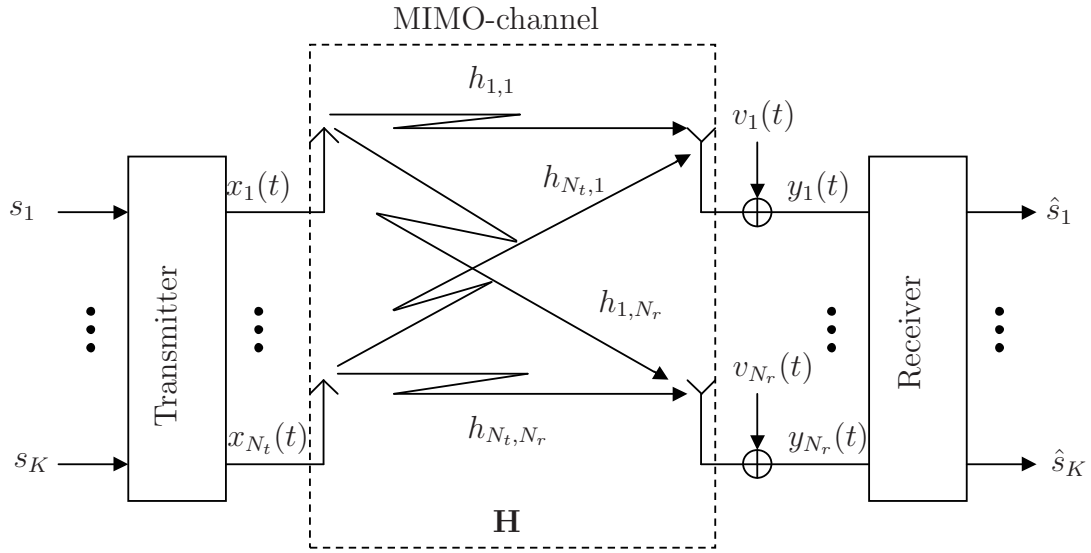

Figure 2.1: Model of the data transmission in a MIMO system with K symbols, N_t transmit and N_r receive antennas.

assumed. By stacking each received signal in a vector, we can express (2.7) as

$$\mathbf{y}(t) = \mathbf{H}\mathbf{x}(t) + \mathbf{v}(t) \tag{2.8}$$

where

$$\mathbf{y}(t) = [y_1(t), \ldots, y_{N_r}(t)]^T \tag{2.9}$$

$$\mathbf{x}(t) = [x_1(t), \ldots, x_{N_t}(t)]^T \tag{2.10}$$

$$\mathbf{v}(t) = [v_1(t), \ldots, v_{N_r}(t)]^T \tag{2.11}$$

$$[\mathbf{H}]_{m,n} = h_{m,n} \tag{2.12}$$

$(\cdot)^T$ is the transpose of a matrix and $[\cdot]_{m,n}$ denotes the entry corresponding to the mth row and the nth column of a matrix.

For the receiver with the known CSI and Rayleigh fading, it can be shown that the MIMO channel capacity at high SNRs is approximately given by

$$C \approx \min\{N_t, N_r\} \log(\text{SNR}) \tag{2.13}$$

where $\min\{a, b\}$ stands for the minimum number between a and b. This means that, with respect to the single-input single-output (SISO) channel capacity, in the case of multiple antennas we obtain a multiplexing gain equal to $\min\{N_t, N_r\}$.

As we assumed that the channel gains remain constant during the length of T channel uses and change independently after that (*block fading*), we can stack T subsequent vectors of (2.8) into matrices and express the input-output relation of the MIMO channel as [88]

$$\mathbf{Y} = \mathbf{H}\mathbf{X} + \mathbf{V} \tag{2.14}$$

where

$$\mathbf{X} = [\mathbf{x}(1), \ldots, \mathbf{x}(T)] \tag{2.15}$$

is the $N_t \times T$ complex matrix of the transmitted signals,

$$\mathbf{V} = [\mathbf{v}(1), \ldots, \mathbf{v}(T)] \tag{2.16}$$

is the $N_r \times T$ complex noise matrix, and

$$\mathbf{Y} = [\mathbf{y}(1), \ldots, \mathbf{y}(T)] \tag{2.17}$$

is the $N_r \times T$ complex matrix of the received signals. The matrix $\mathbf{X}$ is called *space-time code* and is a function of the transmitted symbols.

To design space-time codes, the pairwise error probability $P(\mathbf{X}, \mathbf{X}')$ that the decoder selects an erroneous $\mathbf{X}'$ when the transmitted matrix was in fact $\mathbf{X}$ has been studied in [88] for the ML decoder in (2.14). Two important design criteria for $\mathbf{X}$ were formulated as a result of this study for the high SNR case [88]:

- **Rank criterion:** maximize the minimum rank of $(\mathbf{X} - \mathbf{X}')$ over all pairs of distinct code matrices.
- **Determinant criterion:** maximize the minimum product of the eigenvalues different from zero of the matrix $(\mathbf{X} - \mathbf{X}')$ along the pairs of distinct code matrices with the minimum rank.

Using these criteria, it can be shown that the maximum diversity order that can be obtained in a space-time coded MIMO channel is equal to $N_t N_r$.

A popular choice of $\mathbf{X}$ are the OSTBCs proposed in [3, 86]. They achieve the full diversity with a very low ML decoding complexity. Any $\mathbf{X}$ is said to be an OSTBC [86] if its entries are given by linear combinations of the symbols s_k and their complex conjugates, and for any arbitrary $\mathbf{s}$, it satisfies

$$\mathbf{X}\mathbf{X}^H = \|\mathbf{s}\|^2 \mathbf{I}_{N_t} \tag{2.18}$$

where $\mathbf{I}_{N_t}$ is the $N_t \times N_t$ identity matrix and $(\cdot)^H$ and $\|\cdot\|$ denote the Hermitian transpose and the Euclidean norm, respectively. This property enables a simple symbol-by-symbol ML decoding, i.e., the symbols can be decoded per real dimension independently of each other. The *Alamouti code* was the first OSTBC proposed in the literature [3] for a system with $N_t = 2$ transmit antennas. The code matrix of the Alamouti code is given by

$$\mathbf{X} = \begin{bmatrix} s_1 & -s_2^* \\ s_2 & s_1^* \end{bmatrix} \tag{2.19}$$

where $(\cdot)^*$ stands for the complex conjugate. Despite the advantages in diversity and decoding, the symbol rate of the OSTBCs decreases as a function of N_t [53] and the capacity of the MIMO channel is only achievable in the case of $N_t = 2$ and $N_r = 1$ [75].

Another popular scheme is the *Vertical Bell Laboratories Layered Space-Time* (V-BLAST) technique presented in [96]. This scheme is full-rate and can achieve the MIMO channel capacity (maximum multiplexing gain). However, it does not have the full diversity. Throughout the manuscript, we will refer to a space-time code that can achieve the maximal rate of N_t symbols per channel use as a *full-rate* code.

A natural way to evaluate the performance of space-time codes is the outage probability, i.e. the probability that a certain transmission rate exceeds the channel capacity. This function characterizes, in essence, a tradeoff between the achievable data rate and the error probability. Using the outage probability analysis for the high SNR scenario, the DMG tradeoff of the MIMO channel was derived in [103]. If the achievable rate for a scheme at high SNR grows as $r \log(\mathrm{SNR})$, where r is the multiplexing gain, and its diversity gain for this r is $d(r)$, then the DMG tradeoff of the i.i.d. Rayleigh flat-fading MIMO channel is given by

$$d_{\mathrm{opt}}(r) = (N_t - r)(N_r - r) \tag{2.20}$$

where $d_{\mathrm{opt}}(r)$ is the maximum $d(r)$ that can be obtained. It can be viewed as if r transmit and r receive antennas were dedicated to multiplexing and $(N_t - r)$ transmit and $(N_r - r)$ receive antennas were providing the diversity [103].

Many full-rate and full-diversity space-time code schemes have been proposed in the literature [11, 20, 21, 33, 36, 55, 61, 79, 102]. However, most of them do not

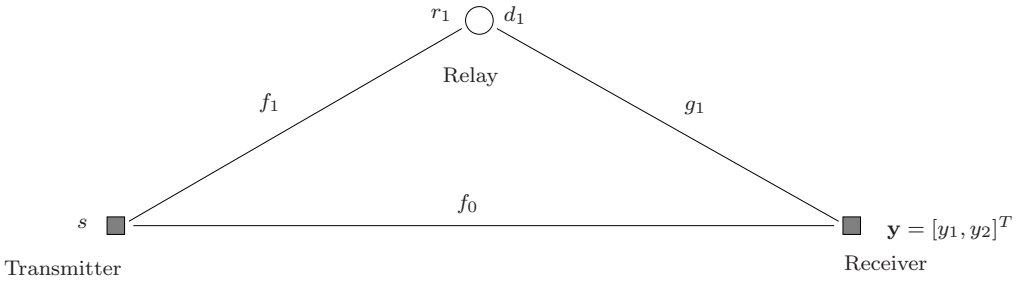

Figure 2.2: Wireless relay network with 3 nodes.

achieve the optimal DMG tradeoff. Recently, a criterion to achieve the optimal DMG tradeoff for any fading distribution was derived in [20, 89]:

- **Non-vanishing determinants (NVD):** the minimum determinant of the matrix $(\mathbf{X} - \mathbf{X}')$ over all pairs of code matrices in a full-rate code should be lower bounded by a positive constant greater than zero for any constellation size and for $N_r \geq N_t$.

An important example of a space-time code for $N_t = 2$ achieving the NVD property is the *Golden code* [7, 17]. Its space-time code matrix is given by:

$$\mathbf{X} = \frac{1}{\sqrt{5}} \begin{bmatrix} \alpha\left(s_1 + s_2\theta\right) & \alpha\left(s_3 + s_4\theta\right) \\ \mathrm{j}\overline{\alpha}\left(s_3 + s_4\overline{\theta}\right) & \overline{\alpha}\left(s_1 + s_2\overline{\theta}\right) \end{bmatrix} \tag{2.21}$$

where $\theta = \frac{1+\sqrt{5}}{2}$, $\overline{\theta} = 1 - \theta$, $\alpha = 1 - \mathrm{j} - \mathrm{j}\theta$, $\overline{\alpha} = 1 + \mathrm{j} + \mathrm{j}\overline{\theta}$ and $\mathrm{j} = \sqrt{-1}$. Although this code achieves the optimal DMG tradeoff, its ML decoding complexity is rather high, as all the symbols should be decoded jointly.

2.3 Wireless Relay Networks

In the case when the use of multi-antenna transceivers is no longer possible due to limitations in power, cost or space, the use of single-antenna nodes in a wireless network as relays can provide gains similar to that achieved in MIMO systems. One simple example of a wireless relay network with three single-antenna nodes is depicted in Fig. 2.2.

In this figure, the channels between the transmitter and the relay, between the transmitter and the receiver and between the relay and the receiver are denoted as

f_1, f_0 and g_1, respectively. Let us consider a half-duplex mode. In the first step of the transmission, the source transmits the signal $\sqrt{P_0}s$ to both the relay and destination nodes with the average transmit power P_0. In this step, the received signals r_1 at the relay and y_1 at the destination are given by

$$r_1 = \sqrt{P_0} f_1 s + v, \qquad y_1 = \sqrt{P_0} f_0 s + w_1 \tag{2.22}$$

where v and w_1 are the noises at the relay and destination, respectively. In the second step, the relay needs to process its receive signal r_1 to obtain the transmitted signal d_1. Then, the relay and the source transmit to the destination the signals $\sqrt{P_1}d_1$ and $\sqrt{P_0}s$, respectively. In the second step, the received signal at the destination is given by

$$y_2 = \sqrt{P_0} f_0 s + \sqrt{P_1} g_1 d_1 + w_2 \tag{2.23}$$

where P_1 is the average transmit power at the relay and w_2 denotes the noise at the destination in the second step.

There are two main strategies for the processing of the signal r_1 at the relay:

- **DF strategy:** the symbol s is decoded at the relay, and its estimate $\hat{s}$ is transmitted to the destination, i.e. $d_1 = \hat{s}$.

- **AF strategy:** as its name implies, the received signal is only amplified and transmitted to the destination, i.e. $d_1 = \gamma_1 r_1 = \gamma_1(\sqrt{P_0} f_1 s + v)$, where γ_1 is the relay weight. Note that in this case, a noisy copy of the signal is transmitted from the relay.

In this thesis, we only consider the AF strategy as its implementation does not require any advanced signal processing at the relays, and, therefore, it is much simpler than that of the DF strategy. As the relay has a limited average transmit power, the relay weight γ_1 should be chosen such that the average transmit power is P_1. Therefore, γ_1 can be chosen either as:

$$\gamma_1 = \frac{1}{\sqrt{P_0 |f_1|^2 + \sigma_v^2}} \tag{2.24}$$

or as

$$\gamma_1 = \frac{1}{\sqrt{P_0 \mathrm{E}\{|f_1|^2\} + \sigma_v^2}} \tag{2.25}$$

where $\mathrm{E}\{\cdot\}$ and σ_v^2 are the statistical expectation and variance of v, respectively. The first option requires to perform channel estimation at the relay while the second one only requires the knowledge of the received signal power at the relay. Therefore, the second option is more attractive due to its simpler implementation.

Using the AF strategy, the received signal vector $\mathbf{y}$ at the destination is given by

$$\mathbf{y} = \begin{bmatrix} \sqrt{P_0} f_0 \\ \sqrt{P_0} f_0 + \gamma_1 \sqrt{P_0 P_1} f_1 g_1 \end{bmatrix} s + \begin{bmatrix} w_1 \\ \gamma_1 \sqrt{P_1} g_1 v + w_2 \end{bmatrix}. \tag{2.26}$$

An important assumption used here is that the system is synchronized at the symbol level. Clearly, (2.26) resembles a multiple antenna system with $N_t = 2$ and $N_r = 1$. Therefore, schemes proposed for MIMO channels can be applied to wireless relay networks but additional constraints on the relay transmissions should be taken into account. For example, in the case of no CSI at the transmitter, space-time codes can be applied in a distributed fashion to AF wireless relay networks. However, the ML decoding complexity and the decoding delay of these schemes increase rapidly with the number of relays. Furthermore, in the case of OSTBCs and more than 2 relays, the linear ML decoding complexity is no longer possible [41]. On the other hand, distributed beamforming techniques that exploit CSI at the transmitter and feedback links to the relays are difficult to implement.

Chapter 3

STBCs with Fast ML Decoding

In this chapter, we propose new full-diversity high-rate space-time codes with a low decoding complexity [63–65].

3.1 Motivation and Preliminary Work

The design of high-performance high-rate space-time codes has been a problem of a great interest and several recent approaches have been developed to obtain such codes. For systems with a coherent decoder (where the complete CSI is known at the receiver), the rank and determinant criteria for the code construction have been proposed in [88] where several space-time trellis codes have been designed. Even though the performance of the latter codes is high, their ML decoding is a numerically difficult task. OSTBCs [3, 86] are able to achieve full-diversity at a low (symbol-by-symbol) ML decoder complexity. However, OSTBCs cannot achieve the ergodic MIMO channel capacity except for the case of two transmit and one receive antennas [75] and their achievable rate is severely limited by the code orthogonality property [53, 95].

To overcome this drawback while retaining low decoding complexity, quasi-orthogonal STBCs (QOSTBCs) have been proposed in [39, 62, 92]. The latter codes achieve higher rates than OSTBCs but at the price of losing the full diversity property. However, the full diversity property of QOSTBCs can be recovered by using symbol rotation [81, 85, 91].

Several other approaches to design space-time codes achieving a rate of one

symbol per channel use and full-diversity for any number of transmit antennas have been proposed, see for example [10,79,98,99] and references therein. However, these space-time codes have a higher or similar ML decoder complexity in comparison to the QOSTBCs.

Recently, several code designs that achieve the full rate and, at the same time, capture full diversity (or a significant portion of the available diversity) have been proposed in the literature; see [11, 20, 21, 29, 33, 36, 55, 61, 82, 102] and references therein. Although rate-one space-time codes can be obtained from designs that achieve full rate, as their originating codes, they have a higher decoding complexity than the QOSTBCs.

In [15, 45, 97, 101], rate-one space-time codes with a lower ML decoding complexity than that of the standard QOSTBCs have been proposed. They are called four-group decodable space-time codes because the ML decoder can separate the decoding task in four groups of real symbols. In the case of four transmit antennas, for instance, the receiver only needs to decode 2 real symbols jointly for each complex symbol transmitted.

In [103], a characterization of the spatial diversity and multiplexing gains in MIMO channels has been studied, and a fundamental tradeoff between these two gains has been found. This has provided a strong motivation to seek for space-time codes that can achieve the optimal DMG tradeoff. The first explicit approach to design space-time codes that achieve this tradeoff has been developed in [100]. Recently, a sufficient condition for a space-time code to achieve the optimal DMG tradeoff (i.e., to be *approximately universal*) for a MIMO channel with an arbitrary fading has been obtained in [89]. This condition implies that for achieving this tradeoff, it is sufficient that a STBC satisfies the so-called non-vanishing determinant (NVD) property, provided that the number of receive antennas is greater or equal than the number of transmit antennas [89]. Apart from achieving the optimal DMG tradeoff, an important advantage of codes that satisfy the NVD property is that their coding gain remains constant when increasing the constellation size.

There have been several powerful approaches to design STBCs that satisfy the NVD property [7, 17, 20, 46, 61, 100]. One of them, the Golden code [7], has been already included in the 2005 IEEE 802.16e standard [37]. Unfortunately, the ML decoding of these codes may be prohibitively expensive as they use a computationally

demanding sphere decoding (SD) technique [1, 12, 22, 71]. Therefore, the design of full-rate full-diversity space-time codes satisfying the NVD property and having a reduced decoding complexity remains an important open problem.

One strategy to lower the complexity is to use sub-optimal decoding schemes. Although such schemes can achieve linear complexity in the number of variables, they usually suffer a significant reduction in performance [12].

In [36], a design of higher-rate codes using the OSTBC structure was proposed. The authors in [36], however, did not consider the fast decoding properties that can result in a simplified SD and the DMG tradeoff optimality. Furthermore, their code design strategy is different from that presented in this chapter.

3.2 System Model

Let us consider a MIMO system with N_r receive and N_t transmit antennas, see Section 2.2. We assume that the antennas are well separated and there is a large number of scatters so that we can model the channel coefficients as i.i.d. random variables with the pdf $\mathcal{CN}(0,1)$. Furthermore, let us use the block flat-fading and noise assumptions discussed in Section 2.2 and use the signal model (2.14)

$$\mathbf{Y} = \mathbf{H}\mathbf{X} + \mathbf{V} \tag{3.1}$$

where $\mathbf{X}$ is the $N_t \times T$ complex matrix of the transmitted signals, $\mathbf{H}$ is $N_r \times N_t$ complex channel matrix, $\mathbf{V}$ is the $N_r \times T$ complex noise matrix, and $\mathbf{Y}$ is the $N_r \times T$ complex matrix of the received signals.

We assume that the K symbols s_k are drawn from a M-QAM constellation $\bar{\mathcal{S}}$ and encoded in a linear fashion to form the matrix $\mathbf{X}$ as [29]

$$\mathbf{X} = \sum_{k=1}^{K} (\mathrm{Re}\{s_k\}\,\mathbf{C}_{2k-1} + \mathrm{Im}\{s_k\}\,\mathbf{C}_{2k}) \tag{3.2}$$

where $\mathrm{Re}\{\cdot\}$ and $\mathrm{Im}\{\cdot\}$ denote the real and imaginary parts, respectively, while $\{\mathbf{C}_k\}_{k=1}^{2K}$ is a set of complex $N_t \times T$ code-specific matrices that are subject to the following energy constraint

$$\sum_{k=1}^{2K} \mathrm{tr}(\mathbf{C}_k^H \mathbf{C}_k) = 2TN_t\,. \tag{3.3}$$

Here tr(·) stands for the trace of a matrix. Since $\mathbf{X}$ is a function of the symbol vector

$$\mathbf{s} \triangleq [s_1 \dots s_K]^T \tag{3.4}$$

we will also often refer to $\mathbf{X}$ as $\mathbf{X}(\mathbf{s})$.

The matrix $\mathbf{X}$ belongs to the transmit codebook

$$\mathcal{X} \triangleq \{\mathbf{X}_1, \dots, \mathbf{X}_L\} \tag{3.5}$$

of cardinality $L = M^K$ where all the members of (3.5) are distinct and equi-probable. Therefore the transmission rate is

$$R = \frac{\log_2 L}{T} \quad \text{(bpcu)}. \tag{3.6}$$

From (3.1), it is clear that, conditioned on $\mathbf{H}$, the signal codebook at the receiver is

$$\mathcal{Y} \triangleq \{\mathbf{Y}_1, \dots, \mathbf{Y}_L\} \tag{3.7}$$

where

$$\mathbf{Y}_l = \mathbf{H}\mathbf{X}_l, \qquad l = 1, 2, \dots, L. \tag{3.8}$$

For any received signal matrix $\mathbf{Y}$, the coherent ML decoder finds [28]

$$l_{\text{opt}} = \arg \min_{\mathbf{Y}_l \in \mathcal{Y}} \|\mathbf{Y} - \mathbf{Y}_l\|_F \tag{3.9}$$

where $\|\cdot\|_F$ denotes the Frobenius norm.

For any $I \times J$ matrix $\mathbf{Z}$, let us define the "underline" operator which transforms this matrix into a $2IJ \times 1$ real column vector as follows

$$\begin{aligned}\underline{\mathbf{Z}} \triangleq [&\operatorname{Re}\{Z_{11}\}, \operatorname{Im}\{Z_{11}\}, \operatorname{Re}\{Z_{21}\}, \operatorname{Im}\{Z_{21}\}, \\ &\dots, \operatorname{Re}\{Z_{IJ}\}, \operatorname{Im}\{Z_{IJ}\}]^T.\end{aligned} \tag{3.10}$$

Note that this operator is a one-to-one function from $\mathbb{C}^{I\times J}$ onto $\mathbb{R}^{2IJ\times 1}$, where $\mathbb{C}$ and $\mathbb{R}$ are the sets of complex and real numbers, respectively. We will refer to $\underline{\mathbf{Z}}$ as the underlined version of $\mathbf{Z}$. Similarly, if $\mathcal{Z}$ is a set of matrices $\mathbf{Z}_1, \mathbf{Z}_2, \dots, \mathbf{Z}_n$ each of size $I \times J$, then we define

$$\underline{\mathcal{Z}} \triangleq \{\underline{\mathbf{Z}_1}, \underline{\mathbf{Z}_2}, \dots, \underline{\mathbf{Z}_n}\} \tag{3.11}$$

and refer to $\underline{\mathcal{Z}}$ as the underlined version of $\mathcal{Z}$. Similarly, we can define

$$\underline{\mathcal{X}} \triangleq \left\{\underline{\mathbf{X}}_1, \ldots, \underline{\mathbf{X}}_L\right\} \tag{3.12}$$

$$\underline{\mathcal{Y}} \triangleq \left\{\underline{\mathbf{Y}}_1, \ldots, \underline{\mathbf{Y}}_L\right\}. \tag{3.13}$$

For any $I \times J$ matrix $\mathbf{Z}$, let us also define the operator $\mathrm{mat}_{I,J}(\cdot)$ such that

$$\mathrm{mat}_{I,J}(\underline{\mathbf{Z}}) = \mathbf{Z}. \tag{3.14}$$

Clearly, this operator is the inverse of the underline operator (3.10).

Applying the operator (3.10) to (3.1), the latter equation can be written as

$$\underline{\mathbf{Y}} = \mathbb{H}\underline{\mathbf{X}} + \underline{\mathbf{V}} \tag{3.15}$$

where (see Appendix 3.A)

$$\mathbb{H} \triangleq \frac{1}{2}\mathbf{I}_T \otimes \left(\mathbf{H} \otimes \mathbf{E} + \mathbf{H}^* \otimes \mathbf{E}^*\right), \tag{3.16}$$

$$\mathbf{E} \triangleq \begin{bmatrix} 1 & \mathrm{j} \\ -\mathrm{j} & 1 \end{bmatrix}. \tag{3.17}$$

Here, $\otimes$ denotes the Kronecker product.

It is obvious that for any complex matrix $\mathbf{Z}$,

$$\|\mathbf{Z}\|_F = \|\underline{\mathbf{Z}}\|. \tag{3.18}$$

Therefore, using (3.13) and (3.18), equation (3.9) can be written as

$$l_{\mathrm{opt}} = \arg \min_{\underline{\mathbf{Y}}_l \in \underline{\mathcal{Y}}} \|\underline{\mathbf{Y}} - \underline{\mathbf{Y}}_l\|. \tag{3.19}$$

Applying the operator (3.10) to $\mathbf{X}$ and using (3.2), we have

$$\underline{\mathbf{X}} = \mathbb{G}\underline{\mathbf{s}} \tag{3.20}$$

where the $2N_tT \times 2K$ real-valued code generator matrix can be defined as

$$\mathbb{G} \triangleq \left[\, \underline{\mathbf{C}}_1 \, \underline{\mathbf{C}}_2 \cdots \underline{\mathbf{C}}_{2K-1} \, \underline{\mathbf{C}}_{2K} \,\right] \tag{3.21}$$

and $\underline{\mathbf{s}}$ is the underlined version of the symbol vector.

The constraint in (3.3) is now equivalent to

$$\mathrm{tr}(\mathbb{G}^T\mathbb{G}) = 2N_tT. \tag{3.22}$$

In the most general case when $\mathcal{X}$ does not have any structure, the decoders (3.9) or (3.19) require an exhaustive search over the receive codebook which may be prohibitively expensive at large symbol constellation sizes (i.e., for large values of L). To reduce the computational cost of the decoder, (3.20) can be used to redefine $\underline{\mathcal{X}}$ as a finite lattice

$$\underline{\mathcal{X}} = \{\mathbb{G}\underline{\mathbf{s}} \,:\, \underline{\mathbf{s}} \in \underline{\mathcal{S}}\} \tag{3.23}$$

where $\underline{\mathcal{S}} \triangleq \{\underline{\mathbf{s}}_1, \ldots, \underline{\mathbf{s}}_L\}$ is the constellation of $\underline{\mathbf{s}}$.

We will refer to the columns of $\mathbb{G}$ as the *axes* of $\underline{\mathcal{X}}$ and to the number of axes as the *dimension* of the lattice. The lattice structure (3.23) $\underline{\mathcal{X}}$ translates into the following lattice structure for $\underline{\mathcal{Y}}$:

$$\underline{\mathcal{Y}} = \{\mathbb{H}\mathbb{G}\underline{\mathbf{s}} \,:\, \underline{\mathbf{s}} \in \underline{\mathcal{S}}\} \tag{3.24}$$

whose generator is $\mathbb{H}\mathbb{G}$. Using (3.24), the ML decoder in (3.19) can be expressed as

$$\hat{\underline{\mathbf{s}}} = \arg\min_{\underline{\mathbf{s}}_l \in \underline{\mathcal{S}}} \|\underline{\mathbf{Y}} - \mathbb{H}\mathbb{G}\underline{\mathbf{s}}_l\| \tag{3.25}$$

where $\hat{\underline{\mathbf{s}}} = \underline{\mathbf{s}}_{l_{\text{opt}}}$.

If $N_r T \geq K$ and $\mathbb{H}$ is full-rank, then (3.25) can be implemented using the SD [1] which in most cases is much more computationally efficient than the exhaustive search.

We will call a lattice *orthogonal* if the columns of its generator are orthogonal. If $\underline{\mathcal{Y}}$ is an orthogonal lattice, then the ML decoder (3.19) will reduce to a real symbol-by-symbol decoder which is much simpler than the SD. However, to make the lattice $\underline{\mathcal{Y}}$ orthogonal, it is not sufficient to simply choose $\underline{\mathcal{X}}$ to be orthogonal because the random channel matrix $\mathbf{H}$, in general, skews the lattice making $\underline{\mathcal{Y}}$ non-orthogonal.

3.3 Orthogonal Structure Based STBCs

First, we introduce the proposed code structure that gives the orthogonal structure based STBCs (OSB-STBCs) the fast ML decoding property. Based on this property, a simplified SD algorithm will be proposed for the OSB-STBCs. Subsequently, a full-rate STBC achieving the optimal DMG tradeoff for two transmit antennas will be presented. Finally, rate-one STBCs for three and four transmit antennas achieving full diversity are developed.

3.3.1 The Proposed Code Structure

If $\mathbf{X}$ in (3.1) were chosen to be an OSTBC, then $\underline{\mathcal{X}}$ would be an orthogonal lattice. According to the constellation space invariance property of OSTBCs [28], the orthogonality of the lattice $\underline{\mathcal{X}}$ remains *invariant* to the skewing effects of the channel, i.e., irrespective of the entries of $\mathbf{H}$ and, as long as $\|\mathbf{H}\|_F \neq 0$, the lattice $\underline{\mathcal{Y}}$ is orthogonal. Therefore, the coherent ML decoder can be implemented as a simple symbol-by-symbol decoder in the OSTBC case [28, 86].

To satisfy (2.18), any OSTBC $\mathbf{X}$ should fulfill the following conditions on the matrices $\mathbf{C}_k$ [24, 51]

$$\mathbf{C}_k\mathbf{C}_k^H = \frac{T}{K}\mathbf{I}_{N_t} \tag{3.26}$$

$$\mathbf{C}_k\mathbf{C}_p^H = -\mathbf{C}_p\mathbf{C}_k^H,\ k \neq p \tag{3.27}$$

for $k = 1, \ldots, 2K$ and $p = 1, \ldots, 2K$. It can be proved (see Appendix 3.B) that

$$\mathbb{G}_{\text{ostbc}}^T\mathbb{H}^T\mathbb{H}\mathbb{G}_{\text{ostbc}} = \|\mathbf{H}\|_F^2\mathbf{I}_{2K} \tag{3.28}$$

where $\mathbb{G}_{\text{ostbc}}$ is the OSTBC generator matrix.

In the proposed design, we are inspired by the constellation space invariance property of OSTBCs [28] which prompts us to select the axes of the lattice of our code to be in the direction of those of the OSTBC lattice as much as possible. The key idea of this selection is to simplify the decoding, as the axes from the OSTBC are "immune" to the skewing effects of the channel and preserve their orthogonality. We choose as many first axes of $\mathbb{G}$ as possible from a proper OSTBC (or equivalently, as many matrices $\mathbf{C}_k$ as possible from this OSTBC) so that K_o complex symbols are encoded. Doing so, we make sure that the corresponding axes of the lattice $\underline{\mathcal{Y}}$ are orthogonal at the decoder. The latter orthogonality property will be used to reduce the complexity of the ML decoder. Now, we add the rest of $2(K - K_o)$ linearly independent columns that are necessary to complete the matrix $\mathbb{G}$. Hence, $\mathbb{G}$ takes the form

$$\mathbb{G} = [\mathbb{G}_{\text{ostbc}}, \mathbb{G}_{\text{add}}] \tag{3.29}$$

where $\mathbb{G}_{\text{add}}$ is the $2N_tT \times 2(K - K_o)$ matrix containing extra-columns added to the code generator matrix to design OSB-STBCs.

We further constrain the columns added to $\mathbb{G}$ to be orthogonal to the original "OSTBC" columns of $\mathbb{G}$ and to each other. In the full-rate case ($N_tT = K$), it has

been shown that an orthogonal $\mathbb{G}$ is a sufficient and necessary condition for the code to be *information lossless* [6,102]. The information lossless property means that the space-time coded MIMO system can achieve the *capacity* and, therefore, the use of the STBC does not induce any information loss.

3.3.2 Full-Rate Full-Diversity OSB-STBC for 2 Transmit Antennas with Optimal DMG Tradeoff

Let us now apply our approach to designing a code for the case of $N_t = T = 2$ and $K = N_t T = 4$. Note that in this case, the code will have full rate at which no OSTBC exist. To design such a code, we should choose $2N_tT = 2K$ linearly independent columns of $\mathbb{G}$, and the particular choice of $\mathbb{G}$ will entirely determine the properties of the code. Using the approach presented in Sec. 3.3.1, we select the first columns for $\mathbb{G}$ from the generator matrix of the Alamouti's code [3] in our particular 2×2 case. As a result, the generator matrix of the designed code has the following form

$$\mathbb{G} = [\mathbb{G}_{\text{OSTBC}}\ \mathbf{g}_1\ \mathbf{g}_2\ \mathbf{g}_3\ \mathbf{g}_4] \tag{3.30}$$

where

$$\mathbb{G}_{\text{OSTBC}} = \frac{1}{\sqrt{2}} \begin{bmatrix} 1 & 0 & 0 & 0 \\ 0 & 1 & 0 & 0 \\ 0 & 0 & 1 & 0 \\ 0 & 0 & 0 & 1 \\ 0 & 0 & -1 & 0 \\ 0 & 0 & 0 & 1 \\ 1 & 0 & 0 & 0 \\ 0 & -1 & 0 & 0 \end{bmatrix} \tag{3.31}$$

is the generator matrix of the Alamouti's code, and $\mathbf{g}_k$ $(k = 1, 2, 3, 4)$ are the remaining columns of $\mathbb{G}$ that have to be chosen yet.

These remaining columns of $\mathbb{G}$ are selected to be orthogonal to the first four OSTBC-based columns and we require the matrix $\mathbb{G}$ to be orthogonal

$$\mathbb{G}^T\mathbb{G} = \mathbb{G}\mathbb{G}^T = \mathbf{I}_{2K} \tag{3.32}$$

so that the resulting code belongs to the class of OSB-STBC codes.

Using (3.31), it can be readily shown that if $\mathbf{g}_k$ $(k = 1, 2, 3, 4)$ are chosen as

$$\mathbf{g}_k = [g_{1k}, g_{2k}, g_{3k}, g_{4k}, g_{3k}, -g_{4k}, -g_{1k}, g_{2k}]^T \tag{3.33}$$

then for any g_{lk} $(l = 1, 2, 3, 4;\ k = 1, 2, 3, 4)$ they are orthogonal to the first K OSTBC-based columns of $\mathbb{G}$. The advantage of using (3.33) lies on its reduced number of parameters that will facilitate the optimization of the code.

To fulfil (3.32), we have to satisfy the following property when choosing the elements of the vectors $\mathbf{g}_k$ $(k = 1, 2, 3, 4)$:

$$\mathbf{g}_k^T \mathbf{g}_l = \begin{cases} 1 & \text{for } k = l \\ 0 & \text{for } k \neq l \end{cases} \tag{3.34}$$

for all $k = 1, 2, 3, 4$ and $l = 1, 2, 3, 4$. Taking into account (3.33), we have that the latter property is equivalent to

$$\tilde{\mathbf{g}}_k^T \tilde{\mathbf{g}}_l = \begin{cases} 1/2 & \text{for } k = l \\ 0 & \text{for } k \neq l \end{cases} \tag{3.35}$$

where the 4×1 vector $\tilde{\mathbf{g}}_k$ contains the four upper entries of $\mathbf{g}_k$. We can satisfy (3.35) by introducing a 4×4 matrix

$$\tilde{\mathbb{G}} \triangleq \sqrt{2}\,[\tilde{\mathbf{g}}_1\ \tilde{\mathbf{g}}_2\ \tilde{\mathbf{g}}_3\ \tilde{\mathbf{g}}_4]. \tag{3.36}$$

If $\tilde{\mathbb{G}}$ were unstructured, then there would be sixteen degrees of freedom (DOFs) available for its design. However, as $\tilde{\mathbb{G}}$ is orthogonal, six out of these sixteen DOFs are used to ensure orthogonality among the different pairs of columns of this matrix, and four more DOFs are required to ensure that the norm of each column is equal to one. As a result, we have only six DOFs left. These remaining DOFs can be used to satisfy some desired performance criterion when designing the code.

The matrix $\tilde{\mathbb{G}}$ can be parameterized using Givens rotations in the following way [16, 72]:

$$\tilde{\mathbb{G}} = \prod_{\substack{1 \leq m \leq 3 \\ m+1 \leq n \leq 4}} \mathbf{G}(m, n, \theta_{m,n}) \tag{3.37}$$

where $\mathbf{G}(m, n, \theta_{m,n})$ is the Givens rotation matrix whose entries coincide with that of the identity matrix except for the entries $[\mathbf{G}]_{m,n}$, $[\mathbf{G}]_{n,m}$, $[\mathbf{G}]_{n,n}$, and $[\mathbf{G}]_{m,m}$ which are given by

$$\begin{aligned} [\mathbf{G}]_{m,n} &= \sin\theta_{m,n}, \quad [\mathbf{G}]_{n,m} = -\sin\theta_{m,n}, \\ [\mathbf{G}]_{m,m} &= [\mathbf{G}]_{n,n} = \cos\theta_{m,n} \end{aligned} \tag{3.38}$$

where $\theta_{m,n}$ is the angular variable. It can be easily seen that the parameterization in (3.37) has six DOFs corresponding to the entries of the vector $\boldsymbol{\theta} = [\theta_{1,2}, \theta_{1,3}, \theta_{1,4}, \theta_{2,3}, \theta_{2,4}, \theta_{3,4}]^T$.

Let us optimize our code over these six variables using the well-known criterion that, to achieve *full diversity*, all non-zero code difference matrices must be full rank [88] (see Section 2.2). Maximizing the absolute value of the worst code difference matrix determinant as

$$\max_{\tilde{\mathbb{G}}} \min_{\substack{\mathbf{X},\mathbf{X}' \in \mathcal{X} \\ \mathbf{X} \neq \mathbf{X}'}} \delta(\tilde{\mathbb{G}}), \qquad \delta(\tilde{\mathbb{G}}) = |\det(\mathbf{X} - \mathbf{X}')|^2 \tag{3.39}$$

we ensure that the designed generator matrix will provide full diversity with a high coding gain. Here, $\det(\cdot)$ stands for the determinant of a matrix. To find the values of the angles used in (3.37), an extensive Monte-Carlo search has been performed followed by local optimization around the resulting maximal value of the objective function. In this search, the constellation has been fixed to be 4-QAM, and a total of 10^5 random values of the Givens rotation angles have been generated to compute δ. The best value of δ has been taken from this set of points, and then used to initialize the downhill simplex algorithm [59] that has been used for local search.

As a result of our numerical optimization, the following matrix $\tilde{\mathbb{G}}$ has been obtained

$$\tilde{\mathbb{G}}_{\text{opt}} = \frac{1}{\sqrt{7}} \begin{bmatrix} -1 & 1 & 1 & 2 \\ 1 & -2 & 1 & 1 \\ 1 & 1 & 2 & -1 \\ 2 & 1 & -1 & 1 \end{bmatrix} \tag{3.40}$$

with the optimal point of the objective function equal to $\delta(\tilde{\mathbb{G}}_{\text{opt}}) = 16/7$ and

$$\boldsymbol{\theta}_{\text{opt}} = [-3\pi/4, -0.6155, -0.8571, -1.2373, -0.6155, \pi/4]. \tag{3.41}$$

Using (3.30), (3.31), (3.33), (3.36) and (3.40) the complete optimal generator matrix

is given by

$$\mathbb{G} = \begin{bmatrix} \frac{1}{\sqrt{2}} \begin{bmatrix} 1 & 0 & 0 & 0 \\ 0 & 1 & 0 & 0 \\ 0 & 0 & 1 & 0 \\ 0 & 0 & 0 & 1 \\ 0 & 0 & -1 & 0 \\ 0 & 0 & 0 & 1 \\ 1 & 0 & 0 & 0 \\ 0 & -1 & 0 & 0 \end{bmatrix} & \frac{1}{\sqrt{14}} \begin{bmatrix} -1 & 1 & 1 & 2 \\ 1 & -2 & 1 & 1 \\ 1 & 1 & 2 & -1 \\ 2 & 1 & -1 & 1 \\ 1 & 1 & 2 & -1 \\ -2 & -1 & 1 & -1 \\ 1 & -1 & -1 & -2 \\ 1 & -2 & 1 & 1 \end{bmatrix} \end{bmatrix}. \tag{3.42}$$

It is worth noting that the designed code generator matrix $\tilde{\mathbb{G}}_{\text{opt}}$ has an intriguingly simple and elegant structure because it is representable in integer values. This structure could not be expected when formulating the optimization problem (3.39). An equivalent generator matrix can also be obtained by interchanging any columns of $\tilde{\mathbb{G}}_{\text{opt}}$.

NVD Property

Having the NVD property for the proposed code means that $\delta \geq \alpha$ for any constellation size, where $\alpha > 0$ is an arbitrary positive constant. This property has been established for several popular STBCs [7, 17, 20, 46, 61, 100, 102]. It has been proven that any space-time code satisfying the latter property achieves the optimal DMG tradeoff not only in the Rayleigh fading channel case [20, 100], but also for an arbitrary fading distribution [89]. In this section, we establish the NVD property for our code.

Let us first introduce the following lemma which is central for the proof of the NVD property.

Lemma 3.3.1. *If $a, b, c, d, w, x, y, z \in \mathbb{Z}$, where $\mathbb{Z}$ is the set of integers, and*

$$a^2 + b^2 + c^2 + d^2 = w^2 + x^2 + y^2 + z^2 \tag{3.43}$$

then

$$\begin{aligned} &a(w + x + 2y - z) + b(-2w - x + y - z) \\ &\quad + c(w - x - y - 2z) + d(w - 2x + y + z) = 0 \end{aligned} \tag{3.44}$$

if and only if $a = b = c = d = w = x = y = z = 0$.

Proof. See Appendix 3.C. □

The following theorem establishes the NVD property for the proposed STBC.

Theorem 3.3.2. *For the proposed code defined by* (3.42)*,*

$$\delta(\tilde{\mathbb{G}}_{\text{opt}}) \geq 16/7 \tag{3.45}$$

for any M-QAM or M-PAM signal constellation.

Proof. Using (3.2), (3.21) and (3.42), it can be readily verified that for any $\mathbf{X}$ and $\mathbf{X}'$ ($\mathbf{X}(\mathbf{s}) \neq \mathbf{X}'(\mathbf{s}')$),

$$\begin{aligned}
&2\det(\mathbf{X}-\mathbf{X}') = |\tilde{s}_1|^2 + |\tilde{s}_2|^2 - |\tilde{s}_3|^2 - |\tilde{s}_4|^2 \\
&+\frac{2\mathrm{j}}{\sqrt{7}}[\mathrm{Re}\{\tilde{s}_3\}(\mathrm{Re}\{\tilde{s}_1\} + \mathrm{Im}\{\tilde{s}_1\} + 2\mathrm{Re}\{\tilde{s}_2\} - \mathrm{Im}\{\tilde{s}_2\}) \\
&+\mathrm{Im}\{\tilde{s}_3\}(-2\mathrm{Re}\{\tilde{s}_1\} - \mathrm{Im}\{\tilde{s}_1\} + \mathrm{Re}\{\tilde{s}_2\} - \mathrm{Im}\{\tilde{s}_2\}) \\
&+\mathrm{Re}\{\tilde{s}_4\}(\mathrm{Re}\{\tilde{s}_1\} - \mathrm{Im}\{\tilde{s}_1\} - \mathrm{Re}\{\tilde{s}_2\} - 2\mathrm{Im}\{\tilde{s}_2\}) \\
&+\mathrm{Im}\{\tilde{s}_4\}(\mathrm{Re}\{\tilde{s}_1\} - 2\mathrm{Im}\{\tilde{s}_1\} + \mathrm{Re}\{\tilde{s}_2\} + \mathrm{Im}\{\tilde{s}_2\})]
\end{aligned} \tag{3.46}$$

where

$$\tilde{s}_k \triangleq s_k - s'_k\,, \qquad k = 1, \ldots, K. \tag{3.47}$$

The value on the right-hand side of (3.46) is zero only if its real and imaginary parts are both zeros. Denoting $w \triangleq \mathrm{Re}\{\tilde{s}_1\}$, $x \triangleq \mathrm{Im}\{\tilde{s}_1\}$, $y \triangleq \mathrm{Re}\{\tilde{s}_2\}$, $z \triangleq \mathrm{Im}\{\tilde{s}_2\}$, $a \triangleq \mathrm{Re}\{\tilde{s}_3\}$, $b \triangleq \mathrm{Im}\{\tilde{s}_3\}$, $c \triangleq \mathrm{Re}\{\tilde{s}_4\}$, $d \triangleq \mathrm{Im}\{\tilde{s}_4\}$, we obtain from (3.46) that

$$\begin{aligned}
\mathrm{Re}\{2\det(\mathbf{X}-\mathbf{X}')\} &= w^2 + x^2 + y^2 + z^2 \\
&- a^2 - b^2 - c^2 - d^2
\end{aligned} \tag{3.48}$$

$$\begin{aligned}
\mathrm{Im}\{2\det(\mathbf{X}-\mathbf{X}')\} &= \frac{2}{\sqrt{7}}\,[a(w + x + 2y - z) \\
&+ b(-2w - x + y - z) \\
&+ c(w - x - y - 2z) \\
&+ d(w - 2x + y + z)]\,.
\end{aligned} \tag{3.49}$$

Comparing (3.48) with (3.43) and (3.49) with (3.44), respectively, we see that according to Lemma 3.3.1, $\det(\mathbf{X}-\mathbf{X}') = 0$ if and only if $\tilde{s}_i = 0$ for all $i = 1, 2, 3, 4$. However, for any two different matrices $\mathbf{X}$ and $\mathbf{X}'$, the latter condition does not hold. Therefore, we have proved that $\det(\mathbf{X}-\mathbf{X}') \neq 0$ and, therefore, $\delta(\tilde{\mathbb{G}}_{\text{opt}}) \neq 0$.

Let us now recall that s_k $(k = 1, 2, 3, 4)$ are drawn from the M-PAM or M-QAM constellation and, therefore, all $\mathrm{Re}\{\tilde{s}_k\}$ and $\mathrm{Im}\{\tilde{s}_k\}$ $(k = 1, 2, 3, 4)$ are integer multiples of 2. Hence, according to this property and equation (3.46), $2\det(\mathbf{X} - \mathbf{X}')$ can be expressed in the following general form

$$2\det(\mathbf{X} - \mathbf{X}') = 4p + \mathrm{j}\,\frac{8}{\sqrt{7}}\,q \tag{3.50}$$

where p and q are some integers. This means that the value of $\delta(\tilde{\mathbb{G}}_{\mathrm{opt}})$ has the following general form

$$\delta(\tilde{\mathbb{G}}_{\mathrm{opt}}) = 4p^2 + \frac{16}{7}\,q^2\,. \tag{3.51}$$

It has been already proved that $\delta(\tilde{\mathbb{G}}_{\mathrm{opt}}) \neq 0$. Hence, the smallest value of $\delta(\tilde{\mathbb{G}}_{\mathrm{opt}})$ is given by $\min\{4,\, 16/7\} = 16/7$. Theorem 3.3.2 is proved. □

According to Theorem 3.3.2, the proposed STBC enjoys the NVD property for any M-QAM or M-PAM signal constellation. Therefore, it can be expected to provide an excellent performance (guaranteed by the optimal DMG tradeoff achieved by this code) for any value of M, even though it was originally designed for the particular 4-QAM case.

3.3.3 Rate-One OSB-STBC for 3 and 4 Transmit Antennas

A reduced complexity of the ML decoder makes OSB-STBCs attractive in the cases when OSTBCs can achieve a reasonably high rate, as it was shown in Section 3.3.2. However, in the case of three or more transmit antennas and full rate, the ratio K_o/K decreases and, therefore, the complexity advantage of the decoder becomes insignificant.

In the practically important case of three and four transmit antennas, we can keep the value of K_o/K high enough by restricting the code rate to be one. For this case, it is only necessary to aggregate one complex symbol to the OSTBC matrix (or, equivalently, two columns to the code generator matrix) to construct our OSB-STBC.

In what follows, we will present different strategies for designing the additional matrices $\mathbf{C}_k$, $k = K_o + 1, \ldots, K$ for the case of $N_t = 4$. In the case of $N_t = 3$, the same code can be used after removing, for instance, the last row of the matrix $\mathbf{X}$.

Our design is based on the following 4×4 OSTBC [51]:

$$\mathbf{X} = \frac{4}{\sqrt{3}} \begin{bmatrix} s_1 & -s_2^* & s_3^* & 0 \\ s_2 & s_1^* & 0 & s_3^* \\ s_3 & 0 & -s_1^* & -s_2^* \\ 0 & s_3 & s_2 & -s_1 \end{bmatrix}. \tag{3.52}$$

Our first strategy is to parameterize the columns added according to the constrains presented in Section 3.3.1. As before, the columns added to $\mathbb{G}$ are orthogonal to the original "OSTBC" columns of $\mathbb{G}$ and to each other. Let $\mathbf{N}$ be a $2N_tT \times 2(N_tT - K_o)$ matrix whose columns form an orthogonal basis for the null-space of $\mathbb{G}_{\text{ostbc}}^T$. Orthogonal columns (that are the candidate columns for $\mathbb{G}_{\text{add}}$) can be obtained as those of the $2N_tT \times 2(N_tT - K_o)$ matrix $\mathbf{NU}$ where $\mathbf{U}$ is any $2(N_tT - K_o) \times 2(N_tT - K_o)$ orthogonal matrix that can be parameterized using, for instance, Givens rotations. Since only two columns are added in the rate-one STBC case with $N_t = 4$, only the first two columns of $\mathbf{U}$ are needed. Using Givens rotations parametrization for the first two columns of $\mathbf{U}$, we can take into account only the rotations that are involved in these two columns, thereby reducing the number of parameters to be optimized.

The Givens rotations parameters are angles between $-\pi$ and π, and any global search algorithm (such as the genetic algorithm) can be employed to optimize the OSB-STBC according to a certain criterion. A suitable criterion for such a design is the *diversity product* [34, 85] that for $T = N_t$ can be defined as

$$\zeta = \frac{1}{2\sqrt{N_t}} \min_{\substack{\mathbf{X},\mathbf{X}' \in \mathcal{X} \\ \mathbf{X} \neq \mathbf{X}'}} |\det(\mathbf{X} - \mathbf{X}')|^{\frac{1}{N_t}}. \tag{3.53}$$

Maximizing ζ, we ensure that the designed OSB-STBC will provide full diversity with a high coding gain. In the maximization of ζ, the code matrix $\mathbf{X}$ is a function of $\mathbb{G}$, whose last two columns depend on the optimization variables (the Givens rotations parameters). We have maximized ζ for the 4-QAM constellation over these parameters using the genetic algorithm and then used the output of such optimization as a starting point for a local search. The resulting code is denoted as OSB-STBC-1.

Our second strategy of the OSB-STBC design is to add s_4 to the anti-diagonal

of (3.52) to obtain the code matrix

$$\mathbf{X} = \begin{bmatrix} s_1 & -s_2^* & s_3^* & s_4 \\ s_2 & s_1^* & s_4 & s_3^* \\ s_3 & s_4 & -s_1^* & -s_2^* \\ s_4 & s_3 & s_2 & -s_1 \end{bmatrix}. \tag{3.54}$$

Clearly, this operation corresponds to adding two orthogonal columns to $\mathbb{G}_{\text{ostbc}}$ and, therefore, the resulting code belongs to the class of OSB-STBC codes. However, as it is presented in the following lemma, the minimal determinant of the code difference matrix is zero, resulting in a code that does not achieve full-diversity.

Lemma 3.3.3. *For the OSB-STBC in* (3.54) *with symbols drawn from the same constellation*

$$\min_{\substack{\mathbf{X},\mathbf{X}'\in\mathcal{X} \\ \mathbf{X}\neq\mathbf{X}'}} |\det(\mathbf{X}-\mathbf{X}')| = 0. \tag{3.55}$$

Proof. See Appendix 3.D. □

From the proof of Lemma 3.3.3, it can be seen that to achieve full diversity, we need to satisfy $\text{Im}\{\tilde{s}_4\}^2 \neq \text{Re}\{\tilde{s}_1\}^2 + \text{Im}\{\tilde{s}_2\}^2 + \text{Im}\{\tilde{s}_3\}^2$ and $\text{Re}\{\tilde{s}_4\}^2 \neq \text{Im}\{\tilde{s}_1\}^2 + \text{Re}\{\tilde{s}_2\}^2 + \text{Re}\{\tilde{s}_3\}^2$ for $\mathbf{X} \neq \mathbf{X}'$. These inequalities can be easily satisfied by rotating the constellation for s_4. For example, if the symbols s_k are drawn from a M-QAM constellation, we need s_4 and its square not to be a rational number. This can be achieved by producing constellation points for s_4 that are multiple of a transcendental number[1]. Therefore, we can multiply s_4 by $e^{\mathrm{j}\beta}$, where β is an algebraic number[2]. This rotation guarantees that the designed OSB-OSTBC will achieve full-diversity for any M-QAM constellation.

Note that it is desirable not only to satisfy the full-diversity property, but also to obtain a high coding gain. In the particular 4-QAM case, both objectives can be achieved by maximizing ζ as follows

$$\beta_{\text{opt}} = \arg\max_{\beta} \zeta\,. \tag{3.56}$$

[1]A transcendental number is a number which is not a solution of non-zero polynomial with rational coefficients.

[2]An algebraic number is a root of a non-zero polynomial with rational coefficients. $e^{\mathrm{j}\beta}$ is transcendental by the Lindemann-Weierstrass theorem [5].

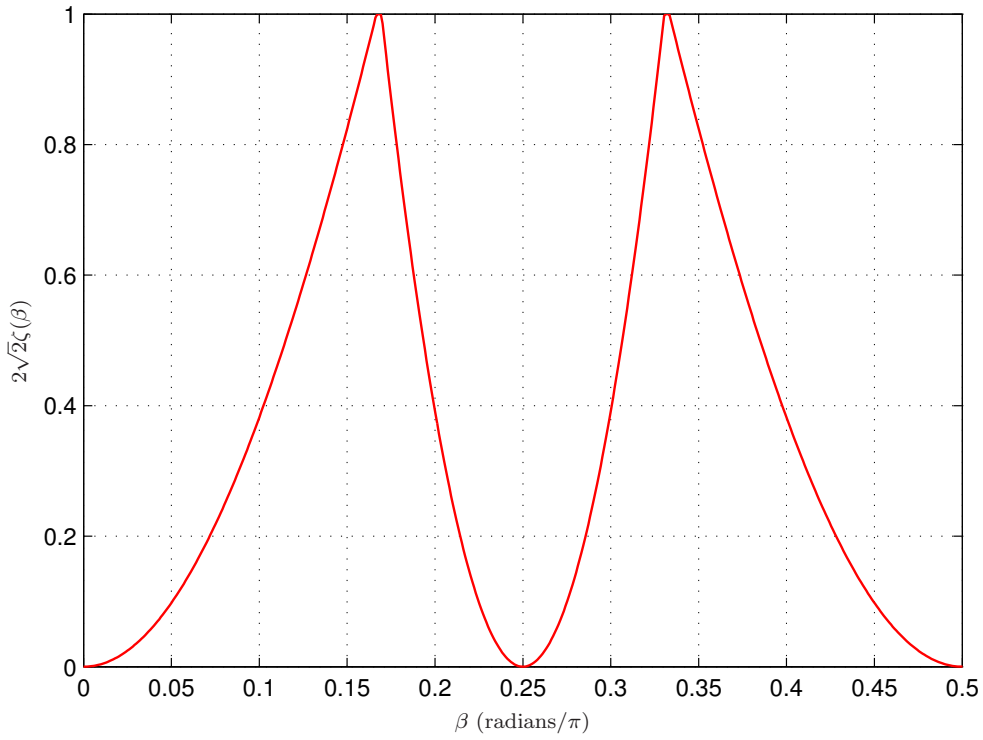

Figure 3.1: Diversity product for 4-QAM versus rotation angle β for s_4 without constellation normalization.

Fig. 3.1 shows the diversity product as a function of β for the proposed STBC with 4-QAM. Since the figure is symmetrical with respect to $\pi/2$, the other half is not shown. It can be observed from the figure that the optimal rotation angles are $\beta_{\text{opt}} = \{\pi/6, \pi/3\}$.

We denote the OSB-STBC with the optimal rotation angles as OSB-STBC-2. A similar strategy was presented in [13] where the two upper anti-diagonal entries were s_4^* rather than s_4 and the coding gain was not optimized.

The previous design has only one degree of freedom that can be utilized by optimizing ζ. Although the optimal ζ can be easily obtained, the performance can be further improved by designing a code with a reduced *kissing number*, that is, a reduced number of code difference matrices $(\mathbf{X} - \mathbf{X}')$ that result in the same worst-case value of ζ. Note that the error probability is dominated not only by the value of ζ but also by the number of code difference matrices that result in the same ζ.

Space-time code	ζ
LCP [99]	$\sqrt{2}/4$
QOSTBC(rot.) [85]	$\sqrt{2}/4$
DAST (real rot.) [10]	$\sqrt{2}/10$
CIOD [45]	$\sqrt{2}/5$
OSB-STBC-1	0.2768
OSB-STBC-2	$\sqrt{2}/4$
OSB-STBC-3	$\sqrt{2}/4$

Table 3.1: Normalized diversity product of different rate-one STBCs for $N_t = 4$ and 4-QAM.

If we let each entry in the anti-diagonal of (3.54) to have an independent rotation and optimize the code over $\boldsymbol{\beta}$, where $\boldsymbol{\beta} = [\beta_{1,4}\ \beta_{2,3}\ \beta_{3,2}\ \beta_{4,1}]^T$ is the vector of rotation angles and $\beta_{m,n}$ denotes the rotation angle for the (m,n)th entry of $\mathbf{X}$, then the kissing number can be reduced. Doing so, we obtain the following optimal value of $\boldsymbol{\beta}$:

$$\boldsymbol{\beta}_{\text{opt}} = [1.9267\ -0.9526\ -1.0622\ -0.9493]^T. \tag{3.57}$$

This code corresponds to our third strategy and is denoted as OSB-STBC-3.

In Table 3.1, we compare the normalized ζ for 4-QAM of the proposed designs with several state-of-the-art rate-one space-time codes:

- STBC based on linear constellation precoding (LCP) [99];
- QOSTBC with rotated constellation [85];
- Diagonal algebraic space-time (DAST) code with real-valued rotation [10];
- Coordinate interleaved orthogonal design (CIOD) [45].

It follows that our designs achieved the maximum diversity product except for OSB-STBC-1. However, it is probable that for OSB-STBC-1 we did not obtain the global maximum.

3.4 ML Decoder for OSB-STBCs

According to (3.25), the objective of the ML decoder is to obtain $\hat{\underline{\mathbf{s}}}$ that results in the minimal norm of the difference between the received data vector $\underline{\mathbf{Y}}$ and the members of the receive codebook $\underline{\mathcal{Y}}$. First, we will develop a real-valued implementation of this decoder for the proposed space-time codes. A complex-valued implementation of the decoder will be developed only for the full-rate 2×2 space-time code due to the resulting structure of $\mathbb{G}_{\text{add}}$ which, as shown in Section 3.4.2, is also an OSTBC.

3.4.1 Real-Valued Implementation

Using a QR-type decomposition of the tall matrix $\mathbb{HG}$, this matrix can be factorized as

$$\mathbb{HG} = \mathbf{QR}, \quad \mathbf{R} \triangleq \begin{bmatrix} \breve{\mathbf{R}} \\ \breve{\mathbf{O}} \end{bmatrix} \tag{3.58}$$

where $\mathbf{Q}$ is a $2N_rT \times 2N_rT$ orthogonal matrix, $\breve{\mathbf{R}}$ is a $2K \times 2K$ upper-triangular matrix, and $\breve{\mathbf{O}}$ is a $(2N_rT - 2K) \times 2K$ matrix of zeros. Inserting (3.58) into (3.25) and using the orthogonality property of $\mathbf{Q}$, we have

$$\hat{\underline{\mathbf{s}}} = \arg \min_{\underline{\mathbf{s}}_l \in \underline{\mathcal{S}}} \|\mathbf{Q}^T \underline{\mathbf{Y}} - \mathbf{R}\underline{\mathbf{s}}_l\| \,. \tag{3.59}$$

As the search in (3.59) is not affected by the last $2N_rT - 2K$ entries of the vector $(\mathbf{Q}^T\underline{\mathbf{Y}} - \mathbf{R}\underline{\mathbf{s}}_l)$, we can rewrite (3.59) in the following equivalent form:

$$\hat{\underline{\mathbf{s}}} = \arg \min_{\underline{\mathbf{s}}_l \in \underline{\mathcal{S}}} \|\breve{\underline{\mathbf{Y}}} - \breve{\mathbf{R}}\underline{\mathbf{s}}_l\| \tag{3.60}$$

where

$$\breve{\underline{\mathbf{Y}}} \triangleq \breve{\mathbf{Q}}^T \underline{\mathbf{Y}} \tag{3.61}$$

and $\breve{\mathbf{Q}}$ is the $2N_rT \times 2K$ matrix composed by the first $2K$ columns of $\mathbf{Q}$.

According to the orthogonality property (3.28), for the resulting OSB-STBC, the matrix $\breve{\mathbf{R}}$ in (3.60) has the following form

$$\breve{\mathbf{R}} = \begin{bmatrix} \gamma \mathbf{I}_{2K_o} & \mathbf{A} \\ \mathbf{O} & \mathbf{B} \end{bmatrix} \tag{3.62}$$

where $\mathbf{A}$ is a $2K_o \times 2(K - K_o)$ general-type matrix, $\mathbf{O}$ is a $2(K - K_o) \times 2K_o$ matrix of zeros, $\mathbf{B}$ is a $2(K - K_o) \times 2(K - K_o)$ upper-triangular matrix, and γ is some

constant. The vector $\underline{\mathbf{s}}_l$ can be represented as

$$\underline{\mathbf{s}}_l = [\underline{\tilde{\mathbf{s}}}_l^T, \underline{\breve{\mathbf{s}}}_l^T]^T \tag{3.63}$$

where

$$\underline{\tilde{\mathbf{s}}}_l \triangleq [\underline{s}_{l,1}, \ldots, \underline{s}_{l,2K_o}]^T \tag{3.64}$$

$$\underline{\breve{\mathbf{s}}}_l \triangleq [\underline{s}_{l,2K_o+1}, \ldots, \underline{s}_{l,2K}]^T. \tag{3.65}$$

Using (3.62) and (3.63), we can rewrite (3.60) as

$$\hat{\underline{\mathbf{s}}} = \arg \min_{\underline{\mathbf{s}}_l \in \underline{\mathcal{S}}} \left\| \underline{\breve{\mathbf{Y}}} - \begin{bmatrix} \gamma \underline{\tilde{\mathbf{s}}}_l + \mathbf{A} \underline{\breve{\mathbf{s}}}_l \\ \mathbf{B} \underline{\breve{\mathbf{s}}}_l \end{bmatrix} \right\|. \tag{3.66}$$

We observe that for any given $\underline{\breve{\mathbf{s}}}$, where $\underline{\mathbf{s}} = [\underline{\tilde{\mathbf{s}}}^T, \underline{\breve{\mathbf{s}}}^T]^T$, the value of $\underline{\tilde{\mathbf{s}}}$ that minimizes the metric in (3.66) can be found by a real symbol-by-symbol decoding procedure. Therefore, in (3.66) it is only necessary to inspect the metric for all possible combinations of $\underline{\breve{\mathbf{s}}}$ in order to find $\hat{\underline{\mathbf{s}}}$.

Using the structure of (3.66), a simplified way of detecting the symbols can be implemented with the standard SD procedure. The SD should conduct a search of possible symbol candidates for the last $2(K - K_o)$ symbols first (that is, for the entries of the vector $\underline{\breve{\mathbf{s}}}$). For each candidate $\underline{\breve{\mathbf{s}}}$ obtained with the SD, symbol-by-symbol decoding can be used to determine the remaining $2K_o$ symbols (the entries of the vector $\underline{\tilde{\mathbf{s}}}^T$).

Summarizing, in contrast to the standard SD, the proposed decoding procedure omits the last $2K_o$ stages of SD and replaces them by a much simpler symbol-by-symbol decoder.

3.4.2 Complex-Valued Implementation

The resulting structure in (3.42) of the matrix $\mathbb{G}_{\text{add}}$ for the 2×2 full-rate code in Section 3.3.2, allow us to develop a complex-valued implementation of the decoder. The main advantage of the real-valued implementation is its simplicity of operation for each visited point, while the main advantage of the complex-valued implementation is a substantially reduced number of visited points [70].

The complex-valued SD [35] can be only used when the real and imaginary parts of each symbol are decoupled in the sense that the decoding of any complex symbol

can be made directly, without any need to decode the real or imaginary part of this symbol first and then to use the result of this decoding to obtain the remaining part of the symbol.

To develop the complex-valued implementation of the ML decoder (3.19), let us first show that the matrix $\mathbf{B}$ in (3.62) is a scaled identity matrix. From our design, it follows that for the first two symbols s_1 and s_2, the matrices $\mathbf{C}_1$, $\mathbf{C}_2$, $\mathbf{C}_3$ and $\mathbf{C}_4$ of our code form an OSTBC. Therefore, they satisfy the properties given in (3.26) and (3.27) for $k = 1, \ldots, 4$ and $p = 1, \ldots, 4$. Interestingly, it can be also readily verified that for the last two symbols s_3 and s_4, the matrices $\mathbf{C}_5$, $\mathbf{C}_6$, $\mathbf{C}_7$ and $\mathbf{C}_8$ of our code form another OSTBC and, hence, they satisfy (3.26) and (3.27) for $k = 5, \ldots, 8$ and $p = 5, \ldots, 8$. Therefore, using the orthogonality property (3.28) we have that

$$\mathbf{B} = \beta \mathbf{I}_K \tag{3.67}$$

where β is a positive constant. Using (3.67) and defining $\underline{\tilde{\mathbf{y}}}$ and $\underline{\breve{\mathbf{y}}}$ as

$$\underline{\breve{\mathbf{Y}}} \triangleq [\underline{\tilde{\mathbf{y}}}^T \, \underline{\breve{\mathbf{y}}}^T]^T \tag{3.68}$$

the metric in (3.66) can be rewritten as

$$\left\| \begin{bmatrix} \underline{\tilde{\mathbf{y}}} \\ \underline{\breve{\mathbf{y}}} \end{bmatrix} - \begin{bmatrix} \gamma \underline{\tilde{\mathbf{s}}}_l + \mathbf{A} \underline{\breve{\mathbf{s}}}_l \\ \beta \underline{\breve{\mathbf{s}}}_l \end{bmatrix} \right\|^2 = \|\underline{\tilde{\mathbf{y}}} - \gamma \underline{\tilde{\mathbf{s}}}_l + \mathbf{A} \underline{\breve{\mathbf{s}}}_l\|^2 + \|\underline{\breve{\mathbf{y}}} - \beta \underline{\breve{\mathbf{s}}}_l\|^2. \tag{3.69}$$

According to (3.69), the decoding of $\underline{\tilde{\mathbf{s}}}_l$ is based on the knowledge of $\underline{\breve{\mathbf{s}}}_l$, and therefore, the vectors $\underline{\tilde{\mathbf{s}}}_l$ and $\underline{\breve{\mathbf{s}}}_l$ should be decoded jointly. However, in the second term of the right-hand side of (3.69), we can use the inverse of the underline operator to obtain $\|\underline{\breve{\mathbf{y}}} - \beta \underline{\breve{\mathbf{s}}}_l\|^2$ where $\breve{\mathbf{y}} = \mathrm{mat}_{2,1}(\underline{\breve{\mathbf{y}}})$ and $\breve{\mathbf{s}} = \mathrm{mat}_{2,1}(\underline{\breve{\mathbf{s}}}) = [s_3, s_4]^T$. Obviously, such a operation does not affect the metric in (3.69). Using this fact, our ML decoder can use the complex-valued SD to visit the possible candidates of $\breve{\mathbf{s}} = [s_3, s_4]^T$ and use the symbol-by-symbol decoder to obtain $\tilde{\mathbf{s}} = \mathrm{mat}_{2,1}(\underline{\tilde{\mathbf{s}}}) = [s_1, s_2]^T$.

3.5 Computer Simulations

In this section, we present simulations results for the STBCs designed in Section 3.2. We compare their performance and decoding complexity to that of other state-of-the-art STBCs. Throughout all our simulations we have assumed a MIMO system with quasi-static Rayleigh flat-fading channel.

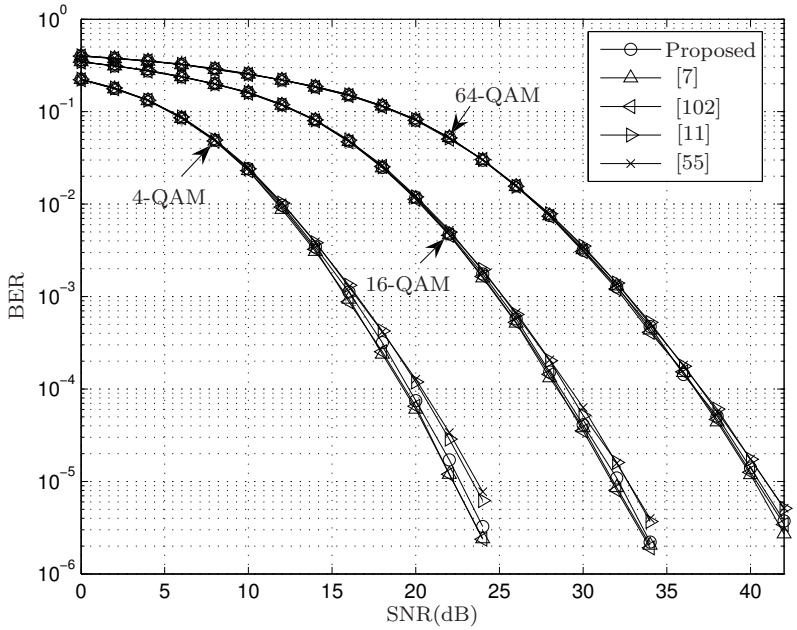

Figure 3.2: BER versus SNR for different STC schemes.

First, the full-rate full-diversity STBC proposed in Section 3.3.2 is tested. We consider a MIMO channel with $N_t = N_r = T = 2$, and compare the performance and decoding complexity of the proposed STBC to that of the following well-known 2×2 full-rate full-diversity codes known from the literature:

- the Golden code of [7];
- the trace-orthogonal cyclotomic STBC of [102];
- the algebraic code of [11];
- the full-rate full-diversity code of [55].

All these codes have been tested for 4-QAM, 16-QAM, and 64-QAM constellations. As recommended in [11], the parameter of the latter code is chosen to be $\lambda = 1/2$ for the 4-QAM constellation, and $\lambda = \pi/6$ for the 16-QAM and 64-QAM constellations. The Schnorr-Euchner variant of the SD has been used for both real- and complex-valued implementations [1, 35].

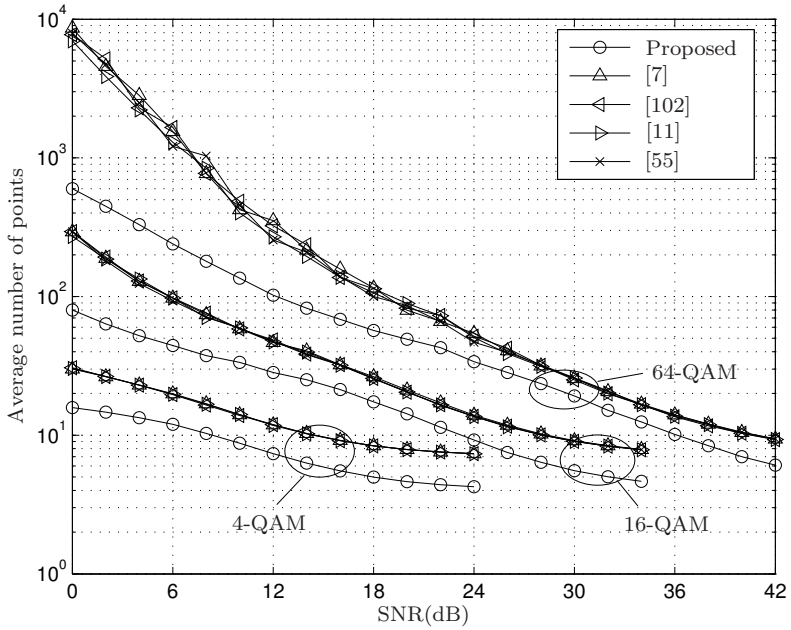

Figure 3.3: Average number of points visited by the real-valued implementation of the decoder versus SNR.

Fig. 3.2 displays the bit error rate (BER) versus SNR for all the codes tested. It should be stressed here that the the BER curves plotted in this figure do not change if the complex-valued decoder is used in lieu of the real-valued one. As can be seen from Fig. 3.2, the performance of the proposed code is nearly the same as of the Golden and trace-orthogonal cyclotomic codes (that have the best performances among the codes tested).

Figs. 3.3 and 3.4 show the average number of points visited by the real-valued and complex-valued versions of the decoder, respectively, versus SNR for all the codes tested. Note that the code of [102] is not included in Fig. 3.4 because the complex-valued decoder is not applicable to this code.

From Figs. 3.3 and 3.4, it can be observed that for both the real-valued and complex-valued decoding cases, the proposed code offers a substantially reduced decoding complexity as compared to the other codes tested. This complexity reduction is especially pronounced in the practically important low and medium SNR regions.

Next, we present the simulation results for the performance of the designed rate-

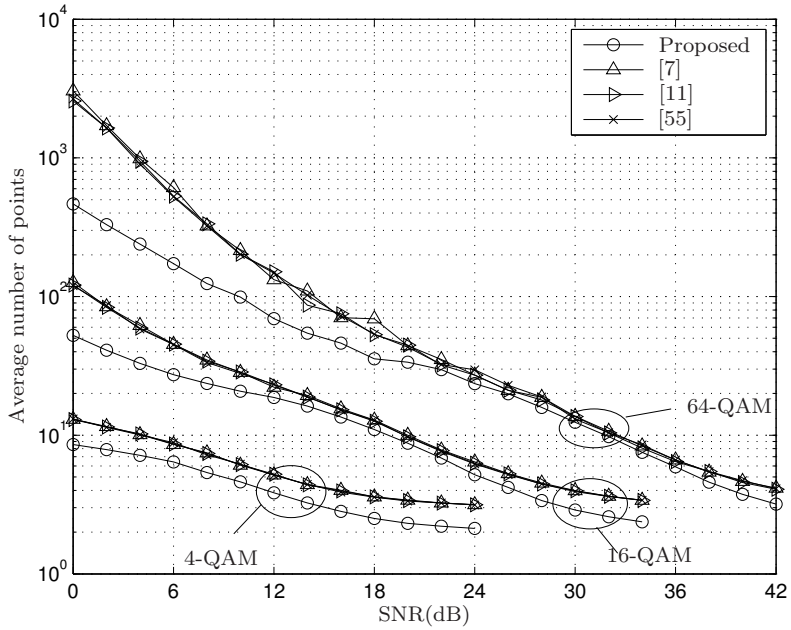

Figure 3.4: Average number of points visited by the complex-valued implementation of the decoder versus SNR.

one OSB-STBCs in Section 3.3.3. We assume a multiple-input single-output (MISO) system with $N_t = T = 4$. To evaluate the difference of the achievable rates of our proposed OSB-STBCs with respect to the MISO channel capacity, we calculate the maximum mutual information (MMI). Using (3.15) and (3.20), the MMI achieved by the space-time coded system is given by [102]

$$C_{\text{MMI}} = \frac{1}{2T}\mathrm{E}_{\mathbb{H}}\left\{\log_2\left(\det\left(\mathbf{I}_{2N_rT} + \frac{\text{SNR}}{N_t}\mathbb{H}\mathbb{G}\mathbb{G}^T\mathbb{H}^T\right)\right)\right\} \tag{3.70}$$

where $\mathrm{E}_{\mathbb{H}}\{\cdot\}$ is the statistical expectation operator with respect to $\mathbb{H}$.

In Fig. 3.5, the capacity for MISO channel with $N_t = 4$ is compared with the MMI achieved by the proposed STBC. It can be observed that OSB-STBC-2 and OSB-STBC-3 achieve a higher MMI than OSB-STBC-1 and suffer a capacity loss of 1.3 dB.

Next, we show simulation results of performance and decoding complexity in the 4-QAM case. In our first example, we compare only the three proposed OSB-STBCs of Section 3.3.3 to identify the best code among them. Fig. 3.6 shows their BERs

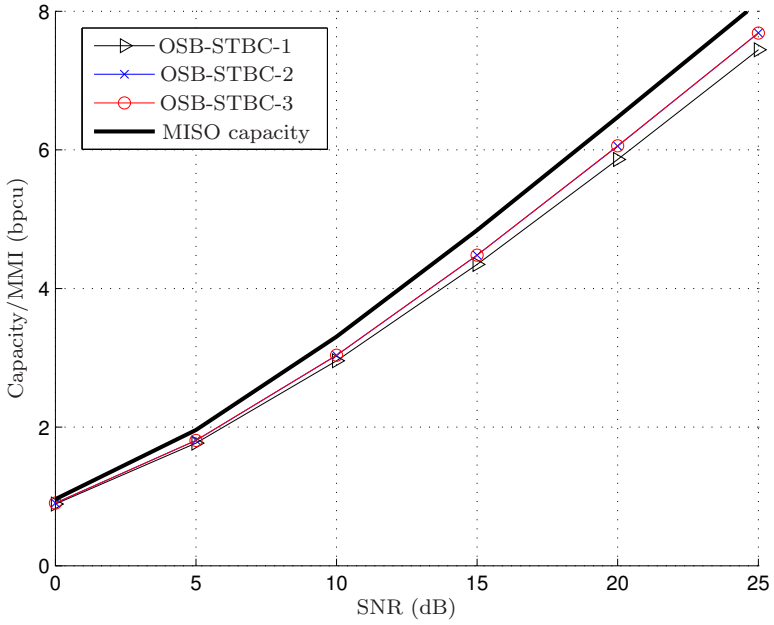

Figure 3.5: Capacity for a MISO channel with $N_t = 4$ and MMI for the proposed OSB-STBCs.

versus the SNR. As it can be seen from this figure, OSB-STBC-3 achieves the best performance among the three proposed codes. This fact can be explained by a lower kissing number of this code.

Next, let us compare the performance of OSB-STBC-3 with the following popular rate-one STBCs:

- QOSTBC with rotated constellation [85];
- CIOD [45];
- STBC based on LCP [99];
- DAST code with real-valued rotation [10].

The Schnorr-Euchner variant of the SD has been employed for decoding [1]. In CIOD of [45], four parallel SDs were used to decode each symbol. In QOSTBC, two parallel SDs were employed to decode each pair s_1, s_4 and s_2, s_3. In the DAST code [10], two parallel SDs were used to decode the imaginary and real parts of each

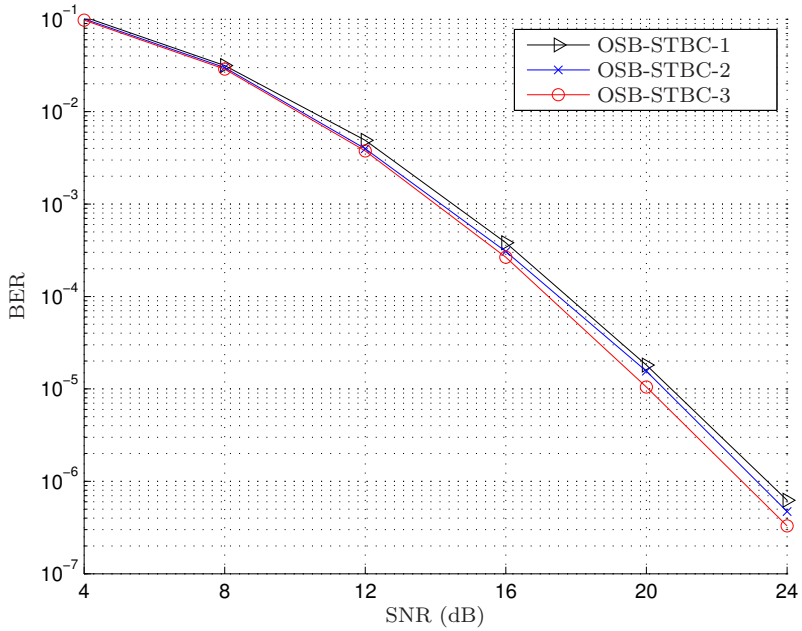

Figure 3.6: BERs of the proposed OSB-STBCs versus SNR.

symbol separately. In the LCP code of [99], only one SD was employed. Note that the proposed OSB-OSTBCs also require one SD which is used to search for s_4, and the other symbols are decoded in the symbol-by-symbol way. From Fig. 3.7, it can be observed that the performances of OSB-STBC-3, QOSTBC, and CIOD are very close to each other and are the best among the codes tested.

Fig. 3.8 displays the average number of points (i.e., the number of vectors $\underline{\mathbf{s}}$) visited by the decoder for all the codes tested versus SNR. From this figure, it can be observed that OSB-STBC-3 has the lowest decoding complexity among these codes.

3.6 Summary

In this chapter, a novel approach to design STBCs that enjoy a fast ML decoding has been presented. First, the case of two transmit antennas and full rate has been addressed, obtaining a space-time code with optimal DMG tradeoff benefit. Next, we developed rate-one STBCs for three and four transmit antennas with full

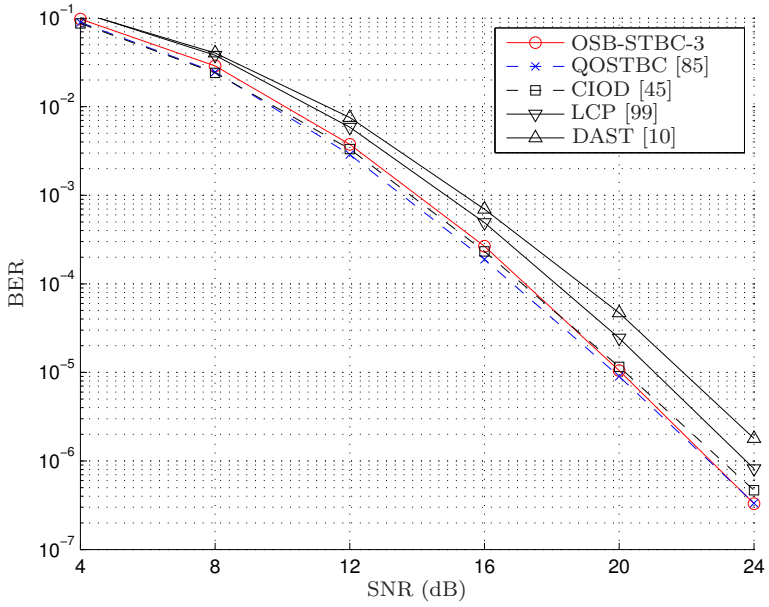

Figure 3.7: BER of different rate-one STBCs versus SNR.

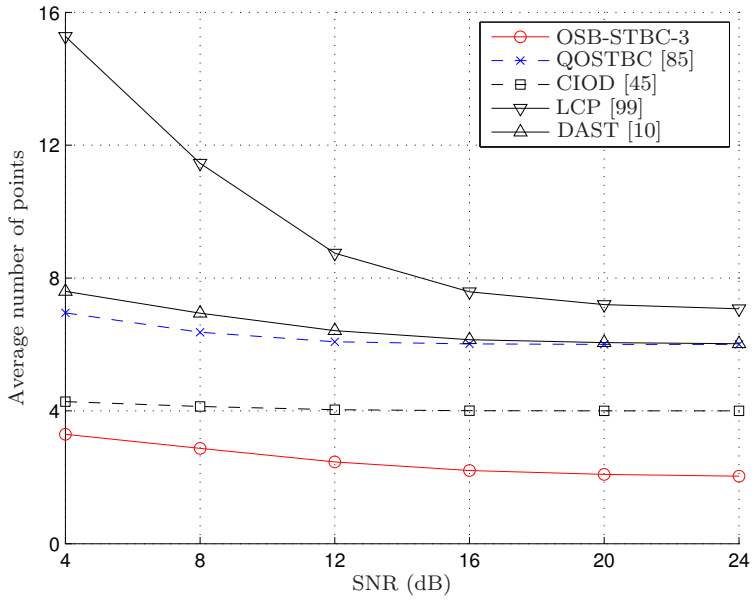

Figure 3.8: Average number of points visited by the decoder versus SNR.

diversity and high-performance. The ML decoding complexity of all designed codes lies in between that of the symbol-by-symbol decoder and the standard SD.

Appendix 3.A Derivation of $\mathbb{H}$

First, let us show that the real and imaginary parts of the multiplication of any two complex numbers $r = a + \mathrm{j}b$ and $q = c + \mathrm{j}d$ can be given by

$$rq = (a + \mathrm{j}b)(c + \mathrm{j}d) = ac - bd + \mathrm{j}(bc + ad) \tag{3.71}$$

where a, b, c, $d \in \mathbb{R}$. Real and imaginary parts of (3.71) can be expressed in the vector form as

$$\begin{bmatrix} \mathrm{Re}\{rq\} \\ \mathrm{Im}\{rq\} \end{bmatrix} = \begin{bmatrix} ac - bd \\ bc + ad \end{bmatrix} = \begin{bmatrix} a & -b \\ b & a \end{bmatrix} \begin{bmatrix} c \\ d \end{bmatrix}. \tag{3.72}$$

The matrix in (3.72) can be obtained as

$$\begin{bmatrix} a & -b \\ b & a \end{bmatrix} = \mathrm{Re}\{r \otimes \mathbf{E}\} = \frac{1}{2}\left(r \otimes \mathbf{E} + r^* \otimes \mathbf{E}^*\right) \tag{3.73}$$

where $\mathbf{E}$ is defined as in (3.17). Applying the vectorization operator to (3.1), we obtain

$$\mathrm{vec}(\mathbf{Y}) = \underbrace{(\mathbf{I}_T \otimes \mathbf{H})}_{\tilde{\mathbf{H}}} \mathrm{vec}(\mathbf{X}) + \mathrm{vec}(\mathbf{V}) \tag{3.74}$$

where $\mathrm{vec}(\cdot)$ stands for the vectorization of any matrix that stacks the columns in a vector, and

$$\tilde{\mathbf{H}} = \begin{bmatrix} \mathbf{H} & & \\ & \ddots & \\ & & \mathbf{H} \end{bmatrix} \tag{3.75}$$

is a $N_tT \times N_rT$ block diagonal matrix. Applying (3.73) to (3.75), we obtain from (3.74) the equivalent underlined version of (3.1) presented in (3.15) where it can be readily verified that

$$\mathbb{H} \;=\; \mathbf{I}_T \otimes \mathrm{Re}\{\mathbf{H} \otimes \mathbf{E}\}. \tag{3.76}$$

Appendix 3.B Proof of the Orthogonality Property of $\mathbb{HG}_{\text{ostbc}}$

Let us note the fact that for any two complex matrices $\mathbf{A}$, $\mathbf{B}$ of the same size,

$$(\underline{\mathbf{A}})^T\underline{\mathbf{B}} = \mathrm{Re}\left\{\mathrm{tr}(\mathbf{A}^H\mathbf{B})\right\}. \tag{3.77}$$

Using the underline operator it can be shown that

$$\mathbb{HG} = \left[\, \underline{\mathbf{HC}_1}\ \underline{\mathbf{HC}_2}\ \cdots\ \underline{\mathbf{HC}_{2K}}\, \right]. \tag{3.78}$$

For the generator matrix of an OSTBC, we can obtain

$$\mathbb{G}_{\text{ostbc}}^T\mathbb{H}^T\mathbb{H}\mathbb{G}_{\text{ostbc}} = \begin{bmatrix} \underline{\mathbf{HC}_1}^T \\ \underline{\mathbf{HC}_2}^T \\ \vdots \\ \underline{\mathbf{HC}_{2K}}^T \end{bmatrix} \left[\, \underline{\mathbf{HC}_1}\ \underline{\mathbf{HC}_2} \cdots \underline{\mathbf{HC}_{2K}}\, \right] \tag{3.79}$$

and using (3.26),(3.27) and (3.77) we obtain

$$\mathbb{G}_{\text{ostbc}}^T\mathbb{H}^T\mathbb{H}\mathbb{G}_{\text{ostbc}} = \|\mathbf{H}\|_F^2\mathbf{I}_{2K}. \tag{3.80}$$

Note that $\mathbf{C}_k\mathbf{C}_p^H$ and $\mathbf{C}_p\mathbf{C}_k^H$, in (3.27), are skew Hermitian and have purely imaginary diagonals for $k \neq p$. Therefore, the real part of their trace is zero.

Appendix 3.C Proof of Lemma 3.3.1

Introducing the new variables

$$f_1 \triangleq w + x + 2y - z \tag{3.81}$$
$$f_2 \triangleq -2w - x + y - z \tag{3.82}$$
$$f_3 \triangleq w - x - y - 2z \tag{3.83}$$
$$f_4 \triangleq w - 2x + y + z \tag{3.84}$$

it can be readily shown that equations (3.43) and (3.44) can be rewritten as

$$7\left(a^2 + b^2 + c^2 + d^2\right) = f_1^2 + f_2^2 + f_3^2 + f_4^2 \tag{3.85}$$
$$af_1 + bf_2 + cf_3 + df_4 = 0 \tag{3.86}$$

respectively. Introducing the vector notation

$$\mathbf{u} \triangleq [f_1, f_2, f_3, f_4]^T \tag{3.87}$$

$$\mathbf{v} \triangleq [a, b, c, d]^T \tag{3.88}$$

the latter equations can be written as

$$\|\mathbf{u}\|^2 = 7\|\mathbf{v}\|^2 \tag{3.89}$$

$$\mathbf{u}^T\mathbf{v} = 0\,. \tag{3.90}$$

Now, let us prove that in the case of integer-valued entries of $\mathbf{u}$ and $\mathbf{v}$, equations (3.89) and (3.90) can be fulfilled only if $\mathbf{u} = \mathbf{v} = \mathbf{0}$ where $\mathbf{0}$ is a vector of zeros.

Let us scale both the vectors $\mathbf{u}$ and $\mathbf{v}$ by the same constant $\sqrt{a^2 + b^2 + c^2 + d^2}$ and rotate these two vectors by the same angle, so that the second, third and fourth entry of the vector $\mathbf{v}$ after such operation become zeros. It can be readily verified that such a common scaling and rotation operation can be expressed as

$$\tilde{\mathbf{v}} = \mathbf{R}\mathbf{v}\,, \qquad \tilde{\mathbf{u}} = \mathbf{R}\mathbf{u} \tag{3.91}$$

where

$$\mathbf{R} \triangleq \begin{bmatrix} a & b & c & d \\ d & -c & b & -a \\ c & d & -a & -b \\ b & -a & -d & c \end{bmatrix}. \tag{3.92}$$

From (3.87)-(3.88) and (3.92), we obtain

$$\tilde{\mathbf{v}} = [n, 0, 0, 0]^T \tag{3.93}$$

$$\tilde{\mathbf{u}} = [0, p, q, r]^T \tag{3.94}$$

where

$$n \triangleq a^2 + b^2 + c^2 + d^2 \tag{3.95}$$

p, q, and r are the integers defined by multiplying the vector $\mathbf{u}$ by the second, third, and fourth rows of $\mathbf{R}$, respectively, and the fact that the first entry of $\tilde{\mathbf{u}}$ is equal to zero follows from (3.86).

Clearly, equations (3.89)-(3.90) should be also satisfied for the vectors $\tilde{\mathbf{v}}$ and $\tilde{\mathbf{u}}$, that is,

$$\|\tilde{\mathbf{u}}\|^2 = 7\|\tilde{\mathbf{v}}\|^2 \tag{3.96}$$

$$\tilde{\mathbf{u}}^T\tilde{\mathbf{v}} = 0\,. \tag{3.97}$$

Inserting (3.93)-(3.94) into (3.96), we obtain that the latter equation can be rewritten as

$$p^2 + q^2 + r^2 = 7n^2. \tag{3.98}$$

The rest of our proof will be made by contradiction. Assume that there is a non-trivial solution to (3.98) and let g be the greatest common divisor (gcd) of p, q, r and n, that is, $g \triangleq \gcd(p, q, r, n)$. Defining

$$N \triangleq \frac{n}{g}, \qquad P \triangleq \frac{p}{g}, \qquad Q \triangleq \frac{q}{g}, \qquad R \triangleq \frac{r}{g} \tag{3.99}$$

we have that $\gcd(N, P, Q, R) = 1$. From (3.98), we notice that

$$n^2 + p^2 + q^2 + r^2 = 8n^2\,. \tag{3.100}$$

Using (3.99) in (3.100), we obtain

$$(N^2 + P^2 + Q^2 + R^2) \bmod 8 = 0 \tag{3.101}$$

and, therefore,

$$(N^2 + P^2 + Q^2 + R^2) \bmod 4 = 0 \tag{3.102}$$

is also true. Here, $a \bmod b$ denotes the remainder of a divided by b.

As for any integer i, the value of $i^2 \bmod 4$ is equal to 0 or 1, it follows from (3.102) that one of the following two equations must hold

$$N^2 \bmod 4 = P^2 \bmod 4 = Q^2 \bmod 4 = R^2 \bmod 4 = 0 \tag{3.103}$$

$$N^2 \bmod 4 = P^2 \bmod 4 = Q^2 \bmod 4 = R^2 \bmod 4 = 1\,. \tag{3.104}$$

Let us first assume (3.103) holds true. However, in this case N^2, P^2, Q^2, and R^2 are divisible by 4, which contradicts to $\gcd(N, P, Q, R) = 1$. Therefore, (3.103) cannot be true.

Let us now assume that (3.104) holds true. Let us use the fact that for any integer i, the value of $i^2 \bmod 8$ can be either 0, or 1, or 4 and, therefore, if $i^2 \bmod 4 = 1$, then $i^2 \bmod 8 = 1$ as well. In this case, we obtain from the latter fact and (3.104) that $(N^2 + P^2 + Q^2 + R^2) \bmod 8 = 4$ which contradicts to (3.101). Therefore, (3.104) cannot be true.

Therefore, by contradiction we conclude that the only possible solution to (3.98) is $p = q = r = n = 0$ which implies $a = b = c = d = w = x = y = z = 0$. Lemma 3.3.1 is proved.

Appendix 3.D Proof of Lemma 3.3.3

Using (3.54) and (3.47) with $K = 4$, it can be readily verified that for any $\mathbf{X}$ and $\mathbf{X}'$ ($\mathbf{X}(\mathbf{s}) \neq \mathbf{X}'(\mathbf{s}')$),

$$\begin{aligned}\det(\mathbf{X}-\mathbf{X}') &= (|\tilde{s}_1|^2+|\tilde{s}_2|^2+|\tilde{s}_3|^2)^2+\tilde{s}_1^2\tilde{s}_4^2-\tilde{s}_2^2\tilde{s}_4^2 \\ &\quad -\tilde{s}_3^2\tilde{s}_4^2+\tilde{s}_4^4+\tilde{s}_4^2(\tilde{s}_1^*)^2-\tilde{s}_4^2(\tilde{s}_2^*)^2-\tilde{s}_4^2(\tilde{s}_3^*)^2. \qquad (3.105)\end{aligned}$$

Let us denote the real and imaginary parts of $\tilde{s}_k$ by $\tilde{s}_{\mathrm{r}k}$ and $\tilde{s}_{\mathrm{i}k}$, respectively. Expanding (3.105), we obtain for the real part

$$\begin{aligned}\mathrm{Re}\{\det(\mathbf{X}-\mathbf{X}')\} &= (|\tilde{s}_1|^2+|\tilde{s}_2|^2+|\tilde{s}_3|^2)^2 \\ &\quad +2\tilde{s}_{\mathrm{i}4}^2(\tilde{s}_{\mathrm{i}1}^2-\tilde{s}_{\mathrm{r}1}^2-\tilde{s}_{\mathrm{i}2}^2+\tilde{s}_{\mathrm{r}2}^2-\tilde{s}_{\mathrm{i}3}^2+\tilde{s}_{\mathrm{r}3}^2) \\ &\quad +2\tilde{s}_{\mathrm{r}4}^2(\tilde{s}_{\mathrm{r}1}^2-\tilde{s}_{\mathrm{i}1}^2+\tilde{s}_{\mathrm{i}2}^2-\tilde{s}_{\mathrm{r}2}^2+\tilde{s}_{\mathrm{i}3}^2-\tilde{s}_{\mathrm{r}3}^2-3\tilde{s}_{\mathrm{i}4}^2) \\ &\quad +\tilde{s}_{\mathrm{r}4}^4+\tilde{s}_{\mathrm{i}4}^4 \qquad (3.106)\end{aligned}$$

and for the imaginary part

$$\begin{aligned}\mathrm{Im}\{\det(\mathbf{X}-\mathbf{X}')\} &= -4\tilde{s}_{\mathrm{r}4}\tilde{s}_{\mathrm{i}4}(\tilde{s}_{\mathrm{i}1}^2-\tilde{s}_{\mathrm{r}1}^2-\tilde{s}_{\mathrm{i}2}^2 \\ &\quad +\tilde{s}_{\mathrm{r}2}^2-\tilde{s}_{\mathrm{i}3}^2+\tilde{s}_{\mathrm{r}3}^2+\tilde{s}_{\mathrm{i}4}^2-\tilde{s}_{\mathrm{r}4}^2). \qquad (3.107)\end{aligned}$$

For (3.105) to be zero, both the real and imaginary parts (3.106) and (3.107) should be zero. For (3.107) to be zero, there are three possibilities:

a) If $\tilde{s}_{\mathrm{r}4} = 0$, then (3.107) is zero and the determinant value is given only by the real part (3.106). After some simplifications of (3.106), we have

$$\begin{aligned}\det(\mathbf{X}-\mathbf{X}') &= (\tilde{s}_{\mathrm{r}1}^2+\tilde{s}_{\mathrm{i}2}^2+\tilde{s}_{\mathrm{i}3}^2-\tilde{s}_{\mathrm{i}4}^2)^2 \\ &\quad +(\tilde{s}_{\mathrm{i}1}^2+\tilde{s}_{\mathrm{r}2}^2+\tilde{s}_{\mathrm{r}3}^2)(|\tilde{s}_1|^2+|\tilde{s}_2|^2+|\tilde{s}_3|^2+\tilde{s}_{\mathrm{r}1}^2+\tilde{s}_{\mathrm{i}2}^2 \\ &\quad +\tilde{s}_{\mathrm{i}3}^2+2\tilde{s}_{\mathrm{i}4}^2). \qquad (3.108)\end{aligned}$$

The last equation can be zero only when $\tilde{s}_{\mathrm{i}1} = 0, \tilde{s}_{\mathrm{r}2} = 0, \tilde{s}_{\mathrm{r}3} = 0$ and $\tilde{s}_{\mathrm{r}1}^2+\tilde{s}_{\mathrm{i}2}^2+\tilde{s}_{\mathrm{i}3}^2 = \tilde{s}_{\mathrm{i}4}^2$.

b) If $\tilde{s}_{\mathrm{i}4} = 0$, then (3.107) is zero again and, following similar steps as in the last case, we obtain from (3.106)

$$\begin{aligned}\det(\mathbf{X}-\mathbf{X}') &= (\tilde{s}_{\mathrm{i}1}^2+\tilde{s}_{\mathrm{r}2}^2+\tilde{s}_{\mathrm{r}3}^2-\tilde{s}_{\mathrm{r}4}^2)^2 \\ &\quad +(\tilde{s}_{\mathrm{r}1}^2+\tilde{s}_{\mathrm{i}2}^2+\tilde{s}_{\mathrm{i}3}^2)(|\tilde{s}_1|^2+|\tilde{s}_2|^2+|\tilde{s}_3|^2+\tilde{s}_{\mathrm{i}1}^2+\tilde{s}_{\mathrm{r}2}^2 \\ &\quad +\tilde{s}_{\mathrm{r}3}^2+2\tilde{s}_{\mathrm{r}4}^2). \qquad (3.109)\end{aligned}$$

The value of (3.109) can be zero only when $\tilde{s}_{\mathrm{r}1} = 0, \tilde{s}_{\mathrm{i}2} = 0, \tilde{s}_{\mathrm{i}3} = 0$ and $\tilde{s}_{\mathrm{i}1}^2 + \tilde{s}_{\mathrm{r}2}^2 + \tilde{s}_{\mathrm{r}3}^2 = \tilde{s}_{\mathrm{r}4}^2$.

c) Finally, if the following condition is true

$$\tilde{s}_{\mathrm{i}1}^2 + \tilde{s}_{\mathrm{r}2}^2 + \tilde{s}_{\mathrm{r}3}^2 + \tilde{s}_{\mathrm{i}4}^2 = \tilde{s}_{\mathrm{r}1}^2 + \tilde{s}_{\mathrm{i}2}^2 + \tilde{s}_{\mathrm{i}3}^2 + \tilde{s}_{\mathrm{r}4}^2, \tag{3.110}$$

then (3.107) is again zero. Using (3.110) with (3.106), we obtain

$$\begin{aligned} \det(\mathbf{X} - \mathbf{X}') &= (|\tilde{s}_1|^2 + |\tilde{s}_2|^2 + |\tilde{s}_3|^2)^2 - |\tilde{s}_4|^4 \\ &= (|\tilde{s}_1|^2 + |\tilde{s}_2|^2 + |\tilde{s}_3|^2 - |\tilde{s}_4|^2)(|\tilde{s}_1|^2 + |\tilde{s}_2|^2 + |\tilde{s}_3|^2 + |\tilde{s}_4|^2). \end{aligned} \tag{3.111}$$

As the second factor is never zero, the determinant is zero only when

$$|\tilde{s}_1|^2 + |\tilde{s}_2|^2 + |\tilde{s}_3|^2 = |\tilde{s}_4|^2. \tag{3.112}$$

Using (3.110) in (3.112), we obtain the same condition as in a) or b).

Since all the symbols are drawn from the same constellation points, there exists a combination in which a) or b) is fulfilled and therefore, (3.55) is zero.

Chapter 4

Distributed Space-Time Coding with Low-Rate Feedback in Relay Networks

In this chapter, we propose a simple distributed space-time coding approach to achieve maximum diversity with a low decoding and implementation complexity using a low-rate feedback [66–68].

4.1 Motivation and Preliminary Work

The performance of wireless communication systems can be severely limited due to channel fading effects. To combat fading, use of multi-antenna systems has been proposed, where the existence of independent paths between the transmitter and receiver can be exploited to achieve a higher degree of diversity than in single-antenna systems [26,51,69]. However, restrictions in size and hardware costs can make the use of multi-antenna systems impractical in wireless networks. Fortunately, similar independent paths are also available in wireless networks with multiple single-antenna nodes, where some nodes are used as relays that help to convey the information through the network. Using such relays between the transmitter and receiver nodes offers the so-called *cooperative diversity* and, hence, can be a good alternative to using multiple antennas at the transmitter and/or receiver. Several cooperation methods between network nodes have been proposed based on different relaying

strategies; see [4, 14, 25, 50, 58, 77, 78] and references therein.

Most of the proposed relaying strategies can be mainly classified into two categories: AF and DF. In the practical scenario, AF is more attractive because it does not require decoding at the relays and can be easily implemented.

The use of space-time codes (originally developed for multi-antenna systems [3,88]) in a distributed fashion has been proposed for relay networks in [40] and [50] using the AF approach. In this cooperative strategy, the source terminal first transmits the information symbols to the relays. Then, the relays encode their received signals and their conjugates in a linear fashion and transmit them to the destination node. This can be viewed as DSTC. The DSTC techniques only require the knowledge of the received signal powers at the relays and can achieve the maximum diversity available in the network.

In [41], OSTBCs [3, 86] and QOSTBCs [39, 85] have been used along with the DSTC strategy of [40]. Both these DSTC approaches have been shown to offer maximum diversity, optimal diversity products, low ML decoding complexity, linear encoding of the information symbols, and robustness against relay failures. Unfortunately, for more than two relays, the maximum rate of OSTBCs reduces [53], the decoding delay increases, and the linear ML decoding complexity is no longer achievable [41]. Furthermore, QOSTBCs are only applicable to particular cases with certain numbers of relays. In addition, their decoding complexity is higher than that of OSTBCs.

In [74], four-group decodable DSTCs for any number of relays are proposed. Although this approach reduces the decoding complexity of a DSTC as compared to the full ML decoder, its complexity is still rather high, especially in the case of more than four relays. To recover the simple symbol-by-symbol ML decoding property of the distributed OSTBCs for more than two relays, the use of backward (source to relay) CSI at the relays [41, 73]. However, as shown in [41], the use of this CSI at the relays (denoted as Network types 2 and 3 in [41]) does not improve the resulting diversity or coding gains.

Another promising approach to AF relaying in wireless networks is distributed beamforming; see [19,30,43,52] and references therein. As most of distributed beamforming techniques require the full knowledge of the instantaneous CSI for both the source-to-relay and relay-to-destination links and, moreover, require a feedback link

between the destination and relays, the complexities of these techniques are rather high. To decrease the distributed beamforming complexity, the use of quantized feedback for selecting beamforming weights from a codebook has been proposed in [47]. However, the codebook design requires a costly numerical optimization and the resulting codebook needs to be transmitted to each relay every time the channel statistics change.

A simple technique to coherently add the signals at the receiver in a sensor network was presented in [56]. However, to achieve convergence, a large number of iterations is needed and more feedback bits than the number of sensors is required.

The use of second-order statistics for power control has been studied in [30, 44]. The approach in [30] maximizes the average SNR, however it does not achieve full diversity. In [44], the power control coefficients were obtained through minimizing an upper bound on the average pairwise error probability in the case of two relays using the distributed Alamouti code. However, extensions of this approach to more higher number of relays are not straightforward.

4.2 System Model

Let us consider a half-duplex wireless relay network with $R+2$ nodes where each node has a single antenna that can transmit or receive signals. Among these $R+2$ nodes, one is the transmitter, one is the receiver, and the remaining R nodes are the relays, see Fig. 4.1. It is assumed that the direct link between the transmitter and the receiver can not be established due to the poor quality of the channel and that the relay channels are statistically independent. We consider the quasi-static flat fading channel case with the block length T, and denote the channel coefficient between the transmitter and the ith relay by f_i. Correspondingly, the channel coefficient between the ith relay and the receiver is denoted by g_i. We assume that f_i and g_i are independent random variables with the pdf's $\mathcal{CN}(\mu_{f_i}, \sigma_{f_i}^2)$ and $\mathcal{CN}(\mu_{g_i}, \sigma_{g_i}^2)$, respectively.

We assume that the transmitter does not have any CSI. However, we consider a low-rate feedback link between the receiver and each relay. This feedback link is used to transmit one bit for every channel realization and can be also used to transmit long-term power control weights (one per relay) every time the channel

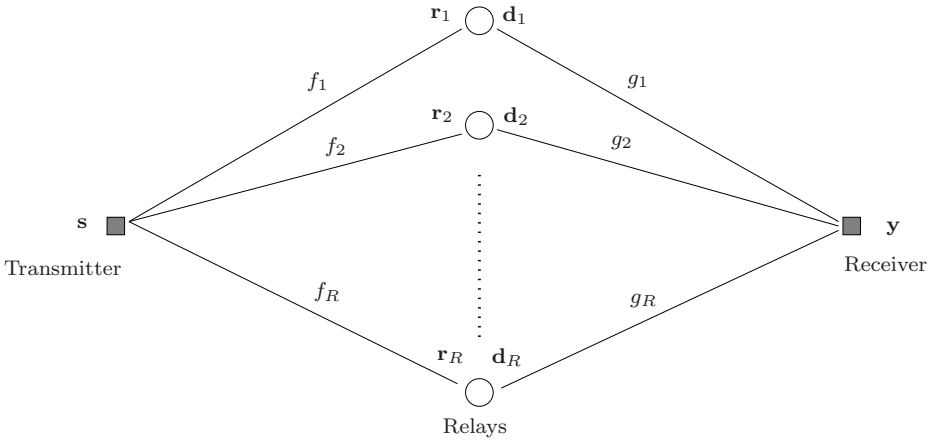

Figure 4.1: Wireless relay network with R relays.

means or variances change significantly. The receiver may or may not enjoy full CSI, depending on the transmission mode (coherent or non-coherent) and the system is synchronized at the symbol level.

The relays are considered to have a feedback link which is used to transmit one feedback bit for every channel realization. Also, in the power control scenario, the feedback link is used to transmit the power control weights (one per relay) every time the channel statistics change. The main idea behind using the one bit feedback is to provide the possibility of adding the signals at the receiver in a quasi-coherent way as presented in the next section.

At the transmitter side, T symbols $\mathbf{s} = [s_1, \ldots, s_T]^T$ are drawn from an M-point constellation according to the information bits to be sent. The signal $\mathbf{s}$ is normalized as $\mathrm{E}\{\mathbf{s}^H\mathbf{s}\} = 1$. The transmission is carried out in two steps. In the first step, the transmitter sends $\sqrt{P_0 T}\mathbf{s}$ from time 1 to T, where P_0 is its average transmitted power. The received signal at the ith relay is given by

$$\mathbf{r}_i = \sqrt{P_0 T} f_i \mathbf{s} + \mathbf{v}_i \tag{4.1}$$

where $\mathbf{v}_i$ is the noise vector at the ith relay. In the second step, the ith relay sends the signal $\mathbf{d}_i$ to the receiver from time $T+1$ to $2T$. At the receiver, we have

$$\mathbf{y} = \sum_{i=1}^{R} g_i \mathbf{d}_i + \mathbf{n} \tag{4.2}$$

where $\mathbf{y} = [y_1, \ldots, y_T]^T$ is the received signal and $\mathbf{n}$ is the receiver noise vector. We assume that the entries of the noise vectors $\mathbf{v}_i$ and $\mathbf{n}$ are i.i.d. random variables with the pdf $\mathcal{CN}(0, \sigma^2)$ and $\sigma^2 = 1$.

The transmitted signal $\mathbf{d}_i$ at each relay is assumed to be a linear function of its received signal and its conjugate [41], that is,

$$\begin{aligned}\mathbf{d}_i &= \sqrt{\frac{P_i}{m_{f_i} P_0 + 1}}\, b_i \theta_i (\mathbf{A}_i \mathbf{r}_i + \mathbf{B}_i \mathbf{r}_i^*) \\ &= \sqrt{\frac{P_0 P_i T}{m_{f_i} P_0 + 1}}\, b_i \theta_i (f_i \mathbf{A}_i \mathbf{s} + f_i^* \mathbf{B}_i \mathbf{s}^*) \\ &\quad + \sqrt{\frac{P_i}{m_{f_i} P_0 + 1}} b_i \theta_i (\mathbf{A}_i \mathbf{v}_i + \mathbf{B}_i \mathbf{v}_i^*) \end{aligned} \tag{4.3}$$

where

$$m_{f_i} \triangleq \mathrm{E}\{|f_i|^2\} = |\mu_{f_i}|^2 + \sigma_{f_i}^2 \tag{4.4}$$

$b_i \in \{-1, 1\}$ is a coefficient selected based on the value of the one-bit feedback, θ_i $(0 \leq \theta_i \leq 1)$ is a real-valued long-term power control weight that is adjusted according to the channel statistics (as it will be explained in Section 4.3.2), P_i is the maximum average transmitted power at the ith relay (while the actual power is $P_i \theta_i^2 \leq P_i$) and the $T \times T$ matrices $\mathbf{A}_i$ and $\mathbf{B}_i$ are assumed to be either $\mathbf{A}_i = \mathbf{O}$ with $\mathbf{B}_i$ being unitary, or $\mathbf{B}_i = \mathbf{O}$ with $\mathbf{A}_i$ being unitary. Here, $\mathbf{O}$ is the $T \times T$ matrix of zeros.

Using this model, let us introduce the following notations:

$$\text{If } \mathbf{B}_i = \mathbf{O} \text{ then } \tilde{\mathbf{A}}_i = \mathbf{A}_i,\ \tilde{f}_i = f_i,\ \tilde{\mathbf{v}} = \mathbf{v}_i,\ \tilde{\mathbf{s}}_i = \mathbf{s} \tag{4.5}$$

$$\text{If } \mathbf{A}_i = \mathbf{O} \text{ then } \tilde{\mathbf{A}}_i = \mathbf{B}_i,\ \tilde{f}_i = f_i^*,\ \tilde{\mathbf{v}} = \mathbf{v}_i^*,\ \tilde{\mathbf{s}}_i = \mathbf{s}^*. \tag{4.6}$$

Taking into account (4.3)-(4.6), the received signal model (4.2) can be written as

$$\mathbf{y} = \mathbf{S}(\mathbf{p} \odot \mathbf{h}) + \mathbf{w} \tag{4.7}$$

where

$$\mathbf{S} \triangleq [\tilde{\mathbf{A}}_1 \tilde{\mathbf{s}}_1, \ldots, \tilde{\mathbf{A}}_R \tilde{\mathbf{s}}_R] \tag{4.8}$$

is the distributed space-time code matrix,

$$\mathbf{h} = [h_1, \ldots, h_R]^T \triangleq [\tilde{f}_1 g_1, \ldots, \tilde{f}_R g_R]^T \tag{4.9}$$

is the equivalent channel vector,

$$\mathbf{w} = [w_1, \ldots, w_T]^T \triangleq \sum_{i=1}^{R} \sqrt{\frac{P_i}{m_{f_i} P_0 + 1}}\, b_i \theta_i g_i \tilde{\mathbf{A}}_i \tilde{\mathbf{v}}_i + \mathbf{n} \tag{4.10}$$

is the equivalent noise vector,

$$\mathbf{p} \triangleq \left[\sqrt{\frac{P_0 P_1 T}{m_{f_i} P_0 + 1}}\, b_1 \theta_1, \ldots, \sqrt{\frac{P_0 P_R T}{m_{f_R} P_0 + 1}}\, b_R \theta_R \right]^T \tag{4.11}$$

and $\odot$ denotes the Schur-Hadamard (element-wise) matrix product.

4.3 The Proposed Cooperative Scheme

In this section, we address the problem of selecting the coefficients b_i $(i = 1, \ldots, R)$ and the long-term power control weights θ_i $(i = 1, \ldots, R)$. We assume that the value of $\mathbf{p} \odot \mathbf{h}$ is known at the receiver and there is a perfect (error-free) low-rate feedback link between the receiver and the relays. We will first introduce the transmission strategy based on one-bit feedback per relay to choose the coefficients b_i for every channel realization. The proposed scheme is based on the ideas of partial phase combining [32, 57] and the group coherent codes [2] originally introduced for traditional multiple-antenna systems. It will be shown by means of an approximate symbol error rate (SER) analysis that the proposed low-rate feedback is sufficient to achieve maximum diversity with an additional power gain. Furthermore, the proposed scheme will be shown to enjoy linear decoding complexity and minimum decoding delay for any number of relays. In comparison to the technique proposed in [56], our scheme needs a lower, fixed number of feedback bits. Subsequently, a further improvement of this scheme will be considered using an additional long-term real-valued power control weight to feed back from the receiver to each relay. These weights will be computed using second-order channel statistics.

For the sake of simplicity, throughout this section we assume that $T = 1$. Hence, matrices $\mathbf{A}_i$ and $\mathbf{B}_i$ become scalars and it is assumed that $\mathbf{A}_i = 1$ and $\mathbf{B}_i = 0$. Correspondingly, $\mathbf{y}$, $\mathbf{v}_i$, $\mathbf{n}$, $\mathbf{w}$ and $\mathbf{s}$ become scalars as well. A more general case when $T > 1$ (and when $\mathbf{A}_i$ and $\mathbf{B}_i$ are matrices rather than scalars) will be considered in Section 4.4.

4.3.1 Using One-Bit Feedback Per Relay

As in the case of one-bit feedback the long-term power control is not taken into account, all the relays transmit with the maximum power P_i (i.e., $\theta_i = 1$ for $i = 1, \ldots, R$). In this particular case, the received signal model (4.7) reduces to

$$y = \mathbf{1}_R^T(\mathbf{p} \odot \mathbf{h})s + w \tag{4.12}$$

where $\mathbf{1}_R$ is the $R \times 1$ column vector of ones. For the sake of simplicity, the sub-indices in all scalar values are hereafter omitted.

Using (4.10) and (4.12), the noise power can be expressed as

$$\begin{aligned} P_w &= \mathrm{E}\{|n|^2\} + \sum_{i=1}^{R} \frac{P_i}{m_{f_i} P_0 + 1} \mathrm{E}\{|v_i|^2\} b_i^2 |g_i|^2 \\ &= 1 + \sum_{i=1}^{R} \frac{P_i}{m_{f_i} P_0 + 1} |g_i|^2. \end{aligned} \tag{4.13}$$

From (4.13) it is clear that the choice of b_i does not affect the noise power. Using (4.12), the signal power can be obtained as

$$\begin{aligned} P_s &= \left(\mathbf{1}_R^T(\mathbf{p} \odot \mathbf{h})\right)^* \left(\mathbf{1}_R^T(\mathbf{p} \odot \mathbf{h})\right) \mathrm{E}\{|s|^2\} \\ &= \left| \sum_{i=1}^{R} \sqrt{\frac{P_0 P_i}{m_{f_i} P_0 + 1}} b_i f_i g_i \right|^2 \\ &= \underbrace{\sum_{i=1}^{R} \rho_{i,i} |f_i g_i|^2}_{\gamma} + \underbrace{\sum_{\substack{i,j=1 \\ i \neq j}}^{R} \rho_{i,j} b_i b_j \mathrm{Re}\left\{ f_i g_i f_j^* g_j^* \right\}}_{\beta} \end{aligned} \tag{4.14}$$

where

$$\rho_{i,j} \triangleq \sqrt{\frac{T P_0 P_i}{m_{f_i} P_0 + 1}} \sqrt{\frac{T P_0 P_j}{m_{f_j} P_0 + 1}} \tag{4.15}$$

for $i, j = 1, \ldots, R$. In general, β can take negative values. Clearly, such negative values of β will reduce the received SNR and affect the achieved diversity. Our key idea here is to use the coefficients b_i to ensure that β is always non-negative. It can be proved using the same approach as presented in [2] that using values of $b_i \in \{-1, 1\}$ is sufficient to guarantee $\beta \geq 0$. This results in a scheme with the diversity order proportional to R, as stated in the following proposition.

Proposition 4.3.1. *If $\beta \geq 0$, then the average symbol error probability ($\overline{\text{SER}}$) for* (4.12) *can be upper bounded by*

$$\overline{\text{SER}} \leq \kappa P^{-R(1-\frac{\log\log P}{\log P})} \tag{4.16}$$

for large R and large P, where P is the total power in the network and κ is a constant.

Proof. The SER for (4.12) is given by [84]

$$\text{SER} = c_1 Q\left(\sqrt{c_2 \frac{P_s}{P_w}}\right) \tag{4.17}$$

where c_1 and c_2 are two constants that depend on the constellation used, and

$$Q(x) = \frac{1}{\sqrt{2\pi}} \int_x^\infty e^{-t^2/2} dt. \tag{4.18}$$

Using the Chernoff bound, we have

$$\overline{\text{SER}} \leq \frac{c_1}{2} \text{E}_{f_i,g_i}\left\{e^{-c_2 \frac{P_s}{2P_w}}\right\}. \tag{4.19}$$

Note that if we establish an upper bound for $\beta = 0$, then it will be also valid for any $\beta > 0$. This follows from the fact that $Q(x)$ is a monotonically decreasing function. Using this fact, let us obtain an upper bound on $\overline{\text{SER}}$ by using the particular value $\beta = 0$. Then, from (4.19) we obtain

$$\overline{\text{SER}} \leq \frac{c_1}{2} \text{E}_{f_i,g_i}\left\{e^{-c_2 \frac{\gamma}{2P_w}}\right\}. \tag{4.20}$$

First, let us calculate the expected value over the channel coefficients f_i. As these coefficients are statistically independent, each term in the sum for γ can be calculated independently. Using the complex Gaussian pdf for f_i

$$p_{f_i}(f_i) = \frac{1}{\pi\sigma_{f_i}^2} e^{-|f_i - \mu_{f_i}|^2/\sigma_{f_i}^2} \tag{4.21}$$

and defining

$$a_i \triangleq \frac{c_2 |g_i|^2 \rho_{i,i}}{2P_w} \tag{4.22}$$

we obtain from (4.20) that

$$\overline{\text{SER}} \leq \frac{c_1}{2} \text{E}_{g_i}\left\{\prod_{i=1}^{R} \Upsilon_i\right\} \tag{4.23}$$

where

$$\Upsilon_i \triangleq \frac{1}{\pi\sigma_{f_i}^2}\int_{-\infty}^{\infty} e^{-a_i|f_i|^2-|f_i-\mu_{f_i}|^2/\sigma_{f_i}^2}\,df_i. \tag{4.24}$$

After straightforward manipulations, (4.24) can be rewritten as

$$\Upsilon_i = \frac{1}{a_i\sigma_{f_i}^2+1} e^{-\frac{|\mu_{f_i}|^2}{\sigma_{f_i}^2}\left(\frac{a_i\sigma_{f_i}^2}{a_i\sigma_{f_i}^2+1}\right)} \int_{-\infty}^{\infty} \frac{a_i\sigma_{f_i}^2+1}{\pi\sigma_{f_i}^2}\, e^{-\frac{(a_i\sigma_{f_i}^2+1)}{\sigma_{f_i}^2}\left|f_i-\frac{\mu_{f_i}}{(a_i\sigma_{f_i}^2+1)}\right|^2} df_i. \tag{4.25}$$

The function inside the integral in (4.25) is equal to the complex Gaussian pdf $\mathcal{CN}\left(\frac{\mu_{f_i}}{a_i\sigma_{f_i}^2+1}, \frac{\sigma_{f_i}^2}{a_i\sigma_{f_i}^2+1}\right)$. Therefore, the integral in (4.25) is equal to one and we obtain that

$$\Upsilon_i = \frac{1}{a_i\sigma_{f_i}^2+1} e^{-\phi_{f_i}\left(\frac{a_i\sigma_{f_i}^2}{a_i\sigma_{f_i}^2+1}\right)} \tag{4.26}$$

where $\phi_{f_i} = |\mu_{f_i}|^2/\sigma_{f_i}^2$. An upper-bound approximation for the expected value in (4.23) can be derived as follows. Since $a_i \geq 0$, we have that

$$0 \leq \frac{a_i\sigma_{f_i}^2}{a_i\sigma_{f_i}^2+1} < 1. \tag{4.27}$$

Therefore, Υ_i can be upper-bounded as $\Upsilon_i \leq 1/(a_i\sigma_{f_i}^2+1)$ and

$$\overline{\mathrm{SER}} \leq \frac{c_1}{2}\mathrm{E}_{g_i}\left\{\prod_{i=1}^{R}\frac{1}{a_i\sigma_{f_i}^2+1}\right\}. \tag{4.28}$$

Let us characterize the power of each transmitting node P_i $(i = 0,\ldots,R)$ as a fraction $P_i = \lambda_i P$ of the total power $P = \sum_{i=0}^{R} P_i$, where $\sum_{i=0}^{R}\lambda_i = 1$. If R is large, then, according to the law of large numbers,

$$\sum_{i=1}^{R}\frac{\lambda_i|g_i|^2}{m_{f_i}\lambda_0 + P^{-1}} \leq \; R\alpha \tag{4.29}$$

where the inequality is satisfied in the almost sure sense,

$$\alpha \triangleq \max_{i=1,\ldots,R}\left(\frac{\lambda_i m_{g_i}}{m_{f_i}\lambda_0 + P^{-1}}\right) \tag{4.30}$$

and $m_{g_i} \triangleq \mathrm{E}\{|g_i|^2\} = |\mu_{g_i}|^2 + \sigma_{g_i}^2$. Therefore, from (4.13) and (4.22), we have that

$$\frac{1}{a_i\sigma_{f_i}^2+1} = \frac{1}{\frac{c_2\sigma_{f_i}^2|g_i|^2\rho_{i,i}}{2P_w}+1} \leq \frac{1}{\frac{c_2\sigma_{f_i}^2|g_i|^2\rho_{i,i}}{2(1+R\alpha)}+1}. \tag{4.31}$$

Using (4.15) and (4.31), from (4.28) we obtain that

$$\overline{\mathrm{SER}} \leq \frac{c_1}{2} \mathrm{E}_{g_i} \left\{ \prod_{i=1}^{R} \frac{1}{\bar{a}_i P |g_i|^2 + 1} \right\} \tag{4.32}$$

where

$$\bar{a}_i \triangleq \frac{c_2 \sigma_{f_i}^2 \lambda_0 \lambda_i}{2(m_{f_i} \lambda_0 + 1/P)(1 + R\alpha)}. \tag{4.33}$$

From (4.32) and the fact that all the channel coefficients are statistically independent, it can be readily seen that for each i the expectation over g_i in the right-hand side can be calculated independently from the other values g_l, $l \neq i$. The random variable $z_i = |g_i|^2$ has the non-central chi-square pdf with two degrees of freedom (see Section 4.A):

$$p_{|g_i|^2}(z_i) = \frac{1}{\sigma_{g_i}^2} e^{-\frac{z_i + |\mu_{g_i}|^2}{\sigma_{g_i}^2}} I_0 \left(\frac{2|\mu_{g_i}| \sqrt{z_i}}{\sigma_{g_i}^2} \right). \tag{4.34}$$

Using (4.34) to compute the expectation in (4.32), we have

$$\overline{\mathrm{SER}} \leq \frac{c_1}{2} \prod_{i=1}^{R} \bar{\Upsilon}_i \tag{4.35}$$

where

$$\begin{aligned} \bar{\Upsilon}_i &\triangleq \int_0^\infty \frac{1}{\bar{a}_i P z_i + 1} \, p_{|g_i|^2}(z_i) \, dz_i \\ &= e^{-\phi_{g_i}} \int_0^\infty \frac{e^{-x_i}}{(\bar{a}_i P \sigma_{g_i}^2 x_i + 1)} I_0 \left(2\sqrt{\phi_{g_i} x_i} \right) dx_i \end{aligned} \tag{4.36}$$

$x_i \triangleq z_i / \sigma_{g_i}^2$ and $\phi_{g_i} \triangleq |\mu_{g_i}|^2 / \sigma_{g_i}^2$. Let us break up the integral (4.36) into two terms as $\int_0^\infty = \int_0^{1/P} + \int_{1/P}^\infty$ and use the following results from [44] to approximate $\bar{\Upsilon}_i$:

$$\int_0^{1/P} e^{-x_i} I_0 \left(2\sqrt{\phi_{g_i} x_i} \right) dx_i = \frac{1}{P} + \mathcal{O}(P^{-2}) \approx \frac{1}{P} \tag{4.37}$$

$$\int_{1/P}^\infty x_i^{-1} e^{-x_i} I_0 \left(2\sqrt{\phi_{g_i} x_i} \right) dx_i = E_1(P^{-1}) + \sum_{k=1}^{\infty} \frac{\phi_{g_i}^k}{k! k} \tag{4.38}$$

where

$$E_1(q) \triangleq -\tilde{c} - \log q - \sum_{k=1}^{\infty} \frac{(-1)^k q^k}{k! k} \tag{4.39}$$

for $q > 0$, and $\tilde{c}$ denotes the Euler's constant. Note that if $\log P \gg 1$, then

$$E_1(P^{-1}) \approx \log P. \tag{4.40}$$

Using the latter fact, from (4.36)-(4.38) we obtain for the case of large P that

$$\overline{\text{SER}} \leq \frac{c_1}{2} \prod_{i=1}^{R} \frac{e^{-\phi_{g_i}}}{\bar{a}_i \sigma_{g_i}^2} \frac{(\log P + q_i)}{P} \tag{4.41}$$

where

$$q_i \triangleq \bar{a}_i \sigma_{g_i}^2 + \sum_{k=1}^{\infty} \frac{\phi_{g_i}^k}{k! k}. \tag{4.42}$$

Defining

$$\kappa \triangleq \frac{c_1}{2} \prod_{i=1}^{R} \frac{e^{-\phi_{g_i}}}{\bar{a}_i \sigma_{g_i}^2} \tag{4.43}$$

and using the properties of the logarithm, we can rewrite (4.41) as

$$\overline{\text{SER}} \leq \kappa \left(P^{-R(1-\frac{\log\log P}{\log P})} + \left(\prod_{i=1}^{R} q_i \right) P^{-R} \right). \tag{4.44}$$

For large values of P, the first term in the sum in (4.44) will dominate. Hence, Proposition 1 is proved. □

It follows from Proposition 1 that the achievable diversity order of the proposed scheme is R.

Since positive values of β will provide an additional signal power gain, the optimal values of b_i $(i = 1, \ldots, R)$ can be obtained through maximizing β. This is an integer maximization problem that requires a full search over all possible values of b_i. Clearly, if the number of relays is large, then such a full search procedure can be impractical. To reduce the complexity, we propose a near-optimal solution based on SDR, that we denote hereafter as *Algorithm 1.*

Note that, according to (4.14), the choice of b_i does not affect the value of γ. Therefore, to maximize P_s, it is sufficient to maximize β in (4.14). Let us express P_s in a more convenient form by extending the notation for $\rho_{i,j}$ in (4.15) with

$$\rho_{i,0} \triangleq \sqrt{\frac{P_i P_0 T}{m_{f_i} P_0 + 1}} \tag{4.45}$$

and denoting

$$\bar{\mathbf{h}} \triangleq [\rho_{1,0} f_1 g_1, \ldots, \rho_{R,0} f_R g_R]^T . \tag{4.46}$$

Using (4.46), the signal power (4.14) can be expressed as

$$P_s = |\bar{\mathbf{h}}^H \mathbf{b}|^2$$

where $\mathbf{b} \triangleq [b_1, \ldots, b_R]^T$. Defining

$$\bar{\mathbf{Q}} \triangleq \bar{\mathbf{h}} \bar{\mathbf{h}}^H \tag{4.47}$$

we can write the optimization problem as

$$\max_{\mathbf{b} \in \{-1,1\}^R} \mathbf{b}^T \bar{\mathbf{Q}} \mathbf{b}. \tag{4.48}$$

As $\mathbf{b}^T \bar{\mathbf{Q}} \mathbf{b} = \mathrm{tr}(\mathbf{b}\mathbf{b}^T \bar{\mathbf{Q}})$, the optimization problem in (4.48) can be rewritten as

$$\begin{aligned} \max_{\mathbf{B}} \mathrm{tr}(\mathbf{B}\bar{\mathbf{Q}}) \quad \text{s.t.} \quad & \mathrm{rank}\{\mathbf{B}\} = 1, \quad \mathbf{B} \succeq 0 \\ & [\mathbf{B}]_{i,i} = 1, \quad i = 1, \ldots, R \end{aligned} \tag{4.49}$$

where

$$\mathbf{B} \triangleq \mathbf{b}\mathbf{b}^T, \quad \mathbf{b} \in \mathbb{R}^R \tag{4.50}$$

and $\mathbf{B} \succeq 0$ means that $\mathbf{B}$ is positive semi-definite. Problems similar to (4.49) arise in the context of ML detection. Solutions close to the optimal one can be efficiently found using the SDR approach [54], whose essence is to omit the rank-one constraint $\mathrm{rank}\{\mathbf{B}\} = 1$ in (4.49) and, therefore, approximate the latter non-convex problem by a convex problem

$$\begin{aligned} \max_{\mathbf{B}} \mathrm{tr}(\mathbf{B}\bar{\mathbf{Q}}) \quad \text{s.t.} \quad & [\mathbf{B}]_{i,i} = 1, \ i = 1, \ldots, R \\ & \mathbf{B} \succeq 0. \end{aligned} \tag{4.51}$$

Thus, our SDR-based approach can be summarized as follows.

Algorithm 1

1. At the receiver, find the solution to (4.51) using the approach of [54].
2. Send the so-obtained b_i from the receiver to the ith relay node for each $i = 1, \ldots, R$ using one-bit per relay feedback.

As it will be shown throughout our simulations, the use of the SDR approach results in a performance that is very close to that of the full search-based approach. The complexity of the SDR approach is much lower than that of the full search; see [54] for details.

To further reduce the complexity, let us discuss a simpler algorithm to obtain acceptable values of b_i that can be formulated using the general idea of [2]. The essence of this algorithm is to use a greedy selection of the values of b_i in a consecutive way. This algorithm can be summarized as the following sequence of steps:

Algorithm 2

1. Set $b_1 = 1$ and $\tau_1 = h_1$.
2. For $i = 2, \ldots, R$, compute

$$b_i = \text{sign}(\text{Re}\{h_i^* \tau_{i-1}\}) \tag{4.52}$$

$$\tau_i = \tau_{i-1} + b_i h_i \tag{4.53}$$

   where $\text{sign}(\cdot)$ is the sign function.
3. Send the so-obtained b_i from the receiver to the ith relay node for each $i = 1, \ldots, R$ using one-bit per relay feedback.

Note that Algorithm 2 does not result in the optimal values of b_i, $i = 1, \ldots, R$. However, Algorithm 2 is computationally much simpler than Algorithm 1. Hence, these two alternative techniques are expected to provide different performance-to-complexity tradeoffs.

4.3.2 Choosing Long-Term Power Control Weights

So far, we have not considered the use of power control weights, θ_i, for each relay. In practical scenarios, relays are distributed randomly in an area between the transmitter and the receiver. As a result, the power loss characteristics in the source-to-relay and relay-to-destination links are different for each relay. Furthermore, different relays may have different transmitted power constraints. Therefore, in such scenarios, some power control strategy should be employed to take into account such differences in channel quality and/or constraints on the relay transmitted power.

From the performance viewpoint, the power control weights should be designed by minimizing the error probability as it was proposed in [44] for a two-relay network using the distributed Alamouti code. However, the approach of [44] does not provide any easy extension to the case of more than two relays. As an alternative, we propose to use the general idea of [30] to obtain the power control weights by maximizing the average SNR subject to individual power constraints. However, we will show that in contrast to [30], full diversity can be achieved in our case only when using the optimal feedback values b_i along with the coefficients θ_i.

First, let us evaluate the average signal power, that is

$$\mathrm{E}\{P_s\} = \mathrm{E}\{\tilde{\gamma}\} + \mathrm{E}\{\tilde{\beta}\} \tag{4.54}$$

where

$$\tilde{\gamma} \triangleq \sum_{i=1}^{R} \rho_{i,i}\theta_i^2 |f_i g_i|^2 \tag{4.55}$$

$$\tilde{\beta} \triangleq \sum_{\substack{i,j=1 \\ i\neq j}}^{R} \rho_{i,j}\theta_i\theta_j b_i b_j \mathrm{Re}\left\{f_i g_i f_j^* g_j^*\right\}. \tag{4.56}$$

Note that in (4.54), the analytical evaluation of $\mathrm{E}\{\tilde{\beta}\}$ is very difficult due to the dependence of b_i $(i = 1, \ldots, R)$ on the instantaneous channel values. Therefore, using (4.55)-(4.56) and assuming that the optimal $b_i (i = 1, \ldots, R)$ are selected, we propose to approximate (4.54) as

$$\mathrm{E}\{P_s\} \approx \sum_{i,j=1}^{R} \rho_{i,j}\theta_i\theta_j |\mathrm{Re}\left\{\mathrm{E}\{f_i g_i f_j^* g_j^*\}\right\}|. \tag{4.57}$$

The quality of this approximation for our optimization problem was verified by means of extensive Monte-Carlo simulations. In Fig. 4.2, we plot the difference between the exact achieved average SNR with optimal θ_i (computed numerically via brute force optimization) and the one achieved with θ_i computed via (4.57) versus the number of relays. Our simulations have involved different channel scenarios, randomly generated channel coefficients for each particular scenario, and different numbers of relays lying in the interval $R = 2, \ldots, 7$. As can be observed from Fig. 4.2, the difference is, in average, less than 2.5%.

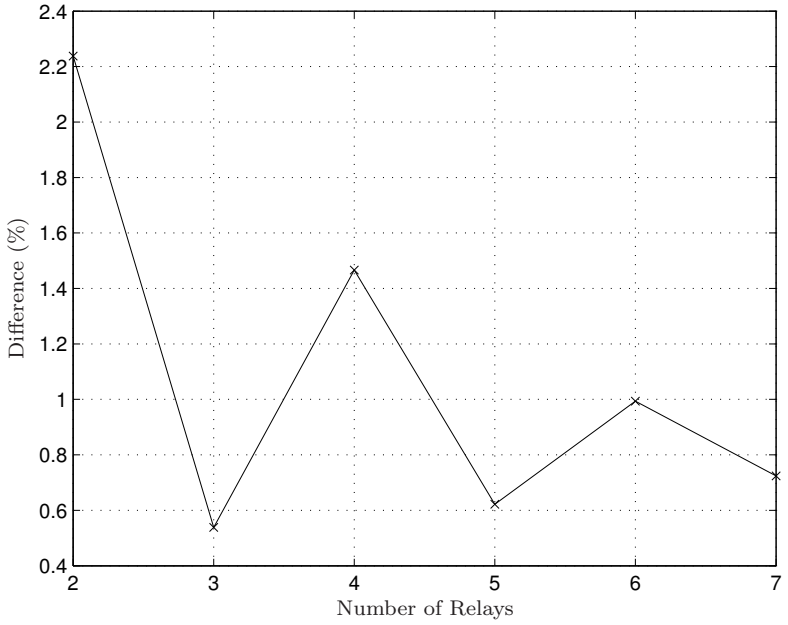

Figure 4.2: Difference between the exact optimal SNR and its approximation.

Using the statistical independence of all source-to-relay and relay-to-destination channels, we can now estimate the expected value in (4.57) as

$$\begin{aligned}\mathrm{E}\{f_i g_i f_j^* g_j^*\} &= \mathrm{E}\{f_i f_j^*\}\mathrm{E}\{g_i g_j^*\} \\ &= (\mu_{f_i}\mu_{f_j}^* + \delta_{ij}\sigma_{f_i}^2)(\mu_{g_i}\mu_{g_j}^* + \delta_{ij}\sigma_{g_i}^2)\end{aligned} \tag{4.58}$$

where δ_{ij} is the Kronecker delta.

Let us define the real-valued matrix $\mathbf{Q}$ with the (i,j) entry as

$$[\mathbf{Q}]_{i,j} = \rho_{i,j}\left|\mathrm{Re}\left\{(\mu_{f_i}\mu_{f_j}^* + \delta_{ij}\sigma_{f_i}^2)(\mu_{g_i}\mu_{g_j}^* + \delta_{ij}\sigma_{g_i}^2)\right\}\right| \tag{4.59}$$

for $i, j = 1, \ldots, R$. Using (4.58) and (4.59), equation (4.57) can be written as

$$\mathrm{E}\{P_s\} \approx \boldsymbol{\theta}^T\mathbf{Q}\boldsymbol{\theta} \tag{4.60}$$

where

$$\boldsymbol{\theta} \triangleq [\theta_1, \ldots, \theta_R]^T. \tag{4.61}$$

Using the fact that the noise waveforms and the channel coefficients are statistically

independent, the noise power can be expressed as

$$\begin{aligned}\mathrm{E}\{P_w\} &= \mathrm{E}\{|n|^2\} + \sum_{i=1}^{R} \frac{\theta_i^2 P_i}{m_{f_i} P_0 + 1} \mathrm{E}\{|v_i|^2\}\mathrm{E}\{|g_i|^2\} \\ &= 1 + \sum_{i=1}^{R} \frac{\theta_i^2 P_i m_{g_i}}{m_{f_i} P_0 + 1} \end{aligned} \tag{4.62}$$

and further rewritten as

$$\mathrm{E}\{P_w\} = \boldsymbol{\theta}^T \mathbf{W} \boldsymbol{\theta} + 1 \tag{4.63}$$

where

$$\mathbf{W} \triangleq \mathrm{diag}\left(\frac{m_{g_1} P_1}{m_{f_1} P_0 + 1}, \ldots, \frac{m_{g_R} P_R}{m_{f_R} P_0 + 1} \right)$$

and $\mathrm{diag}\,(\cdot)$ denotes a diagonal matrix. Using (4.60) and (4.63), the maximization of the receiver SNR over $\boldsymbol{\theta}$ can be approximately written as

$$\max_{\boldsymbol{\theta}} \frac{\boldsymbol{\theta}^T \mathbf{Q} \boldsymbol{\theta}}{\boldsymbol{\theta}^T \mathbf{W} \boldsymbol{\theta} + 1} \qquad \text{s.t.} \quad \theta_i^2 \leq 1, \quad i = 1, \ldots, R \tag{4.64}$$

where instead of the signal power we use its approximation given by (4.57).

If the aggregate power constraint ($\boldsymbol{\theta}^T \boldsymbol{\theta} = R$) is used instead of the individual relay power constraints in (4.64), the resulting problem becomes

$$\max_{\boldsymbol{\theta}} \frac{\boldsymbol{\theta}^T \mathbf{Q} \boldsymbol{\theta}}{\boldsymbol{\theta}^T (\mathbf{W} + (1/R)\mathbf{I}_R) \boldsymbol{\theta}} \qquad \text{s.t.} \quad \boldsymbol{\theta}^T \boldsymbol{\theta} = R. \tag{4.65}$$

Solving (4.65) amounts to the unconstrained optimization of the objective function in (4.65) (that boils down to solving a generalized eigenvector problem) followed by rescaling the so-obtained vector $\boldsymbol{\theta}$ to satisfy the constraint $\boldsymbol{\theta}^T \boldsymbol{\theta} = R$.

In what follows, we consider a more practical case of individual power constraints rather than the aggregate power constraint.

As mentioned above, the design of power control weights by maximizing the average SNR does not take into account the diversity aspect of the problem. In fact, maximizing the average SNR can result in a solution with a poor performance in terms of the error probability. This can particularly be the case if some of the resulting values of θ_i are small, so that the diversity order suffers. In Fig. 4.3, we show an example, where the BER as a function of P is shown for $R = 10$ relays and $4-$QAM modulation. The relays are randomly located between the source and destination, without LOS, i.e., the channels are zero-mean but have different

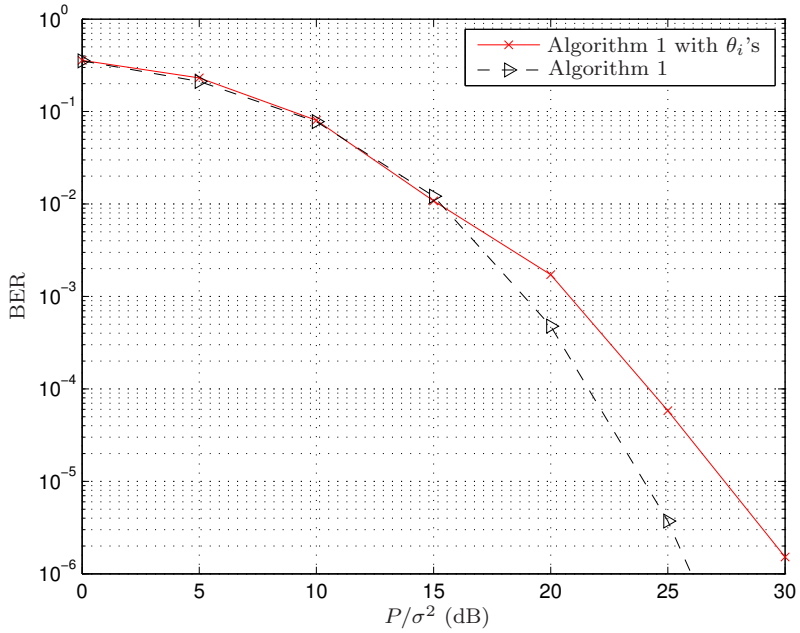

Figure 4.3: Diversity order loss using optimized weights θ_i without $\bar{\theta}_i$.

variances. As can be verified from the figure, the scheme using the optimized weights θ_i and b_i's has a lower diversity order than the scheme that sets $\theta_i = 1$, i.e., the one that only uses the b_i values.

In order to prevent such a loss of diversity, an additional constraint $\theta_i^2 \geq \bar{\theta}_i^2$ can be used where $\bar{\theta}_i^2$ is a preselected minimum weight value that establishes a tradeoff between the diversity and the performance with power control. If $\bar{\theta}_i$ is chosen too large, then the interval for θ_i will be smaller, and this may prevent the scheme from achieving a significant improvement in performance with power control. Reversely, if $\bar{\theta}_i$ is chosen too small, a substantial diversity loss can occur.

Defining $\mathbf{\Theta} \triangleq \boldsymbol{\theta}\boldsymbol{\theta}^T$, we can rewrite (4.64) as

$$\max_{\mathbf{\Theta}} \frac{\mathrm{tr}(\mathbf{Q}\mathbf{\Theta})}{\mathrm{tr}(\mathbf{W}\mathbf{\Theta}) + 1} \quad \text{s.t. } \bar{\theta}_i^2 \leq [\mathbf{\Theta}]_{i,i} \leq 1, \quad i = 1, \ldots, R \\ \mathrm{rank}\{\mathbf{\Theta}\} = 1, \quad \mathbf{\Theta} \succeq 0. \tag{4.66}$$

Introducing the auxiliary variable t, (4.66) can be written as

$$\begin{aligned} \max_{\boldsymbol{\Theta},t} t \quad \text{s.t.} \quad & \operatorname{tr}(\boldsymbol{\Theta}(\mathbf{Q}-t\mathbf{W})) \geq t \\ & \bar{\theta}_i^2 \leq [\boldsymbol{\Theta}]_{i,i} \leq 1, \quad i=1,\ldots,R \\ & \operatorname{rank}\{\boldsymbol{\Theta}\}=1, \quad \boldsymbol{\Theta} \succeq 0. \end{aligned} \tag{4.67}$$

As the rank constraint in (4.67) is non-convex, this optimization problem can not be solved efficiently. Using the SDR approach (i.e., ignoring the constraint $\operatorname{rank}\{\boldsymbol{\Theta}\} = 1$ in (4.67)), a quasi-convex optimization problem can be obtained from (4.67) that can be directly solved using the bisection technique [8, 30]. Based on the latter technique, the optimal value t_{opt} is found in the interval $[t_{\text{low}}, t_{\text{up}}]$, where t_{low} is a feasible value and therefore, $t_{\text{opt}} \geq t_{\text{low}}$, and t_{up} is not a feasible value and therefore, $t_{\text{opt}} \leq t_{\text{up}}$. The algorithm solves the feasibility problem

$$\begin{aligned} \text{find } \boldsymbol{\Theta} \qquad \text{s.t.} \qquad & \operatorname{tr}(\boldsymbol{\Theta}(\mathbf{Q}-t\mathbf{W})) \geq t, \quad \boldsymbol{\Theta} \succeq 0 \\ & \bar{\theta}_i^2 \leq [\boldsymbol{\Theta}]_{i,i} \leq 1, \quad i=1,\ldots,R \end{aligned} \tag{4.68}$$

at the midpoint of the interval, $t = (t_{\text{low}} + t_{\text{up}})/2$. If it is feasible, t_{low} is updated as $t_{\text{low}} = t$. If it is not feasible, t_{up} is updated as $t_{\text{up}} = t$. Then, the algorithm continues to solve the feasibility problem with the new interval until $t_{\text{up}} - t_{\text{low}} < \epsilon$, where ϵ is a parameter denoting the acceptable tolerance of the solution. The optimal matrix $\boldsymbol{\Theta}_{\text{opt}}$ is selected as $\boldsymbol{\Theta}$ for the last feasible t, (i.e., $t = t_{\text{low}}$ in the last step). If the matrix $\boldsymbol{\Theta}_{\text{opt}}$ is rank-one, then its principal eigenvector is the optimal solution to (4.64). If $\boldsymbol{\Theta}_{\text{opt}}$ is not rank-one, then a proper approximate solution for $\boldsymbol{\theta}$ can be obtained using randomization techniques [83].

4.4 Extended Distributed Alamouti Code

The scheme developed in the previous section applies to the case of $T = 1$. In what follows, we extend it to the case of $T = 2$ by developing an approach based on the distributed Alamouti code to reduce the total feedback rate. Using computer simulations, the latter scheme will be shown to provide robustness against feedback errors. Such improvements in the feedback rate and robustness are, however, achieved at the price of an increased decoding delay and a moderate performance loss as compared to the case of $T = 1$.

Let us consider the case of an even number of relays[1], i.e., let $R = 2K$ where K is some positive integer. The distributed Alamouti code is used by relay pairs. Let each kth relay pair receive a low-rate feedback to select the binary coefficient $b_k \in \{-1, 1\}$ and the real-valued power control coefficient $\theta_k \in [0, 1]$. Since the same b_k and θ_k should be used by the two relays of the kth relay pair, the receiver can broadcast them to both these relays, thereby reducing the feedback rate almost by half.

The relays use the basic distributed Alamouti code matrices [41] to form the signal transmitted by each relay pair as:

$$\tilde{\mathbf{A}}_{2k-1} = \mathbf{I}_2 \quad \text{with} \quad \mathbf{B}_{2k-1} = \mathbf{O} \tag{4.69}$$

$$\tilde{\mathbf{A}}_{2k} = \begin{bmatrix} 0 & -1 \\ 1 & 0 \end{bmatrix} \quad \text{with} \quad \mathbf{A}_{2k} = \mathbf{O}. \tag{4.70}$$

Using (4.7)-(4.11), we obtain the following distributed space-time code matrix for the proposed scheme:

$$\mathbf{S} = [\mathbf{S}_a, \cdots, \mathbf{S}_a] \tag{4.71}$$

where

$$\mathbf{S}_a = \begin{bmatrix} s_1 & -s_2^* \\ s_2 & s_1^* \end{bmatrix} \tag{4.72}$$

is the conventional Alamouti code matrix.

The channel and relay power vectors are given by

$$\mathbf{h} = [f_1 g_1, f_2^* g_2, \ldots, f_{2K-1} g_{2K-1}, f_{2K}^* g_{2K}]^T \tag{4.73}$$

$$\begin{aligned} \mathbf{p} &= [p_1, p_2, \ldots, p_{2K-1}, p_{2K}]^T \\ &= \left[\sqrt{\frac{P_0 P_1 T}{m_{f_1} P_0 + 1}}\, b_1\theta_1, \ldots, \sqrt{\frac{P_0 P_{2K} T}{m_{f_{2K}} P_0 + 1}}\, b_K \theta_K \right]^T \end{aligned} \tag{4.74}$$

respectively.

Note that in contrast to (4.11), any $(2k-1)$th and $(2k)$th relays use the same $b_k\theta_k$.

Conjugating the second entry y_2 of the vector $\mathbf{y} = [y_1, y_2]^T$ in (4.7) and using (4.71)-(4.74), we obtain the following equivalent model

$$\breve{\mathbf{y}} = \mathbf{H}\breve{\mathbf{s}} + \breve{\mathbf{w}} \tag{4.75}$$

[1]The case of an odd number of relays can be addressed in the same way and, therefore, is omitted below.

where

$$\breve{\mathbf{y}} \triangleq [y_1, y_2^*]^T \tag{4.76}$$

$$\breve{\mathbf{s}} \triangleq [s_1, s_2^*]^T \tag{4.77}$$

$$\breve{\mathbf{w}} \triangleq [w_1, w_2^*]^T \tag{4.78}$$

$$\mathbf{H} = \sum_{k=1}^{K} \mathbf{H}_k \tag{4.79}$$

$$\mathbf{H}_k = \begin{bmatrix} p_{2k-1}h_{2k-1} & -p_{2k}h_{2k} \\ p_{2k}h_{2k}^* & p_{2k-1}h_{2k-1}^* \end{bmatrix}. \tag{4.80}$$

Note that

$$\mathbf{H}^H\mathbf{H} = \begin{bmatrix} \gamma_a + \beta_a & 0 \\ 0 & \gamma_a + \beta_a \end{bmatrix} \tag{4.81}$$

where

$$\gamma_a \triangleq \|(\mathbf{p} \odot \mathbf{h})\|^2 \tag{4.82}$$

$$\beta_a \triangleq \sum_{i,j=1, i\neq j}^{K} \theta_i b_i \theta_j b_j \mathrm{Re}\{\rho_{2i-1,2j-1} h_{2i-1} h_{2j-1}^* + \rho_{2i,2j} h_{2i} h_{2j}^*\}. \tag{4.83}$$

Throughout (4.71)-(4.83), the subindex $(\cdot)_a$ stands for the extended Alamouti scheme.

Since the matrices $\tilde{\mathbf{A}}_i$ satisfy the property $\tilde{\mathbf{A}}_i\tilde{\mathbf{A}}_i^H = \mathbf{I}_T$, the noise covariance matrix $\mathbf{R}_{\breve{\mathbf{w}}} \triangleq \mathrm{E}\{\breve{\mathbf{w}}\breve{\mathbf{w}}^H\}$ is a scaled identity matrix. Therefore, the ML decoding

$$\arg\min_{\breve{\mathbf{s}}} \|\breve{\mathbf{y}} - \mathbf{H}\breve{\mathbf{s}}\| \tag{4.84}$$

reduces to simple symbol-by-symbol decoding.

As $|h_k|^2 = |\tilde{f}_k g_k|^2$, it is clear from (4.82), (4.83) and Proposition 1 that the maximum diversity can be achieved if $\beta_a \geq 0$. Similar to [2], it can be proved that if $b_k \in \{-1, 1\}$, it can be guaranteed that $\beta_a \geq 0$.

As in Section 4.3, the coefficients b_k can be selected using the exhaustive full search, a suboptimal SDR approach similar to Algorithm 1, or an iterative procedure similar to Algorithm 2. To develop the SDR approach for the extended distributed Alamouti code case, we define the $K \times 1$ vector

$$\mathbf{b}_a \triangleq [b_1, \ldots, b_K]^T \tag{4.85}$$

and the $2 \times K$ matrix

$$\mathbf{F} \triangleq \begin{bmatrix} p_1 h_1 & p_3 h_3 & \cdots & p_{2K-1} h_{2K-1} \\ p_2 h_2 & p_4 h_4 & \cdots & p_{2K} h_{2K} \end{bmatrix}. \tag{4.86}$$

Using (4.86), we obtain that

$$\gamma_a + \beta_a = \mathbf{b}_a^T \mathbf{F}^H \mathbf{F} \mathbf{b}_a. \tag{4.87}$$

Defining

$$\bar{\mathbf{Q}}_a \triangleq \mathbf{F}^H \mathbf{F} \tag{4.88}$$

we can write the problem of optimal selection of the coefficients b_k $(k = 1, \ldots, K)$ as

$$\max_{\mathbf{b}_a \in \{-1,1\}^K} \mathbf{b}_a^T \bar{\mathbf{Q}}_a \mathbf{b}_a. \tag{4.89}$$

Using the notation

$$\mathbf{B}_a \triangleq \mathbf{b}_a \mathbf{b}_a^T \tag{4.90}$$

this problem can be rewritten as

$$\begin{aligned} \max_{\mathbf{B}_a} \operatorname{tr}(\mathbf{B}_a \bar{\mathbf{Q}}_a) \quad \text{s.t.} \quad & [\mathbf{B}_a]_{k,k} = 1, \quad k = 1, \ldots, K \\ & \operatorname{rank}\{\mathbf{B}_a\} = 1, \quad \mathbf{B}_a \succeq 0 \end{aligned} \tag{4.91}$$

and using the SDR approach, it can be approximately converted to the following convex form

$$\begin{aligned} \max_{\mathbf{B}_a} \operatorname{tr}(\mathbf{B}_a \bar{\mathbf{Q}}_a) \text{ s.t.} \quad & [\mathbf{B}_a]_{k,k} = 1, \, k = 1, \ldots, K \\ & \mathbf{B}_a \succeq 0 \end{aligned} \tag{4.92}$$

by omitting the rank-one constraint $\operatorname{rank}\{\mathbf{B}_a\} = 1$ in (4.91).

The SDR-based algorithm for the proposed distributed Alamouti approach be summarized as follows.

Algorithm 3

1. At the receiver, find the solution to (4.92) using the approach of [54].

2. Send the so-obtained b_k from the receiver to the kth relay pair for each $k = 1, \ldots, K$ using one-bit per relay pair feedback.

In turn, the greedy algorithm of Section 4.3 can be modified as follows.

Algorithm 4

1. Set $b_1 = 1$ and $\boldsymbol{\tau}_1 = [h_1\, h_2]^T$.

2. For $k = 2, \ldots, K$, compute

$$b_k = \text{sign}(\text{Re}\left\{[h_{2k-1}^*\, h_{2k}^*]\boldsymbol{\tau}_{k-1}\right\}) \tag{4.93}$$

$$\boldsymbol{\tau}_k = \boldsymbol{\tau}_{k-1} + b_k[h_{2k-1}\, h_{2k}]^T. \tag{4.94}$$

3. Send the so-obtained b_k from the receiver to the kth relay pair for each $k = 1, \ldots, K$ using one-bit per relay pair feedback.

To derive the weights θ_k, an approach similar to that presented in Section 4.3.2 can be applied. We first develop an approximation to the expected value of the signal power and then maximize a lower bound on the SNR. Using (4.75), the average signal power can be written as

$$\text{E}\{P_s\} = \text{E}\{\gamma_a\} + \text{E}\{\beta_a\}. \tag{4.95}$$

Using (4.82), (4.83) and the same arguments as in Section 4.3.2, $\text{E}\{P_s\}$ can be approximated as

$$\text{E}\{P_s\} \approx \sum_{i,j=1}^{K} \theta_i\theta_j |\text{Re}\{\text{E}\{\rho_{2i-1,2j-1}h_{2i-1}h_{2j-1}^* + \rho_{2i,2j}h_{2i}h_{2j}^*\}\}| \tag{4.96}$$

where it is assumed that the optimal values of b_i $(i = 1, \ldots, K)$ are selected.

The expected value of the noise is given by

$$\text{E}\{P_w\} = 1 + \sum_{k=1}^{K} \theta_k^2 \left(\frac{P_{2k-1}m_{g_{2k-1}}}{P_0 m_{f_{2k-1}} + 1} + \frac{P_{2k}m_{g_{2k}}}{P_0 m_{f_{2k}} + 1} \right). \tag{4.97}$$

Using (4.96) and (4.97), the SNR maximization problem can be approximated as

$$\max_{\boldsymbol{\theta}_a} \frac{\boldsymbol{\theta}_a^T \mathbf{Q}_a \boldsymbol{\theta}_a}{\boldsymbol{\theta}_a^T \mathbf{W}_a \boldsymbol{\theta}_a + 1} \quad \text{s.t.} \quad \bar{\theta}_k \le \theta_k^2 \le 1,\ i = 1, \ldots, K \tag{4.98}$$

where $\boldsymbol{\theta}_a \triangleq [\theta_1 \ \ldots \ \theta_K]^T$,

$$\mathbf{W}_a \triangleq \text{diag}\left(\sum_{l=1}^{2} \frac{m_{g_l}P_l}{m_{f_l}P_0 + 1}, \ldots, \sum_{l=2K-1}^{2K} \frac{m_{g_l}P_l}{m_{f_l}P_0 + 1} \right) \tag{4.99}$$

$\mathbf{Q}_a$ is a $K \times K$ matrix with the entries

$$[\mathbf{Q}_a]_{i,j} \triangleq \left|\mathrm{Re}\left\{\rho_{2i-1,2j-1}\mathrm{E}\{h_{2i-1}h_{2j-1}^*\} + \rho_{2i,2j}\mathrm{E}\{h_{2i}h_{2j}^*\}\right\}\right| \tag{4.100}$$

and $\bar{\theta}_k$ constrains the weights θ_k to prevent diversity losses in a way similar to that described in Section 4.3. Now, the expected value in (4.100) can be estimated using the statistical independence of the channels as in (4.58). In particular, for the $(2i, 2j)$th factor in (4.100), we have

$$\mathrm{E}\{h_{2i}h_{2j}^*\} = \left(\mu_{f_{2i}}\mu_{f_{2j}}^* + \delta_{(2i)(2j)}\sigma_{f_{2i}}^2\right) \cdot \left(\mu_{g_{2i}}\mu_{g_{2j}}^* + \delta_{(2i)(2j)}\sigma_{g_{2i}}^2\right). \tag{4.101}$$

Following the same steps as in Section 4.3, the optimization problem in (4.98) can be turned into a convex feasibility problem that extends (4.68) to the distributed Alamouti coding case.

4.5 Differential Transmission

The concept of differential transmission is used in this section to extend the proposed approach to the case where no CSI is available at the receiver. Let us assume that $T = 1$ and let the transmitter encode differentially the information symbols s_l selected from some constant-modulo constellation $\mathcal{S}$ as

$$u_l = u_{l-1}s_l, \quad u_0 = 1 \tag{4.102}$$

where u_l and u_0 are the current and initial transmitted symbols, respectively. Similar to the coherent scheme in (4.12), we have

$$y_l = \mathbf{1}_R^T(\mathbf{p} \odot \mathbf{h})u_l + w_l. \tag{4.103}$$

Using (4.103) and the previous received signal y_{l-1}, the ML symbol estimate can be obtained from maximizing [51]

$$\mathrm{Re}\left\{y_{l-1}y_l^* s_l\right\} \tag{4.104}$$

over $s_l \in \mathcal{S}$. We assume that no power control is used, i.e., set $\theta_i = 1$ for $i = 1, \ldots, R$. Since the receiver has no CSI to select the feedback bits for b_i $(i = 1, \ldots, R)$, the following simple sequential feedback bit assignment scheme can be

used. Before the beginning of the frame in which the information symbols should be transmitted, there is an extra transmission stage to select the coefficients b_i. First, u_0 is transmitted from the source to the relays and then it is retransmitted by the relays to the destination with $b_i = 1$ $(i = 1, \ldots, R)$. Then, the second relay only alters its coefficient b_2 to -1 and the relays retransmit again. The received powers corresponding to the latter two relay-to-destination transmissions are compared at the receiver and the receiver sends one bit of feedback. This bit is used by the second relay to select b_2 that corresponds to the maximum received power. The process continues with the remaining relays in the same way. This makes it possible to select all the coefficients b_i $(i = 2, \ldots, R)$ in a sequential (greedy) way. After the process of selecting the coefficients b_i is completed, the source starts the transmission of its information symbols. The overall transmission strategy can be summarized as follows:

Algorithm 5

1. Set $b_i = 1$, $i = 1, \ldots, R$. Transmit u_0 from the source to relays and then retransmit it from the relays to the destination to obtain

$$y_1 = \mathbf{1}_R^T(\mathbf{p} \odot \mathbf{h})u_0 + w_1 \tag{4.105}$$

   at the receiver.

2. For $j = 2, \ldots, R$:

   - At the jth relay, set $b_j = -1$ and, using (4.3), update the signal d_j to be transmitted from this particular relay.
   - Transmit signals from all relays to obtain

$$y_j = \mathbf{1}_R^T(\mathbf{p} \odot \mathbf{h})u_0 + w_j \tag{4.106}$$

     at the receiver.

   - If $|y_j|^2 > |y_{j-1}|^2$, then feed "1" from the receiver back to the relay; otherwise feed "0" back to the relay. In the latter case, set $y_j = y_{j-1}$.
   - If the received feedback at the jth relay is 1, then select $b_j = -1$. Otherwise, select $b_j = 1$.

Similarly, a differential modification of the extended distributed Alamouti code of Section 4.4 can be developed in the case when $T = 2$. At the transmitter, a unitary matrix $\mathbf{S}_l$ should be formed from the constant-modulo information symbols s_{2l-1}, s_{2l} as

$$\mathbf{S}_l = \frac{1}{\sqrt{2}} \begin{bmatrix} s_{2l-1} & -s_{2l}^* \\ s_{2l} & s_{2l-1}^* \end{bmatrix}. \tag{4.107}$$

Let the differential encoding

$$\mathbf{u}_l = \mathbf{S}_l \mathbf{u}_{l-1} \tag{4.108}$$

be used at the transmitter. It amounts to sending the vector $\mathbf{u}_l = [u_{2l-1}, u_{2l}]^T$ instead of $\mathbf{s}_l = [s_{2l-1}, s_{2l-1}]^T$ to the relays where l denotes the transmitted block number. The first vector $\mathbf{u}_l$ can be chosen as $\mathbf{u}_0 = [1, 0]^T$.

Similar to (4.7) and using the matrices $\tilde{\mathbf{A}}_{2k-1}$ and $\tilde{\mathbf{A}}_{2k}$ defined in the previous section for the extended distributed Alamouti code, the following equivalent relation can be obtained

$$\mathbf{y}_l = \mathbf{S}_l \mathbf{U}_{l-1} \left(\sum_{k=1}^{K} \mathbf{p}_k \odot \mathbf{h}_k \right) + \mathbf{w}_l \tag{4.109}$$

where

$$\mathbf{U}_0 = \mathbf{I}_2 \tag{4.110}$$

$$\mathbf{U}_{l-1} \triangleq \begin{bmatrix} u_{2l-3} & -u_{2l-2}^* \\ u_{2l-2} & u_{2l-3}^* \end{bmatrix}, \quad l > 1 \tag{4.111}$$

$$\mathbf{p}_k \triangleq \left[\sqrt{\frac{P_0 P_{2k-1} T}{m_{f_{2k-1}} P_0 + 1}} b_k \theta_k, \sqrt{\frac{P_0 P_{2k} T}{m_{f_{2k}} P_0 + 1}} b_k \theta_k \right]^T \tag{4.112}$$

$$\mathbf{h}_k \triangleq [f_{2k-1} g_{2k-1}, f_{2k}^* g_{2k}]^T. \tag{4.113}$$

The ML decoding amounts to maximizing [51]

$$\mathrm{Re}\left\{ \mathrm{tr}\left(\mathbf{y}_{l-1} \mathbf{y}_l^H \mathbf{S}_l \right) \right\} \tag{4.114}$$

over $s_{2l-1}, s_{2l} \in \mathcal{S}$. Note that the detection can be done symbol-by-symbol.

As in the previous scheme without DSTC, we set $\theta_i = 1$ and use a similar strategy to select the coefficients b_i using relay pairs and blocks of length $T = 2$. This strategy can be summarized as follows:

Algorithm 6

1. Set $b_i = 1$, $i = 1, \ldots, K$. Transmit the vector $\mathbf{u}_0$ from the source to relays and then retransmit it from the relays to the destination to obtain

$$\mathbf{y}_1 = \mathbf{U}_0 \left(\sum_{k=1}^{K} \mathbf{p}_k \odot \mathbf{h}_k \right) + \mathbf{w}_1 \tag{4.115}$$

   at the receiver.

2. For $j = 2, \ldots, K$:

   - At the $(2j-1)$th and $(2j)$th relays, set $b_j = -1$ and, using (4.3), update the signals $\mathbf{d}_{2j-1}$ and $\mathbf{d}_{2j}$ to be transmitted from this particular relay pair.
   - Transmit signals from all relays to obtain

$$\mathbf{y}_j = \mathbf{U}_0 \left(\sum_{k=1}^{K} \mathbf{p}_k \odot \mathbf{h}_k \right) + \mathbf{w}_j \tag{4.116}$$

     at the receiver.
   - If $\|\mathbf{y}_j\|^2 \geq \|\mathbf{y}_{j-1}\|^2$, then feed "1" from the receiver back to the relay; otherwise feed "0" back to the relay. In the latter case, set $\mathbf{y}_j = \mathbf{y}_{j-1}$.
   - If the received feedback at the $(2j-1)$th and $(2j)$th relays is 1 then select $b_j = -1$. Otherwise, select $b_j = 1$.

Similar to Algorithms 2 and 4, Algorithms 5 and 6 are suboptimal. However, the latter two algorithms do not require any CSI at the receiver and, moreover, our simulations show that they achieve maximum diversity with a linear decoding complexity.

4.6 Computer Simulations

Throughout our simulation examples, the QPSK modulation is used and the channels are assumed to be statistically independent from each other. Unless a different assumption is explicitly mentioned, we consider all the channels to be complex circular Gaussian random variables with zero-mean and unit variance and assume that $\theta_i = 1$, $i = 1, \ldots, R$ (which are the optimal power control weights in this case) in our

No.	R	Channels	Power distribution	Feedback
1	20	Zero-mean, unit variance	$P_i = P/(R+1)$	error free
2	4	Zero-mean, unit variance	$P_0 = P/2$, $P_i = P/(2R)$	error free
3	4	Zero-mean, unit variance	$P_0 = P/2$, $P_i = P/(2R)$	error free
4	10	NLOS, LOS, path-loss exp. 3	$P_i = P/(R+1)$	error free
5	4	NLOS, LOS, path-loss exp. 3	$P_i = P/(R+1)$	error free
6	4	Zero-mean, unit variance	$P_0 = P/2$, $P_i = P/(2R)$	erroneous

Table 4.1: Parameters of the six simulation examples.

simulation examples. In Table 4.1, we present the parameters for each simulation example in detail.

In the first example, we compare the BER performances of the algorithms that select the coefficients b_i using the cooperative transmission scheme of Section 4.3.1 with $R = 20$ relays and the same maximum power $P_0 = \ldots = P_R = P/(R+1)$. In this example, the full search-based (optimal) algorithm is compared with Algorithms 1 and 2. Fig. 4.4 displays the BERs of these algorithms versus P/σ^2. It can be seen from this figure that the SDR-based approach (Algorithm 1) performs about 1 dB better than the iterative procedure of Algorithm 2. The performances of the optimal full search algorithm and Algorithm 1 are nearly identical.

In our second example, the performances of the cooperative transmission schemes of Sectons 4.3.1 (Algorithm 1) and 4.4 (Algorithm 3) are compared with that of the best relay selection scheme and the distributed version of the QOSTBC [41]. Throughout this example, $R = 4$ and the source and relay powers are chosen from the optimal power distribution for DSTC [41] as $P_0 = P/2$ and $P_i = P/(2R)$ ($i = 1, \ldots, R$). In the best relay selection scheme, the relay with the largest received SNR is selected. Fig. 4.5 displays the BERs of the techniques evaluated versus P/σ^2.

It can be clearly seen from this figure that the extended Alamouti code with one-bit total feedback outperforms the best relay selection (that requires two bits of the total feedback) and the distributed QOSTBC technique (that does not require any feedback). However, the distributed QOSTBC approach requires a more complicated decoder and imposes the decoding delay of $T = 4$. From Fig. 4.5, it also follows that Algorithm 1 outperforms the extended Alamouti with the performance gain of

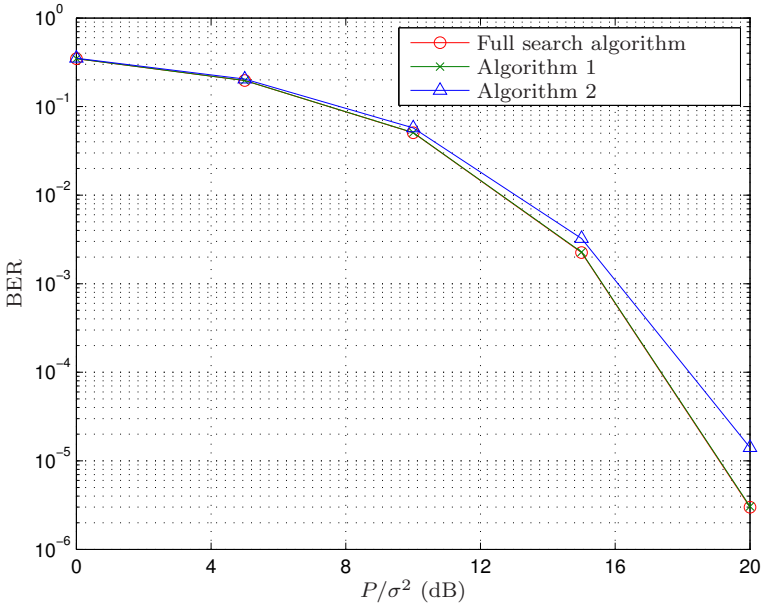

Figure 4.4: BERs versus P/σ^2; first example. Comparison of the proposed suboptimal algorithms for the selection of b_i and the optimal algorithm using full-search.

more than 2 dB at the cost of a higher feedback rate.

In our third example, the performance of the differential techniques developed in Section 4.5 is compared to that of the Sp(2) DSTC of [42], the coherent distributed QOSTBC of [41] (this code requires full CSI at the receiver) and the relay selection technique with differential transmission in which the relay with the largest received power is selected (this approach requires a total of two feedback bits). In this example, $R = 4$ is chosen. For the Sp(2) code, we use the 3-PSK constellation for the first two symbols and the 5-PSK constellation for the other two symbols. With that, a total rate of 0.9767 bpcu is achieved. The other schemes use the QPSK symbol constellations to achieve the total rate of 1 bpcu.

Fig. 4.6 compares the block error rate (BLER) performance of the techniques evaluated versus P/σ^2. The values of BLER are computed using blocks of four symbols. As can be observed from Fig. 4.6, both Algorithms 5 and 6 achieve same diversity order as the other evaluated schemes, outperform the Sp(2) code and the differential relay selection approach, and their performance is close to the distributed QOSTBC (which requires the full CSI knowledge). These improvements come at

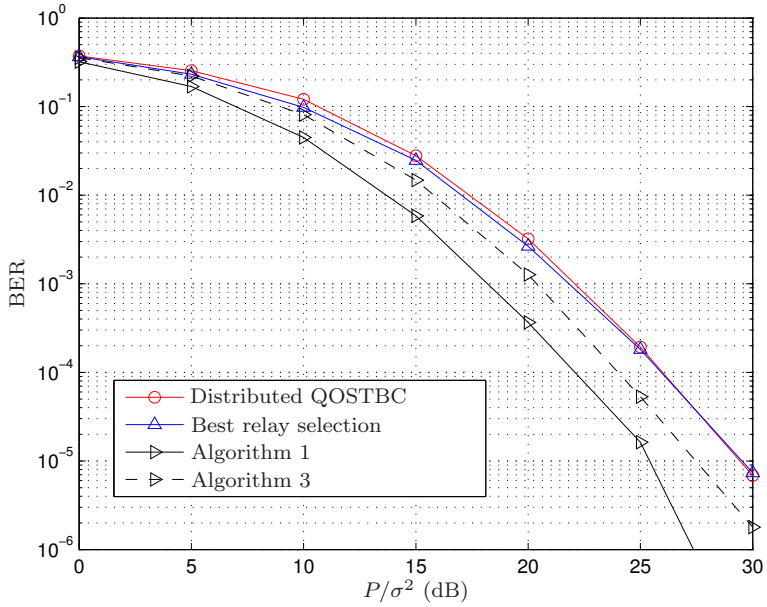

Figure 4.5: BERs versus P/σ^2; second example. Comparison of the proposed schemes with the best relay selection technique and distributed QOSTBC.

the price of three bits and one bit of feedback for Algorithms 5 and 6, respectively. Also, note that Algorithm 5 uses a total of $2R$ auxiliary time-slots before starting the transmission of information bits, while Algorithm 6 uses $3K+1$ time-slots (one time-slot for each feedback bit). On the other hand, the Sp(2) code uses $2R$ auxiliary time-slots.

For our next example, we test the algorithms proposed combined with long-term power control (which is developed in Section 4.3.2) for $R = 10$. For long-term power control, the approach of (4.68) with bisection search is used. To select an appropriate value for $\bar{\theta}_i$ $(i = 1, \ldots, R)$, we assume $\bar{\theta}_1 = \ldots = \bar{\theta}_R$ and conduct simulations for the following values: $\bar{\theta}_i = 0.05, 0.1, 0.2, 0.3, 0.4, 0.5$. The value of $\bar{\theta}_i$ that provides the best BER performance averaged over different random relay locations was selected. In Fig. 4.7 we show the averaged BER performance over different relay locations of Algorithm 1 for the $\bar{\theta}_i$ values evaluated in the case of zero-mean channels, $R = 10$ and $P_0 = P_1 = \ldots = P_R = P/(R+1)$. As can be seen from Fig. 4.7, the value of $\bar{\theta} = 0.1$ results in the best performance. Similar results are obtained for channels with LOS.

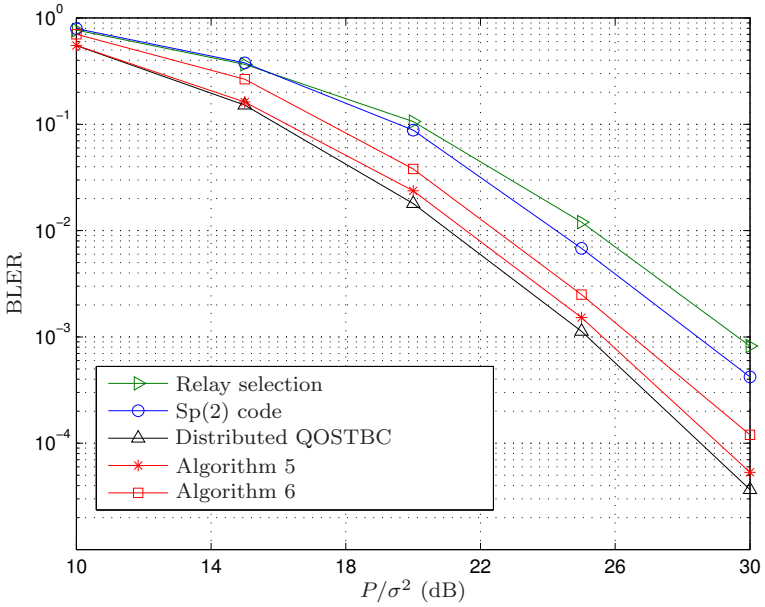

Figure 4.6: BLER versus P/σ^2; third example. Comparison of the proposed schemes for the non-coherent receiver with the best relay selection technique, the Sp(2) code and the coherent distributed QOSTBC.

Using $\bar{\theta} = 0.1$, we compare in our fourth example the performance of Algorithm 1 with and without long-term power control with the best relay selection technique and the approach of [30]. The relay locations have been uniformly drawn from a circle of normalized radius 0.5, while the distance between the source and destination is equal to 2; see Fig. 4.8 that explicitly clarifies the relay network geometry. The values of m_{f_i} and m_{g_i} depend on the distance from the transmitter to the ith relay, where $m_{f_i} = m_{g_i} = 1$ in the center of the circle. We assume that the path-loss exponent is equal to 3. The performance is averaged over random channel realizations whereas the relay locations are kept fixed over all simulation runs. Both the LOS and non-LOS (NLOS) scenarios are considered and equal maximum powers of the transmitter and relay nodes ($P_0 = P_1 \ldots = P_R = P/(R+1)$) are taken. In the LOS channel case, it is assumed that $\phi_{f_i} = \phi_{g_i} = 1$.

In Fig. 4.9, the BERs of the algorithms evaluated are shown versus P/σ^2. As can be observed from the figure, the approach of [30] shows a lower order of diversity resulting in a poor performance at high and medium SNR. Although Algorithm

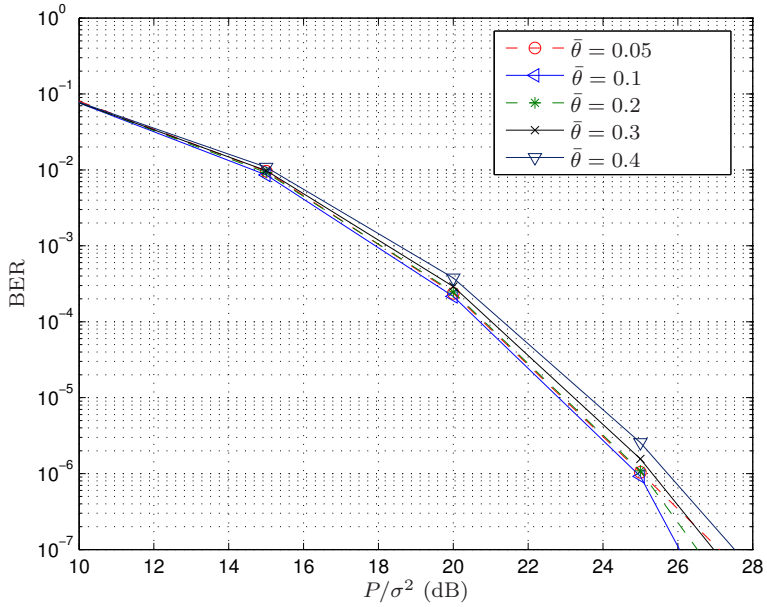

Figure 4.7: BERs versus P/σ^2; $R = 10$. Performance of the proposed power control scheme for different values of $\bar{\theta}$. The performance is averaged over different random relay locations for zero-mean channels and equal power distribution.

1 with and without long-term power control requires more feedback bits than the relay selection technique, our approach substantially outperforms it. Using the same scenario, Fig. 4.10 displays the BER performance of Algorithm 3 of Section 4.4 with and without long-term power control and best relay selection. In this case, all the techniques require the same total amount of instantaneous feedback. However, our proposed approach still outperforms the relay selection technique and achieves a significantly better performance when the long-term power control coefficients are used.

In our fifth example, the performance of Algorithm 1 combined with long-term power control is compared with Algorithm 1 of Section 4.3 and with the analytical results obtained from (4.19) by means of brute force optimization. In this example, $R = 4$ and the nearly optimal value of $\bar{\theta} = 0.1$ has been chosen. The relay locations were drawn in the same way as in the previous example and are shown in Fig. 4.11. Hence, the values of m_{f_i} and m_{g_i} depend again on the distance from the transmitter to the ith relay and from the ith relay to the receiver. Equal maximum powers of

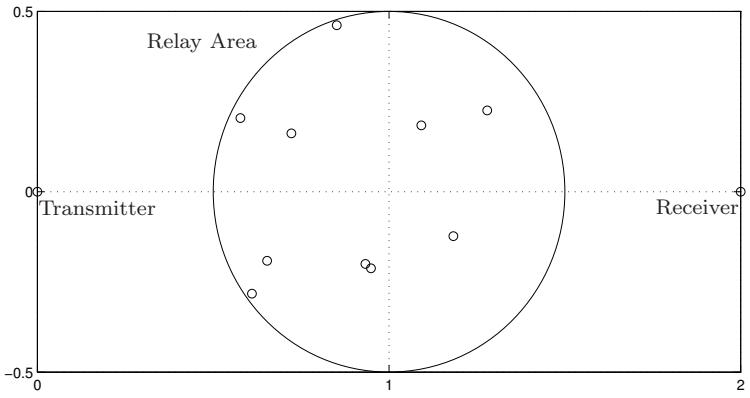

Figure 4.8: Geometry of the fourth example.

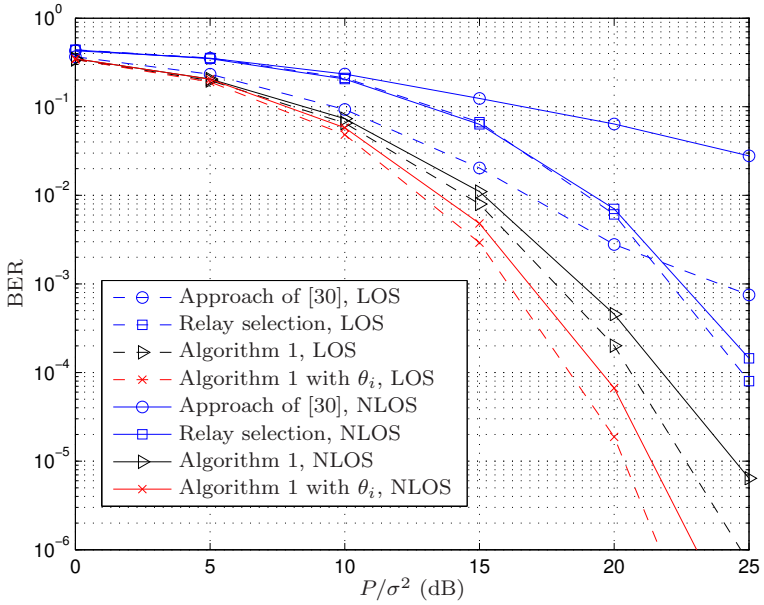

Figure 4.9: BER versus P/σ^2; fourth example. Comparison of the proposed Algorithm 1 with and without power control with the best relay selection technique and the approach of [30].

the transmitter and relay nodes ($P_0 = P_1 \ldots = P_R = P/(R+1)$) are taken. In the LOS channel case, it is again assumed that $\phi_{f_i} = \phi_{g_i} = 1$.

In Fig. 4.12, the BERs of the algorithms evaluated are shown versus P/σ^2. As

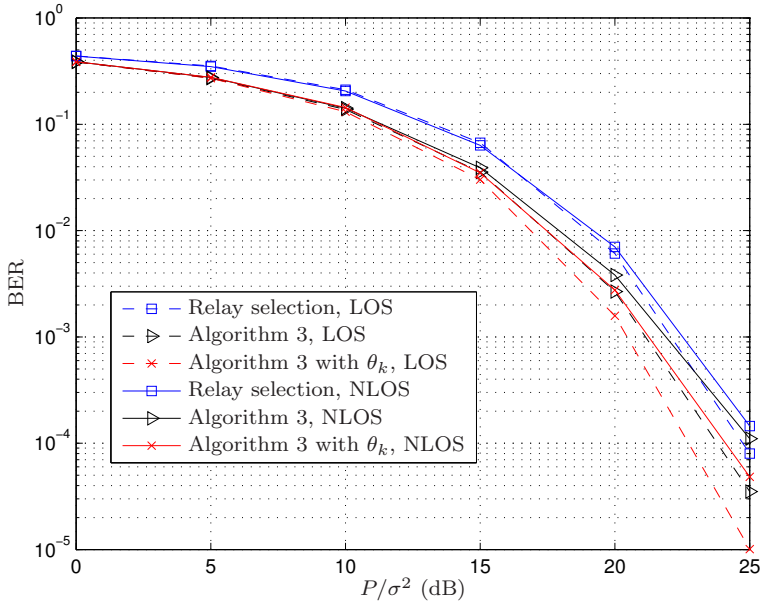

Figure 4.10: BER versus P/σ^2; fourth example. Comparison of the proposed Algorithm 3 with and without power control with the best relay selection technique.

can be clearly seen from the figure, the proposed approach with long-term power control achieves nearly the same performance as predicted by (4.19) and substantially outperforms Algorithm 1 without power control.

In our sixth example, we compare the performances of Algorithm 1 of Section 4.3 and Algorithm 3 of Section 4.4 in the cases of perfect and imperfect feedback. In this example, $R = 4$, and the feedback error probabilities $P_e = 10^{-2}$ and $P_e = 10^{-3}$ are evaluated.

Fig. 4.13 displays the BERs of the methods evaluated versus P/σ^2. As can be observed from this figure, the performance of Algorithm 1 becomes sensitive to feedback errors when the BER values are smaller than the feedback error probability itself. Therefore, as the same link quality can be normally expected in both directions, the performance of Algorithm 1 should not be significantly affected by feedback errors.

It can also be seen from Fig. 4.13 that, in contrast to Algorithm 1, the performance of Algorithm 3 is not sensitive to feedback errors. The latter fact can be explained by the spatial diversity of the Alamouti code.

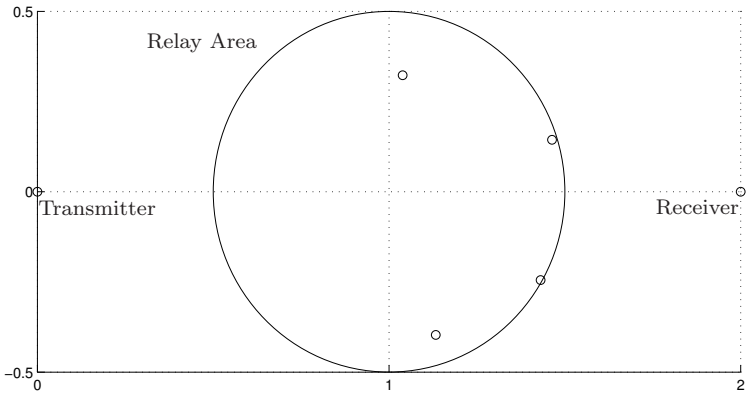

Figure 4.11: Geometry of the fifth example.

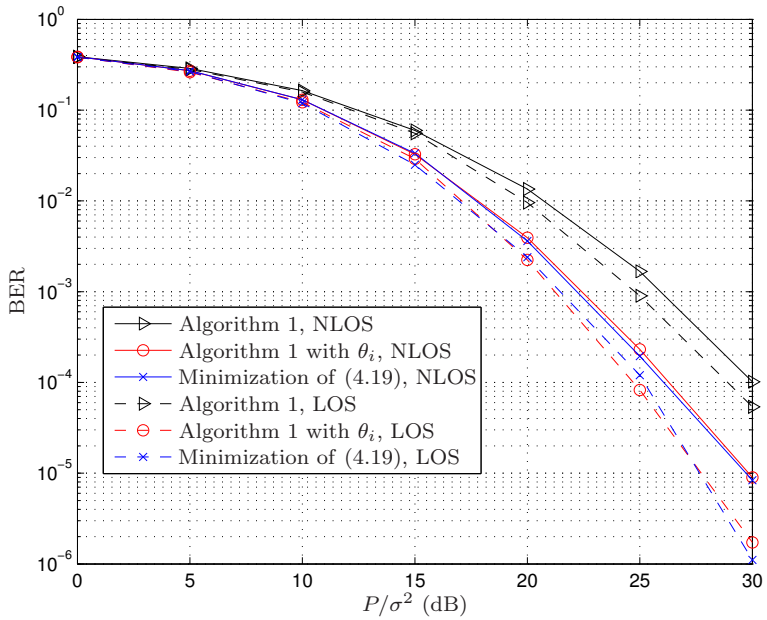

Figure 4.12: BER versus P/σ^2; fifth example. Comparison of the proposed Algorithm 1 using power control with the technique that minimizes the Chernoff bound on the error probability using brute force optimization to obtain the power control coefficients.

4.7 Summary

A new approach to use of low-rate feedback in wireless relay networks has been proposed. It has been shown that our scheme achieves the maximum possible diversity

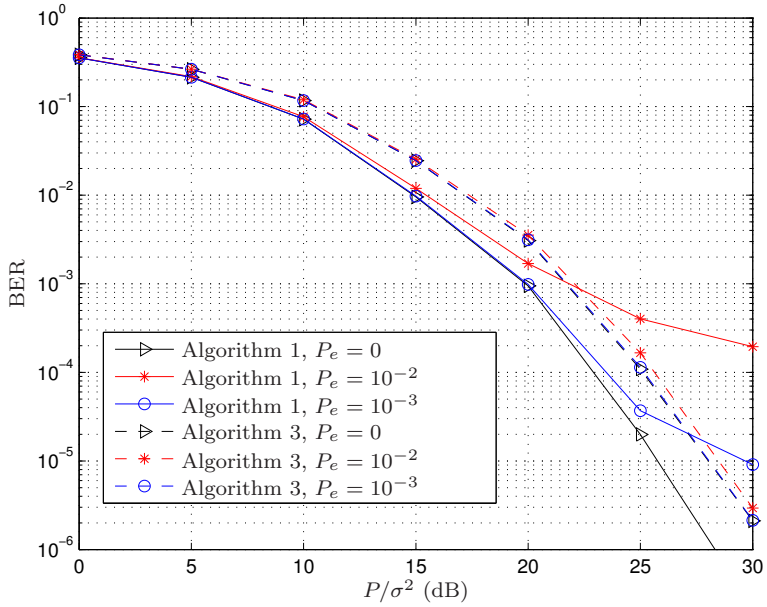

Figure 4.13: BER versus P/σ^2; sixth example. Comparison of the proposed techniques in case of erroneous feedback link.

offered by the relay network. To further improve the performance of the proposed scheme in practical scenarios, the knowledge of second-order channel statistics has been used to obtain long-term power control coefficients by means of maximizing the receiver SNR with proper power constraints. This maximization problem has been shown to be approximately equivalent to a convex feasibility problem whose solution has been demonstrated to be close to the optimal one in terms of the error probability. To improve the robustness of our scheme against feedback errors and further decrease the feedback rate, an extended version of the distributed Alamouti code has been developed. Extensions of the proposed approach to the differential transmission case have been discussed.

The proposed schemes achieve linear ML decoding complexity with low delays and can also be used for any number of relays.

Simulations have verified an improved performance-to-feedback tradeoff of the proposed techniques as compared to other popular DSTC techniques such as distributed QOSTBC of [41], best relay selection method, and the Sp(2) distributed code of [42].

Appendix 4.A Derivation of the Non-Central Chi-Square pdf for $|g_i|^2$

Using (2.5), the pdf of $|g_i|$ is given by

$$p_{|g_i|}(|g_i|) = \frac{|g_i|}{\sigma_{g_i}^2} e^{-\frac{|g_i|^2+|\mu_{g_i}|^2}{2\sigma_{g_i}^2}} I_0\left(\frac{|g_i||\mu_{g_i}|}{\sigma_{g_i}^2}\right). \tag{4.117}$$

The pdf of $|g_i|^2$ is given by

$$p_{|g_i|^2}(z_i) = \frac{p_{|g_i|}(\sqrt{z_i})}{\left|\frac{dz_i}{d(|g_i|)}\right|} \tag{4.118}$$

where $z_i \triangleq |g_i|^2$ and the derivative of z_i with respect to $|g_i|$ is

$$\frac{dz_i}{d(|g_i|)} = 2|g_i| = 2\sqrt{z_i}. \tag{4.119}$$

Using (4.117) and (4.119), (4.34) can be directly obtained from (4.118).

Chapter 5

Conclusions

In this thesis, we have proposed several advanced techniques for exploiting the gains available in wireless communication systems at a low decoding/implementation complexity. We have considered two important practical cases of point-to-point multi-antenna systems and wireless cooperative relay networks.

In the first part of this thesis, new high-rate OSB-STBCs are developed that enjoy fast ML decoding for multi-antenna systems. A new 2×2 full-rate full-diversity information lossless OSB-STBC has been proposed. Our code has been proved to fulfil the NVD property and, therefore, to achieve the optimal DMG tradeoff. Our simulation results have demonstrated that the performance of the proposed code is nearly identical to that of the best existing full-rate full-diversity codes. At the same time, our code is shown to enjoy a substantially reduced decoding complexity with respect to these state-of-the-art STC schemes. For three and four transmit antennas, new rate-one STBCs have been developed. The proposed designs add extra-symbols to the OSTBC matrix using different meaningful strategies. The proposed codes have been demonstrated to achieve a substantially improved performance-to-complexity tradeoff as compared to current state-of-the-art rate-one STBCs.

In the second part of this thesis, a new way of using a low-rate feedback has been proposed for half-duplex wireless relay networks. It has been shown analytically that the maximum diversity provided by the relay network can be achieved by using one bit feedback per relay. Low-complexity algorithms to select the one bit feedback have been developed. The use of second-order channel statistics has been proposed to design long-term power control weights in a combination with low-

rate feedback to further improve the performance in practical scenarios (where the channel quality for different relay nodes can vary significantly). The problem of designing the weight vector by maximizing an approximate expression of the receive SNR is turned into a convex feasibility problem. Simulations have shown that the solution to this optimization problem is close to the optimal solution obtained by a direct minimization of the Chernoff bound on the error probability. Additionally, the proposed schemes exhibit linear ML decoding complexity with low decoding delays and can be used in the case of an arbitrary number of relays. It is also shown that the proposed schemes can perform reliably in the case of imperfect feedback links. Furthermore, an extended Alamouti code has been proposed to increase the robustness against feedback errors. Finally, a blind modification of the proposed schemes for the non-coherent receiver using differential transmission was presented. It has been demonstrated via computer simulations that the proposed blind techniques performance close to the coherent receiver of a DSTC only at the cost of a low-rate feedback.

Bibliography

[1] E. Agrell, T. Eriksson, A. Vardy, and K. Zeger, "Closest point search in lattices," *IEEE Trans. Inform. Theory*, vol. 48, no. 8, pp. 2201–2214, August 2002.

[2] J. Akhtar and D. Gesbert, "Extending orthogonal block codes with partial feedback," *IEEE Trans. Wireless Commun.*, vol. 3, pp. 1959–1962, Nov. 2004.

[3] S. Alamouti, "A simple transmit diversity technique for wireless communications," *IEEE J. Select. Areas Commun.*, vol. 16, no. 8, pp. 1451–1458, October 1998.

[4] K. Azarian, H. El Gamal, and P. Schniter, "On the achievable diversity-multiplexing tradeoff in half-duplex cooperative channels," *IEEE Trans. Inform. Theory*, vol. 51, pp. 4152–4172, Dec. 2005.

[5] A. Baker, *Transcendental Number Theory.* London: Cambridge University Press, 1975.

[6] S. Barbarossa, *Multiantenna Wireless Communication Systems.* Artech House, 2005.

[7] J.-C. Belfiore, G. Rekaya, and E. Viterbo, "The golden code: A 2 x 2 full-rate space-time code with non-vanishing determinants," *IEEE Trans. Inform. Theory*, vol. 51, no. 4, pp. 1432–1436, April 2005.

[8] S. Boyd and L. Vandenberghe, *Convex Optimization.* Cambridge University Press, 2004.

[9] T. M. Cover and A. A. El Gamal, "Capacity theorems for the relay channel," *IEEE Trans. Inform. Theory*, vol. 25, no. 5, pp. 572–584, Sept. 1979.

[10] M. O. Damen, K. Abed-Meraim, and J.-C. Belfiore, "Diagonal algebraic space-time block codes," *IEEE Trans. Inform. Theory*, vol. 48, no. 3, pp. 628–636, Mar. 2002.

[11] M. O. Damen and N. C. Beaulieu, "On two high-rate algebraic space-time codes," *IEEE Trans. Inform. Theory*, vol. 49, no. 4, pp. 1059–1063, April 2003.

[12] M. O. Damen, A. Chkeif, and J.-C. Belfiore, "Lattice code decoder for space-time codes," *IEEE Commun. Lett.*, vol. 4, pp. 161–163, May 2000.

[13] M. O. Damen, H. El Gamal, and N. C. Beaulieu, "On the design of quasi-orthogonal constellations: Filling the empty threads," in *Proc. IEEE Vehicular Technology Conference (VTC'03) – Fall*, Oct. 2003, pp. 1753–1756.

[14] A. F. Dana and B. Hassibi, "On the power-efficiency of sensory and ad hoc wireless networks," *IEEE Trans. Inform. Theory*, vol. 7, pp. 2890–2914, July 2006.

[15] D. N. Dao, C. Yuen, C. Tellambura, Y. L. Guan, and T. T. Tjhung, "Four-group decodable space-time block codes," *IEEE Trans. Signal Processing*, vol. 56, pp. 424–430, Jan. 2008.

[16] V. M. DaSilva and E. S. Sousa, "Fading-resistant modulation using several transmitter antennas," *IEEE Trans. Commun.*, vol. 45, no. 10, pp. 1236–1244, Oct. 1997.

[17] P. Dayal and M. K. Varanasi, "An optimal two transmit antenna space-time code and its stacked extensions," *Proc. Asilomar Conference on Signals, Systems and Computers*, pp. 987–991, Nov. 2003.

[18] S. N. Diggavi, N. Al-Dhahir, A. Stamoulis, and A. R. Calderbank, "Great expectations: the value of spatial diversity in wireless networks," *Proc. IEEE*, vol. 92, no. 2, pp. 219–270, Feb. 2004.

[19] Z. Ding, W. H. Chin, and K. K. Leung, "Distributed beamforming and power allocation for cooperative networks," *IEEE Trans. Wireless Commun.*, vol. 7, pp. 1817–1822, May 2008.

[20] P. Elia, K. R. Kumar, S. A. Pawar, P. V. Kumar, and H. Lu, "Explicit construction of space-time block codes: Achieving the diversity-multiplexing gain tradeoff," *IEEE Trans. Inform. Theory*, vol. 52, no. 9, pp. 3869–3884, Sept. 2006.

[21] A. Fasano and S. Barbarossa, "Information lossless full-rate full-diversity trace-orthogonal space-time codes," in *Proc. IEEE Workshop on Signal Processing Advances in Wireless Commun. (SPAWC)*, Cannes, France, July 2006, pp. 1–5.

[22] U. Fincke and M. Pohst, "Improved method for calculating vectors of short length in a lattice, including a complexity analysis," *Math. Comput.*, vol. 44, pp. 463–471, Apr. 1985.

[23] G. J. Foschini and M. J. Gans, "On limits of wireless communications in a fading environment when using multiple antennas," *Wireless Personal Communications*, vol. 6, pp. 311–335, March 1998.

[24] G. Ganesan and P. Stoica, "Space-time block codes: a maximum SNR approach," *IEEE Trans. Inform. Theory*, vol. 47, pp. 1650–1656, May 2001.

[25] M. Gastpar and M. Vetterli, "On the capacity of large Gaussian relay networks," *IEEE Trans. Inform. Theory*, vol. 51, pp. 765–779, March 2005.

[26] A. B. Gershman and N. D. Sidiropoulos, Eds., *Space-Time Processing for MIMO Communications*, 1st ed. UK: John Wiley & Sons, 2005.

[27] D. Gesbert, M. Shafi, D. Shiu, P. Smith, and A. Naguib, "From theory to practice: an overview of MIMO space-time coded wireless systems," *IEEE J. Select. Areas Commun.*, vol. 21, pp. 281–302, April 2003.

[28] M. Gharavi-Alkhansari and A. B. Gershman, "Constellation space invariance of orthogonal space-time block codes," *IEEE Trans. Inform. Theory*, vol. 51, pp. 1051–1055, Jan. 2005.

[29] B. Hassibi and B. M. Hochwald, "High-rate codes that are linear in space and time," *IEEE Trans. Inform. Theory*, vol. 48, pp. 1804–1824, July 2002.

[30] V. Havaray-Nassab, S. Shahbazpanahi, A. Grami, and Z.-Q. Luo, "Network beamforming based on second order statistics of the channel state information," in *Proc. IEEE Int. Conf. on Acoust., Speech and Signal Processing (ICASSP)*, Las Vegas, USA, Apr. 2008, pp. 2605–2608.

[31] S. Haykin, *Communication Systems*, 3rd ed. USA: John Wiley & Sons, 1994.

[32] R. W. Heath, Jr. and A. J. Paulraj, "A simple scheme for transmit diversity using partial channel feedback," in *Proc. Asilomar Conf. on Signals, Systems and Computers*, Pacific Grove, USA, Nov. 1998, pp. 1073–1078.

[33] R. W. Heath, Jr. and A. J. Paulraj, "Linear dispersion codes for MIMO systems based on frame theory," *IEEE Trans. Signal Processing*, vol. 50, no. 10, pp. 2429–2441, Oct. 2002.

[34] B. M. Hochwald and W. Sweldens, "Differential unitary space-time modulation," *IEEE Trans. Commun.*, vol. 48, pp. 2041–2052, Dec. 2000.

[35] B. M. Hochwald and S. ten Brink, "Achieving near-capacity on a multiple-antenna channel," *IEEE Trans. Commun.*, vol. 51, pp. 389–399, Mar. 2003.

[36] A. Hottinen and O. Tirkkonen, "Precoder designs for high rate space-time block codes," in *Proc. Conf. on Inform. Sciences and Systems*, Princeton, NJ, March 2004.

[37] *IEEE Standard for Local and Metropolitan Area Networks*, IEEE 802.16e - 2005, Feb. 2006.

[38] IEEE 802.16's Relay Task Group, http://www.ieee802.org/16/relay/, 2006.

[39] H. Jafarkhani, "A quasi-orthogonal space-time block code," *IEEE Trans. Commun.*, vol. 49, pp. 1–4, Jan. 2001.

[40] Y. Jing and B. Hassibi, "Distributed space-time coding in wireless relay networks," *IEEE Trans. Wireless Commun.*, vol. 5, pp. 3524–3536, Dec. 2006.

[41] Y. Jing and H. Jafarkhani, "Using orthogonal and quasi-orthogonal designs in wireless relay networks," *IEEE Trans. Inform. Theory*, vol. 53, pp. 4106–4118, Nov. 2007.

[42] Y. Jing and H. Jafarkhani, "Distributed differential space-time coding for wireless relay networks," *IEEE Trans. Commun.*, vol. 56, pp. 1092–1100, July 2008.

[43] Y. Jing and H. Jafarkhani, "Network beamforming using relays with perfect channel information," *IEEE Trans. Inform. Theory*, submitted in 2008.

[44] Y. Jing and H. Jafarkhani, "Network beamforming with channel mean and covariance at relays," in *Proc. IEEE International Conference on Communications*, Beijing, May 2008, pp. 3743–3747.

[45] M. Z. A. Khan and S. B. Rajan, "Single-symbol maximum likelihood decodable linear STBCs," *IEEE Trans. Inform. Theory*, vol. 52, no. 5, pp. 2062–2091, May 2006.

[46] T. Kiran and S. B. Rajan, "STBC-Schemes with non-vanishing determinant for certain number of transmit antennas," *IEEE Trans. Inform. Theory*, vol. 51, no. 8, pp. 2984–2992, August 2005.

[47] E. Koyuncu, Y. Jing, and H. Jafarkhani, "Distributed beamforming in wireless relay networks with quantized feedback," *IEEE J. Select. Areas Commun.*, vol. 26, pp. 1429–1439, Oct. 2008.

[48] G. Kramer, M. Gatspar, and P. Gupta, "Cooperative strategies and capacity theorems for relay networks," *IEEE Trans. Inform. Theory*, vol. 51, no. 9, pp. 3037–3063, Sept. 2005.

[49] J. N. Laneman, D. N. C. Tse, and G. W. Wornell, "Cooperative diversity in wireless networks: efficient protocols and outage behavior," *IEEE Trans. Inform. Theory*, vol. 50, pp. 3062–080, Dec. 2004.

[50] J. N. Laneman and G. W. Wornell, "Distributed space-time-coded protocols for exploiting cooperative diversity in wireless networks," *IEEE Trans. Inform. Theory*, vol. 49, pp. 2415–2425, Oct. 2003.

[51] E. Larsson and P. Stoica, *Space-Time Block Coding for Wireless Communications*. Cambridge: Cambridge University Press, 2003.

[52] P. Larsson, "Large-scale cooperative relaying network with optimal combining under aggregate relay power constraint," in *Proc. of Future Telecomm. Conf.*, Beijing, China, Dec. 2003, pp. 166–170.

[53] X.-B. Liang, "Orthogonal designs with maximal rates," *IEEE Trans. Inform. Theory*, vol. 49, pp. 2468–2503, Oct. 2003.

[54] W. K. Ma, T. N. Davidson, K. M. Wong, Z.-Q. Luo, and P.-C. Ching, "Quasi-maximum-likelihood multiuser detection using semi-definite relaxation with application to synchronous CDMA," *IEEE Trans. Signal Processing*, vol. 50, pp. 912–922, April 2002.

[55] X. Ma and G. Giannakis, "Full-diversity full-rate complex-field space-time coding," *IEEE Trans. Signal Processing*, vol. 51, pp. 2917–2930, Nov. 2003.

[56] R. Mudumbai, J. Hespanha, U. Madhow, and G. Barriac, "Scalable feedback control for distributed beamforming in sensor networks," in *Proc. International Symposium on Information Theory (ISIT)*, Adelaide, Australia, Sept. 2005, pp. 137–141.

[57] K. K. Mukkavilli, A. Sabharwal, M. Orchard, and B. Aazhang, "Transmit diversity with channel feedback," in *Proc. Int. Symposium on Telecommunications*, Tehran, Iran, Sept. 2001, pp. 900–901.

[58] R. U. Nabar, H. Bölcskei, and F. W. Kneubühler, "Fading relay channels: Performance limits and space-time signal design," *IEEE J. Select. Areas Commun.*, vol. 22, pp. 1099–1109, August 2004.

[59] J. A. Nelder and R. Mead, "A simplex method for function minimization," *Computer Journal*, vol. 7, pp. 308–313, 1965.

[60] A. Nosratinia, T. E. Hunter, and A. Hedayat, "Cooperative communication in wireless networs," *IEEE Commun. Mag.*, vol. 42, pp. 74–80, Oct. 2004.

[61] F. Oggier, G. Rekaya, J.-C. Belfiore, and E. Viterbo, "Perfect space time block codes," *IEEE Trans. Inform. Theory*, vol. 52, pp. 3885–3902, Sept. 2006.

[62] C. B. Papadias and G. J. Foschini, "Capacity-approaching space-time codes for systems employing four transmitter antennas," *IEEE Trans. Inform. Theory*, vol. 49, pp. 726–732, Mar. 2003.

[63] J. Paredes and A. B. Gershman, "High-rate space-time block codes with fast maximum-likelihood decoding," in *Proc. IEEE Int. Conf. on Acoust., Speech and Signal Processing (ICASSP)*, Las Vegas, USA, Apr. 2008, pp. 2385–2388.

[64] J. Paredes, A. B. Gershman, and M. Gharavi-Alkhansari, "A 2x2 space-time code with non-vanashing determinants and fast maximum likelihood decoding," in *Proc. IEEE Int. Conf. on Acoust., Speech and Signal Processing (ICASSP)*, Honolulu, Hawaii, Apr. 2007, pp. 877–880.

[65] J. Paredes, A. B. Gershman, and M. Gharavi-Alkhansari, "A new full-rate full-diversity space-time block code with non-vanishing determinants and simplified maximum likelihood decoding," *IEEE Trans. Signal Processing*, vol. 56, pp. 2461–2469, June 2008.

[66] J. M. Paredes, B. H. Khalaj, and A. B. Gershman, "Using orthogonal designs with feedback in wireless relay networks," in *Proc. IEEE Workshop on Signal Processing Advances in Wireless Commun. (SPAWC)*, Recife, Brazil, July 2008, pp. 61–65.

[67] J. M. Paredes, B. H. Khalaj, and A. B. Gershman, "Cooperative transmission for wireless relay networks using low-rate feedback," *IEEE Trans. Signal Processing*, Submitted. 2009.

[68] J. M. Paredes, B. H. Khalaj, and A. B. Gershman, "A differential cooperative transmission scheme with low rate feedback," in *Proc. IEEE Int. Conf. on Acoust., Speech and Signal Processing (ICASSP)*, Taipei, Taiwan, April 2009, pp. 2621–2624.

[69] A. Paulraj, R. Nabar, and D. Gore, *Introduction to Space-Time Wireless Communications*. Cambridge University Press, 2003.

[70] D. Pham, K. Pattipati, P. Willet, and J. Luo, "An improved complex sphere decoder for V-BLAST systems," *IEEE Signal Processing Lett.*, vol. 11, pp. 748–751, Sept. 2004.

[71] M. Pohst, "On the computation of lattice vectors of minimal length, successive minima and reduced bases with applications," in *Proc. ACM SIGSAM*, 1981, pp. 37–44.

[72] D. Rainish, "Diversity transform for fading channels," *IEEE Trans. Commun.*, vol. 44, pp. 1653–1661, Dec. 1996.

[73] G. S. Rajan and B. S. Rajan, "Distributed space-time codes for cooperative networks with partial CSI," in *Proc. IEEE Wireless Communications and Networking Conference (WCNC 2007)*, Hong Kong, March 2007, pp. 902–906.

[74] G. S. Rajan and B. S. Rajan, "Multi-group ML decodable collocated and distributed space-time block codes," *IEEE Trans. Inform. Theory*, Submitted 2008.

[75] S. Sandhu and A. J. Paulraj, "Space-time block codes: A capacity perspective," *IEEE Commun. Lett.*, vol. 4, no. 12, pp. 384–386, Dec. 2000.

[76] M. Sauter, *Grundkurs Mobile Kommunikationssysteme*. Wiesbaden: Fried. Vieweg & Sohn Verlag, 2008.

[77] A. Sendonaris, E. Erkip, and B. Aazhang, "User cooperation diversity–Part I: System description," *IEEE Trans. Commun.*, vol. 51, pp. 1927–1938, Nov. 2003.

[78] A. Sendonaris, E. Erkip, and B. Aazhang, "User cooperation diversity–Part II: Implementation aspects and performance analysis," *IEEE Trans. Commun.*, vol. 51, pp. 1938–1948, Nov. 2003.

[79] B. A. Sethuraman, B. S. Rajan, and V. Shashidhar, "Full-diversity, high-rate space-time block codes from division algebras," *IEEE Trans. Inform. Theory*, vol. 49, no. 10, pp. 2596–2616, Oct. 2003.

[80] C. E. Shannon, "A mathematical theory of communication," *The Bell System Technical J.*, vol. 27, pp. 379–423, 623–656, July, Oct. 1948.

[81] N. Sharma and C. B. Papadias, "Improved quasi-orthogonal codes through constellation rotation," *IEEE Trans. Commun.*, vol. 51, no. 3, pp. 332–335, Mar. 2003.

[82] N. D. Sidiropoulos and R. S. Budampati, "Khatri-Rao space-time codes," *IEEE Trans. Signal Processing*, vol. 50, pp. 2396–2407, Oct. 2002.

[83] N. D. Sidiropoulos, T. N. Davidson, and Z.-Q. Luo, "Transmit beamforming for physical layer multicasting," *IEEE Trans. Signal Processing*, vol. 54, pp. 2239–2251, June 2006.

[84] M. K. Simon and M.-S. Alouni, *Digital Communication over Fading Channels*, 2nd ed. John Wiley & Sons, 2005.

[85] W. Su and X. Xia, "Signal constellations for quasi-orthogonal space-time block codes with full diversity," *IEEE Trans. Inform. Theory*, vol. 50, no. 10, pp. 2331–2347, Oct. 2004.

[86] V. Tarokh, H. Jafarkhani, and A. R. Calderbank, "Space-time block codes from orthogonal designs," *IEEE Trans. Inform. Theory*, vol. 45, pp. 1456–1467, July 1999.

[87] V. Tarokh, A. Naguib, N. Seshadri, and A. R. Calderbank, "Space-time codes for high date rate wireless communication: Performance criteria in the presence of channel estimation errors, mobility and multiple paths," *IEEE Trans. Commun.*, vol. 47, pp. 199–207, Feb. 1999.

[88] V. Tarokh, N. Seshadri, and A. R. Calderbank, "Space-time codes for high date rate wireless communication: Performance criterion and code construction," *IEEE Trans. Inform. Theory*, vol. 44, pp. 744–765, March 1998.

[89] S. Tavildar and P. Viswanath, "Approximately universal codes over slow fading channels," *IEEE Trans. Inform. Theory*, vol. 52, no. 7, pp. 3233–3258, July 2006.

[90] I. E. Telatar, "Capacity of multiple antenna Gaussian channels," *European Trans. Telecommunications*, vol. 10, pp. 585–595, Nov./Dic. 1999.

[91] O. Tirkkonen, "Optimizing STBCs by constellation rotations," in *Proc. Finnish Wireless Communications Workshop (FWCW)*, Tampere, Finland, Oct. 2001, pp. 59–60.

[92] O. Tirkkonen, A. Boariu, and A. Hottinen, "Minimal nonorthogonality rate 1 space-time block code for 3+ tx antennas," in *Proc. IEEE ISSSTA'00*, Parsippany, NJ, USA, Sept. 2000, pp. 429–432.

[93] D. Tse and P. Viswanath, *Fundamentals of Wireless Communication*. Cambridge: Cambridge University Press, 2005.

[94] J. Villare, G. Vazquez, and M. Lamarca, "Maximum likelihood blind carrier synchronization in space-time coded ofdm systems," in *Proc. IEEE Workshop on Signal Processing Advances in Wireless Commun. (SPAWC)*, Rome, Italy, Sept. 2003, pp. 610–614.

[95] H. Wang and X.-G. Xia, "Upper bounds of rates of complex orthogonal space-time block codes," *IEEE Trans. Inform. Theory*, vol. 49, pp. 2788–2796, April 2003.

[96] P. W. Wolniansky, G. J. Foschini, G. D. Golden, and R. A. Valenzuela, "V-BLAST: an architecture for realizing very high data rates over the rich-scattering wireless channel," in *Proc. URSI Int. Symp. Signals, Syst., Electron.*, Italy, Sept. 1998, pp. 295–300.

[97] A. Wong, J. K. Zhang, and K. M. Wong, "Full diversity group decodable orthogonal linear dispersion codes for MISO flat fading channels," in *Proc. IEEE Int. Conf. on Acoust., Speech and Signal Processing (ICASSP)*, Las Vegas, USA, Apr. 2008, pp. 2929–2932.

[98] L. Xian and H. Liu, "Rate-one space-time block codes with full diversity," *IEEE Trans. Commun.*, vol. 53, no. 12, pp. 1986–1990, Dec. 2005.

[99] Y. Xin, Z. Wang, and G. B. Giannakis, "Space-time diversity systems based on linear constellation precoding," *IEEE Trans. Wireless Commun.*, vol. 2, no. 2, pp. 294–309, Mar. 2003.

[100] H. Yao and G. Wornell, "Achieving the full mimo diversity-multiplexing frontier with rotation based space-time codes," in *Proc. of the Allerton Conf. on Commun., Control and Computing*, Monticelo, Illinois, October 2003, pp. 400–409.

[101] C. Yuen, Y. L. Guan, and T. T. Tjhung, "Quasi-orthogonal STBC with minimum decoding complexity," *IEEE Trans. Wireless Commun.*, vol. 4, no. 5, pp. 2089–2095, Sept. 2005.

[102] J. K. Zhang, J. Liu, and K. M. Wong, "Trace-orthogonal full diversity cyclotomic space-time codes," in *Space-Time Processing for MIMO Communications*, A. B. Gershman and N. D. Sidiropoulos, Eds. John Wiley & Sons, 2005, ch. 5, pp. 169–208.

[103] L. Zheng and D. N.C. Tse, "Diversity and multiplexing: A fundamental tradeoff in multiple-antenna channels," *IEEE Trans. Inform. Theory*, vol. 45, no. 5, pp. 1073–1096, May 2003.

Wissenschaftlicher Werdegang

Ausbildung

- October 2005 - März 2009. Technische Universität Darmstadt, Darmstadt, Deutschland. Promotionsstudium. DAAD Stipendiat.
- März 2002 - Januar 2004. Technische Universität Kaiserslautern, Kaiserslautern, Deutschland. M.Sc. in Electrical Engineering. Vertiefungsrichtung: Nachrichtentechnik. Masterarbeit: "Optimum transmit signal design for the downlink of future mobile radio systems".
- Januar 1993 - September 1998. Universidad de los Andes, Bogota, Kolumbien. Elektrotechnikingenieur, mit Auszeichnung.
- Januar 1993 - September 1998. Universidad de los Andes, Bogota, Kolumbien. Maschinenbauingenieur, mit Auszeichnung.

Berufserfahrung

- Februar 2004 - September 2005. Centuritech Ltda., Bogota, Kolumbien. Senior Software Entwickler.
- Juni 2002 - Januar 2004. Fraunhofer Institut für experimetelles Software Engineering (IESE), Kaiserslautern, Deutschland. Wissenschaftliche Hilfskraft.
- Dezember 1998 - Februar 2002. Forschungs- und Entwicklungsabteilung, ITEC-TELECOM, Bogota, Kolumbien. Entwicklungsingenieur.
- Januar 1994 - Juli 1998. Universidad de los Andes, Bogota, Kolumbien. Wissenschaftliche Hilfskraft.